EVIDENCE FOR DIFFERENTIAL COMMINUTION / AEOLIAN SORTING AND CHEMICAL WEATHERING OF MARTIAN SOILS PRESERVED IN MARS METEORITE EET79001

M.N.Rao,
Lockheed Martin, NASA Road One, Houston. TX. 77058
and
D.S.McKay,
Jhonson Space Center, NASA, Houston. TX. 77058

Geochimica Cosmochemica Acta , submitted in February, 2004.

ABSTRACT

Impact-melt glasses containing Martian atmospheric gases in Mars meteorite EET79001 are formed from Martian soil fines that had undergone meteoroid-comminution and aeolian sorting accompanied by chemical weathering near Mars surface. Using SiO_2 and SO_3 as proxy for silicates and salts respectively in Mars soils, we find that SiO_2 and SO_3 correlate negatively with FeO and MgO and positively with Al_2O_3 and CaO in these glasses, indicating that the mafic and felsic components are depleted and enriched relative to the bulk host (Lith A/B) respectively as in the case of Moon soils. Though the overall pattern of mineral fractionation is similar between the soil fines on Mars and Moon, the magnitudes of the enrichments / depletions differ between these sample-suites because of pervasive aeolian activity on Mars.

In addition to this mechanical processing, the Martian soil fines, prior to impact-melting, have undergone acid-sulfate dissolution under oxidizing / reducing conditions. The SO_3 content in EET79001,507 (Lith B) glass is ~18% compared to < 2% in EET79001, 506 (Lith A). SiO_2 and SO_3 negatively correlate with each other in ,507 glasses similar to Pathfinder soils. The positive correlation found between FeO and SO_3 in ,507 glasses as well as Pathfinder rocks and soils is consistent with the deposition of ferric-hydroxysulfate on regolith grains in an oxidizing environment. As in the case of Pathfinder soils, the Al_2O_3 vs SiO_2 positive correlation and FeO vs SiO_2 negative correlation observed in ,507 glasses indicate that SiO_2 from the regolith is mobilized as soluble silicic acid at low pH. The large off-set in the end-member FeO abundance (SO3=0) between Pathfinder soil-free rock and sulfur-free rock in ,507 glass precursors suggests that the soils comprising the ,507 glasses contain much larger proportion of fine-grained Martian soil fraction that registers strong mafic depletion relative to Lith B. This inference is strongly supported by the Al2O3 – SO3 negative correlation observed in both ,507 glasses and pathfinder soils. Furthermore, the flat MgO-SO_3 correlation observed in the case of ,507 glasses shows that the solubilized $MgSO_4$ is mobilized by the aqueous solutions leaving behind the rock-residue with ~2-3% MgO. This value is similar to the ~ 2% MgO found for the soil-free rock at the Pathfinder site.

The EET79001, 506 glasses, in contrast, show that Al_2O_3 and CaO positively correlate with SO_3 indicating that Al is precipitated as amorphous hydroxysulfate at relatively high pH. The FeO - SO_3 negative correlation observed in ,506 glasses yields an end-member FeO abundance of ~21% for the sulfur-free rock, which is consistent with the 22% FeO deduced for the Viking soil-free rock. Further, the FeO and MgO negative correlation with SO_3 observed in ,506 glasses indicates that the divalent Fe and Mg released from ferromagnesian minerals by acid sulfate dissolution are mobilized away from the reaction sites as soluble sulfates under reducing environment. A similar negative correlation between FeO and SO_3 and a positive correlation between Al_2O_3 and SO_3 found in Viking soils suggest that they also had undergone acid-sulfate dissolution under relatively reducing conditions.

Taking Martian atmospheric gases as soil-markers, we present a weathering-model for calculating the composition of the end products after dissolution and mobilization from (or precipitation at) the reaction site. We show that one set of assumptions used for calculating these

compositions in Cases A, B and C (discussed in text) is able to reproduce both negative and positive correlation trends observed between major element oxides versus SO3 / SiO2 in EET79001 glasses.

1. INTRODUCTION

Elephant Moraine 79001 is a shergottite meteorite originating from Mars surface (Trieman et al., 2000; McSween, 2002). Some impact melt glasses in these shergottite meteorites, that contain large concentrations of Martian atmospheric noble gases (Bogard and Johnson, 1983; Becker and Pepin, 1984; Swindle et al., 1986) likely contain Martian soil fines (MSF) mixed with other coarser regolith rock-materials in varying proportions. These glasses also show large variations in $^{87}Sr/^{86}Sr$ ratios when compared with the host lithology (Wooden et al., 1982). These impact glasses in EET79001 are also found to contain volatiles having hydrogen isotopic composition similar to the Martian atmosphere (Boctor et al., 2003; Leshin et al., 1996). The Martian gases were presumably incorporated into these glasses when they were produced by shock-melting of the soil constituents during meteoroid impact. The silicate melts, thus generated during impact, were shock-injected into the fractures and voids in the surrounding rocks which were quickly quenched into glass. In some impact melt glass veins in EET79001, (also called Lithology C), large enrichments of sulfur, which is abundantly present in Mars soil, were found by Gooding and Muenow, (1986) and Rao et al., (1999). Furhermore, in these samples, secondary sulfate minerals such as calcium sulfate and sulfur-rich aluminosilicates formed during aqueous alteration on Mars were found trapped as relict grains in these glasses (Gooding and Muenow,1986; Gooding et al., 1988). Recently, in the glass veins from EET79001 and other shergottites (Shergotty), Rao et al., (1999b) ad Rao and McKay, (2001 & 2002) have observed systematic depletion of mafic component (FeO, MgO & TiO_2) accompanied by simultaneous enrichment of felsic (Al_2O_3, CaO and NaO) component with respect to the bulk host phase . This characteristic feature of MSF fraction was attributed to the occurrence of varying proportions of Martian soil fines (MSF), prior to melting, in the precursor regolth materials, which were presumably produced as result of continuous meteoroid bombardment of basement and regolith rocks, accompanied by sorting due to pervasive Aeolian activity on Mars.

Though innumerable publications have appeared in literature regarding the study of Martian soils with and without using Viking and Pathfinder rock and soil data, very few attempts were made to search for Martian soil components in SNC meteorites. Early on, McSween and Jarosewich (1983) studied these glasses using EMPA and found significant plagioclase (maskelynite) enrichments. But, Gooding and Meunow (1986) were the first to recognize the significance of the fact that the Martian atmospheric noble gases (discovered by Bogard and Johnson (1983) in EET79001) were not homogeneously distributed in this Martian meteorite but is concentrated in selected glass-rich pockets (mm to cm in size) designated as Lithology C. During a EMPA study of these petrologically documented glass inclusions, Gooding et al. (1986) found several anherdral grains of CaCO3 intimately associated with CaSO4, suggesting that they were trapped during rapid solidification of quench-textured pyroxenes and glass from the impact melt on Mars. They, further, found significant enrichment of sulfur and Al2O3 in Lith C

relative to Lith A suggesting the occurrence of sulfur-rich aluminosilicate mineraloids (~10 um in size) in trace quantities. Using high vacuum pyrolisis of glass inclusions in EET79001, bearing Martian atmospheric noble gases, Gooding and Meunow (1986) showed that significant amounts of sulfur in these glasses exist as sulfate in higher oxidation state and it is sometimes associated with S-rich aluminosilicates occluded in these glasses. Also, Burgess et al. (1988) carried out stepped combustion analysis of sulfur bearing phases in some SNC meteorites such as Shergotty and Nakhla (both falls) and showed that sulfates and sulfides are widespread and sulfur exists as sulfate in varying proportions in these meteorites. They showed that shergottites contain much larger amounts of sulfates compared to nakhlites, another group of Martian meteorites. Burgess et al. (1988) and recently Shearer et al. (2000) tried to measure sulfur isotopic composition in EET79001, Lith C samples with little success. Furthermore, in Martian meteorites such as Nakhla and Lafayette (and also in another meteorite ALH84001), Gooding et al. (1991) and Bridges et al. (2001) among others found secondary mineral assemblages of carbonates and sulfates sometimes associated with clay-minerals of Martian origin based on textural and isotopic evidence. As the present study is focused on impact melt glasses bearing Martian atmospheric noble gases, other Martian meteorites such as nakhlites and ALH84001 (having no impact glasses) are not discussed further.

In addition to the above mechanical processing, we present evidence that shows that shows these Martian soil fines, prior to impact-melting, had undergone chemical (acid-sulfate) weathering near the martian surface to varying degrees. The acid-sulfate weathering is caused by aqueous fluids dissolving sulfurous gases released in volcanic eruptions during the last few hundred million years on Mars. The acid-sulfate (H_2SO_4) weathering reactions seem to have preferentially dissolved pyroxenes releasing Fe and Mg and Ca and soluble silica from the mineral matrix into these solutions, when compared to feldspars. The dissolved mineral-material is locally mobilized by transgressing solutions depending on the water availabilty and was eventually deposited as evaporation products or amorphous coatings on grain surfaces. Subsequently, these secondary salt and silicate assemblages episodically come into contact with the transgressing aqueous solutions generated as result of favorable climatic and other conditions near mid-latitude and equatorial regions on Mars. These solutions mobilize soluble salts from the reaction sites leaving behind insoluble hydrolysis products. The ferrihydrite, produced by the hydrolysis of iron sulfate, partially reacts with H_2S dissolved in the subsurface aqueous media resulting in sporadic secondary FeS formation. These mixed assemblages of iron sulfates and sulfides were occasionally found in melt pockets in these impact glasses. We present a simple model describing the characteristics of Martian soil fines that gave rise to the impact melt glasses, using a combination of surface processes such as comminution of basaltic rocks followed by aeolian sorting on Mars to generate the soil fines and subsequent acid-sulfate weathering of soil fines under limited aqueous alteration in the Martian regolith. We present here additional features characterizing these precursor Martian soil fines (before impact-melting into glass), deciphered during recent EMPA and FE SEM studies of EET79001 impact glasses.

2. EXPERIMENTAL

EET79001 thin sections were studied using Electron Microprobe (EMPA) and Field Emission SEM (FESEM) instruments at JSC. Several polished thin sections (TS) of EET79001, Lithology A (,77; ,78; ,18; ,20A; and ,506) and one TS of EET79001, Lithology B (,507) were analyzed using a state of the art Cameca SX100 microbeam automated electron microprobe

equipped with standard Cameca instrument controls and PAP reduction software. Standard analytical methods and calibration procedures were used at 15 kV accelerating potential and 20 nA beam current, for determining 12 element oxides for major and some accessory elements. Quantitative chemical analysis was performed on impact melt glass veins in 77; 78; 18; 20A and 506 thin sections (TS) of EET79001, Lith A by raster beam as well as point mode techniques. The data are obtained in the raster mode along line traverses (in 10 x 8 pixel). Also the data are taken along the same line profiles by the point mode technique and the data from both these methods agree with each other within experimental limits. Most of the technical details regarding the SX100 micro-probe use was reported in Rao et al. (1999). Similar experimental procedures were employed in the present study.

Figs. 1a-d show the WDS (wavelength dispersive spectrometer) elemental maps of glass bearing regions in EET79001 for studying the spatial distribution of elements such as Fe, Mg, Al, Ca and S and Si in veins and pods of Lith C.

3. RESULTS AND DISCUSSION

3.1 Elemental abundances in impact-melt glasses in EET79001, Lith A

Several relatively homogenous areas in the glass veins and pods in ,77; ,78; ,18; ,20A; and ,506 thin sections (TS) were micro-probed. The data were sequentially collected along different line-traverses across the veins and pods (as explained in Rao et al., 1999). The data, in turn, were summed up to yield line-average values in each case. For purposes of the present discussion, it is assumed that the silicate components constituting the glass matrix are relatively well-mixed prior to shock-melting at the Martian site where the impact occurred. The glass samples in EET79001 sometimes show signs of incipient melting of the parent mineral components. Small local variations exist in samples from different sites of a thin section. The average composition deduced by summing up the data points along a line traverse is considered to be a close approximation to the true composition of the source materials composing the regolith mix (prior to melting) at the impact site on Mars. For reference normalization, Lith A composition is used because the parent material for different mineral components in EET 79001 glasses veins belongs to Lith A (McSween and Jarosewich, 1983). The justification for using the line-traverse average data in Lith A glasses is provided later in this sub-section. Though we use average values here for discussion, note that we discuss the individual data points for specific samples such as TS,506 and TS,507 in the other sections 4 and 5).

3.1.1. FeO and MgO & Al_2O_3 and CaO vs SiO_2 : The FeO & MgO as well as Al_2O_3 & CaO line average-abundances determined at different locations in the glass veins in TS ,77 ; ,78; ,18; ,20A and ,506 are plotted against SiO_2 in Figs.2a-d. For comparison, Lith A data point is also shown in these figures. Though the data points show significant scatter without plotting along correlation lines, some general features are discernable in these diagrams. The FeO and MgO abundances in Fig.2a & 2b plot generally at lower levels than the host Lith A point. Further, one finds that the FeO and MgO points negatively correlate with SiO_2, i.e. as the SiO_2 content increases from ~48 to 51%, the FeO abundance in the glasses decreases from ~18% to 15% and the MgO abundance also decreases from ~17% to 11%. On the other hand, the data points for Al_2O_3 and CaO plotted against SiO_2 in Fig.2c & 2d yield higher abundances than Lith A. They indicate a positive correlation trend. Here, we notice that as the SiO_2 content increases from ~48 to 51 %, the AlO_3 content correspondingly increases from ~5.5% to 9.5% and the CaO content also increases from ~6.7% to ~9.2% in these glasses. If we choose the maximum

abundance levels observed in these elemental correlation trends, 2c & 2d, we find that Al_2O_3 shows an enrichment up to a max of ~60% and CaO, up to a max of ~20% and Na_2O (figure not shown), up to a max of ~60% with reference to host Lith A. Similarly, if we consider the minimum abundance levels in Figs. 2a & 2b, FeO, MgO and TiO_2 (figure not shown) abundances in these glasses show depletion levels of ~15%, 36% and 30% respectively with reference to Lith A.

3.1.2. FeO & MgO vs SO_3 : We attempted, above, to sketch a simple description of the differential distribution of major elements Fe and Mg (representing pyroxenes) and Al and Ca (representing feldspars) with respect to SiO_2 (representing silicates) in these glasses. Feldspars and pyroxenes are the two major silicate constituents in the basaltic regolith on Mars. On partial dissolution with acidic solutions near the Martian surface, this mineral assemblage yields a variety of secondary salts such as sulfates. In the present study, we focus our attention on the interaction of acid-sulfate solutions with these primary minerals in martian regolith resulting in the production of sulfates. To begin with, we plot FeO & MgO as well as Al_2O_3 & CaO line-average abundances against SO_3 in Figs.3a & 3b and 3c & 3d respectively. Though the sulfate in these glasses is associated with varying amounts of sulfide, all sulfur is considered as sulfate for the purpose of discussion here. In the MgO versus SO_3 plot (Fig.3b), one finds that the dissolution of pyroxenes by acid-sulfate break-down is moderate (or limited) because the deposited SO_3 (sulfate) content in these glasses amounts only to a maximum of ~1.6% (in contrast to ~18% found in the case of EET790001,507 discussed later). But, significant amounts of MgO (as soluble $MgSO_4$) seem to have been mobilized from the grain-surfaces during leaching of constituent soil grains prior to melting on Mars surface. The element concentration profiles in Fig.3b suggest that as more acid-sulfate becomes available for mineral dissolution, more MgO is released from pyroxenes and mobilized by the transgressing solutions. The residual pyroxenes, consequently, yield lower MgO abundance compared to the host-phase, resulting in a negative correlation between SO_3 (proxy for salts) and MgO. (We show later that this depleted pyroxene residue in the regolith is shock- melted by impact and quenched as glass into the meteorite crevices / fractures). Similarly, FeO in pyroxenes (Fig.3a) is also solubilized and mobilized from the pyroxene matrix probably as ferrous iron hydroxysulfate into solution under reducing conditions (which is later discussed under ,506 glass, section 4) because oxidation of ferrous to ferric iron yields insoluble precipitates under the ambient environment resulting in positive correlation. So, in the FeO versus SO_3 plot (Fig.3a), as the SO_3 content increases from ~0.4% to ~1.2%, the FeO content decreases from ~19% to ~15% in these glasses resulting in a negative correlation between these two elements (eg. MgO vs SO_3 system). Therefore, we infer that the mildly acidic solutions permeating through the subsurface martian soil regime under reducing conditions have mobilized and transported the dissolved ferrous hydroxy-sulfate and soluble magnesium sulfate away from the reaction sites leaving behind depleted mineral residues which yield negative correlation profiles. In both cases of FeO and MgO, the trend lines pass through the host Lith A data point in Figs.3a and 3b (the implications of these inferences are again discussed under TS,506 subsection) implying a controlled mineral dissolution and mobilization.

3.1.3. Al_2O_3 & CaO vs SO_3 : As a continuation of the discussion of mineral-dissolution in the martian soils, we plot Al_2O_3 & CaO contents against SO_3 in Figs.3c and 3d to examine the contrasting behavior of feldspars. Although the SO_3 content is found to vary only from 0.4% to ~1.6%, the $Al2O_3$ content shows a significant variation from ~5 to ~10%, resulting in positive correlation between the two elements. Note that most of the data points in the Al_2O_3-SO_3

diagram (Fig.3c) plot above the Lith A data point. The positive correlation trend between $Al2O_3$ and SO_3 suggests that the dissolved and mobilized Al from feldspar dissolution is probably re-precipitated as poorly-crystalline aluminum hydroxysulfate (jurbanite- or basaluminite- type) on the regolith grains under moderately high pH conditions. It appears that the acid-sulfate equivalent of the excess sulfate (i.e. SO_3= 0.4% to 1.6%), responsible for the dissolution and re-precipitation of aluminum on grain surfaces in this case may not be sufficient to account for all the observed increase in Al_2O_3 content (from ~5% to ~10% max) in these glasses. This observation suggests that there may be already some excess plagioclase existing in the soil as enriched mineral component relative to Lith A host. The behavior of CaO is similar to a lesser extent to that of Al_2O_3 in these Lith C glass precursor materials (the glasses in Lith A are referred to as Lith C). The mobilized and re-precipitated CaO from feldspars and pyroxenes shows a positive correlation with SO_3 similar to Al_2O_3, suggesting that the excess CaO is precipitated as insoluble $CaSO_4$ (gypsum) on the soil grains. These results suggest that the Al_2O_3 and CaO excesses are probably due to the plagioclase enrichment in these glasses relative to Lith A.

The rationale behind averaging the line-profile data of these glasses for constructing these plots (Figs. 2a-2d and 3a-3d) is as follows: (a) the veins in these glass pockets in Lith A are physically situated close to each other and sometimes one finds these glasses filling the narrow cracks and faults inter-connecting with one another as shown in the case of Zagami by McCoy et al., (1990). The impact-melt glass veins in Lith A are fairly homogeneous and seem to emanate from glass pockets. (McSween and Jarosewich, 1983; McCoy et al.,1990). (b) Further, McSween and Jarosewich (1983) plotted the modal compositions of several Lith A impact glasses (Lith C) in a ternary diagram, Fig.5 of McSween and Jarosewich (1983), where all the Lith C data points representing the dark brown glasses in Lith A tightly cluster together plotting close to the host Lith A composition. This ternary diagram (Fig.5) clearly shows that all these Lith A glasses are closely related to each other. Further, they note that the shergottite impact glasses appear to have incorporated plagioclase in greater than modal proportions. Hence, the data-averaging procedure employed for the line-profiles here could be meaningfully used to examine the general trends in major element distribution characterizing the parent materials of these glass melts.

3.1.4. Enrichment / Depletion : Considering that all the different glass assemblages studied here in Lith A originate from a common well-mixed source-material reservoir, we attempt to characterize the composition of the parent soil on Mars based on the total data set (maximum to minimum) plotted in Fig.4 as a box-graph. In this figure, the range of measured abundances for a given element oxide (minimum to maximum) is given in rectangular boxes in comparison to the host Lith A (McSween and Jarosewich, 1983) whose composition is also given in the adjoining square boxes. In Fig.4, one finds that SiO_2, Al_2O_3, CaO, Na_2O and K_2O are enriched to a maximum of 6.6%, 74.1%, 31%, 58.5 %and 66% respectively with reference to Lith A (Na_2O and K_2O data not plotted here). As these elements are the major constituents of feldspars, these excesses indicate that there is an enrichment of felsic component in the source materials at this martian site, prior to impact-melting. Similarly, one finds that FeO, MgO ,MnO and TiO_2 are depleted up to a maximum of 16.1%, 35.5% $_2$3.1% and 29.7% respectively with reference to Lith A (TiO_2 and MnO data not plotted here). These elements, in turn, are the major constituents of pyroxenes and their depletions indicate that there is a depletion of mafic mineral component in the source materials prior to impact-melting. Furthermore, these results indicate that the degree of enrichment and depletion in these glasses differ from one sample to another.

The enrichment of felsic component and depletion of mafic component to different degrees in these glasses could be a result of the interplay of several processes including (a) acid-sulfate degradation of Martain soil samples (Banin et al., 1997; Tosca et al., 2003; Morris et al.,2000) or (b) meteoroid comminution of basaltic rocks on Martian surface (Hoerz et al., 1999 ; Hartmann et al., 2001) or (c) lateral transport and sorting involving saltation / deflation of the fine grained materials due to aeolian activity (Greely et al., 1999; McSween and Keil, 2000) . Below, we address these issues briefly.

3.1.5. Hawaian basalts (lab experiments): First, we look into the data obtained for acid-sulfate weathering studies of Hawaian volcanic basalts in the laboratory simulation experiments carried out by Morris et al. (2000). Morris et al. (2000) extensively studied elemental fractionation patterns associated with hydrolytic and sulfuric alteration of the volcanic tephra samples from Mauna Kea. Sulfuric alteration trends are found to be distinctly different from those observed in palagonitic tephra. In the acid-sulfate altered basalt, they found that MgO and MnO are depleted and all other major elements are either essentially un-fractionated or slightly to moderately enriched relative to unaltered basalt tephra. However, sulfur, present as sulfate, is highly enriched. Morris et al. suggest that this behavior is a result of the relatively high solubility of Mg and Mn sulfates and the precipitation of Na and K, along with ferric iron, as insoluble jarosite. The fractionation trends observed in palogenitic tephra are found to be inconsistent with what is observed in the impact-melt glass samples in this study. Note that we do not find the occurrence of K-rich jarosite in our glass samples which is consistent with low K abundance near Mars surface. In contrast to the findings of Morris et al., in the analyzed glass samples of Lith A (and Lith B as shown later), we find varying degrees of feldspathic enrichment and mafic depletion with respect to host Lith A. These findings suggest that, in addition to the sulfatetic alteration-processing of regolith fines on Mars, there are other processes operating on these martian soil materials to produce varying degrees of enrichment and depletion of feldspathic and mafic components in the mineral residues. To further constrain these possibilities, below we look into the details of a physical process involving differential comminution of basalts by meteoroid bombardment on the surface of Mars (similar to that on Moon) as described by Hartmann et al. (2001), Hoerz et al. (1999) and Papike et al. (1981).

3.1.6. Mineral- specific comminution : Impact-induced comminution of bed rock materials by meteoroids constantly occurs on planetary surfaces, resulting in the in-situ generation of fragmental products having a range of grain sizes (Hoerz and Cintala,1997 ; Hoerz et al., 1999; Hartmann et al. 2001). Repetitive impacts commonly occur over long periods of time and the unconsolidated materials undergo increased fracturing and shock-processing with time. During detailed chemical and petrologic characterization of various grain-size fractions of lunar soil fines, Papike et al. (1981) and McKay and Basu (1979) found that the fine-size (<10 um) fraction of lunar soils is indeed severely fractionated with respect to the parental material, indicating that their bulk chemistry is generally consistent with mineral specific comminution. McKay and Basu (1979) further showed that the <10 um fractions of both highland and mare soils from Apollo 15 are enriched in feldspars relative to pyroxenes. In order to quantify this comminution model, Horz and Cintala (1997) carried out lab simulation experiments, subjecting a coarse-grained gabbro target rock to differential comminution by impacting the fragmental gabbro several hundred times with stainless steel projectiles having impact velocities of ~1.4 km/sec. Subsequently, they isolated and petrographically- examined the individual grain size fractions from the multiple impact- comminuted target rock assemblages and showed that plagioclase comminutes more efficiently than pyroxenes and the finest grain-size fraction (<10

um) indeed is most severely affected by differential comminution. Bulk chemical analysis of the grain size fractions by Horz et al. revealed that, in the fine grain size fractions, Al_2O_3, CaO and Na_2O are enriched and FeO and MgO are depleted with respect to the host rock.

3.1.7. Comparison : Below, we attempt to draw a limited comparison of the results obtained in the present study on EET79001 impact-melt glasses, produced as a result of melting of the source regolith materials which are generated by meteoroid comminution accompanied by aeolian sorting on Mars, with the complementary results obtained in the case of lunar samples by Papike et al. (1981) and in the lab simulation experiments by Hoerz and Cintala, (1997). In a histogram (Fig.5), we present the data (in percentage units) corresponding to the enrichment of feldspathic component and the depletion of mafic component, observed in the impact glasses studied here. For comparison, in the same figure, we also plot the enrichment and depletion factors as percentages obtained for feldspathic and mafic components by Hoerz and Cintala, (1997) during lab simulation experiments. In the case of EET79001, LithA impact glasses, SiO2 is enriched upto ~6 % (max) whereas in the case of simulation experiments (Horz and Cintala, 1997), the SiO_2 enrichment is only between ~1-2 %. In the case of Al_2O_3 and CaO in these glasses, the enrichment is up to 74% and 30% (max) respectively, whereas in simulation experiments they are only up to ~20% and 7% respectively. In contrast, the depletion of FeO and MgO in the glass samples is ~16 % and 35% (max) respectively whereas, in the simulation experiments, they are up to 35% (65% in some cases) and 40% respectively. Note that FeO shows large variations in the case of lab simulation experiments. Though the overall pattern of the mineral-specific comminution trends are similar in the case of shergottite impact glasses studied here and simulation experiments of Horz and Cintala (1997) as well as lunar soils studied by Papike et al. (1981), the magnitude of these variations differ from one sample to another. These differences may partly be attributed to the fact that the Martian soil samples are subjected to both comminution and aeolian sorting whereas lunar soil samples (and lab simulation studies by Horz and Cintala, 1997) involve only comminution but no aeolian sorting. Some of these variations may be due to the incorporation of varying amounts of fine-grained material in a given soil sample that shock-melted to produce these impact glasses. Furthemore, these variations may additionally be influenced by other processes such as chemical weathering on Mars which is discussed below.

3.2 Volcanic gases and acid-sulfate weathering of soils on Earth and Mars:

3.2.1. Sulfurous gases from volcanoes and their oxidation characteristics :

Volcanic gas emissions and their interactions with water in the atmosphere on Earth and Mars relevant to the present study are briefly addressed here. On Earth, detailed analysis of high-temperature volcanic gas samples from convergent- and divergent-plate and hot-spot volcanoes indicate that H_2O, CO_2 and SO_2 are the dominant species in the volcanic gas emanations, although H_2S is considered significant only in gases in equilibrium with some convergent plate magmas at depth. Otherwise, H_2S is considered as minor species. The H_2S contribution to SO_2, in most of the cases, varies from ~0.1 to 1%. But, in some fumaroles, higher concentrations of H_2S are found (Symonds et al., 1995). If the composition of volcanic

gases from Earth and Mars are considered to be similar, SO_2 seems to dominate over H_2S in sulfurous gases from Martian volcanoes.

On Earth, SO_2 and H_2S, released into the atmosphere by volcanoes, eventually get oxidized to sulfuric acid depending on O_2 and H_2O availability in the atmosphere and the crust. The oxidation state of sulfur in SO_2 is 4^+. The released SO_2 is converted rapidly to H_2SO_4 by the reactions: SO (O_2, HO_2) → SO_2 (O) → SO_3 (H_2O) → H_2SO_4 (Stumm and Morgan, 1996). In contrast, the oxidation state of sulfur in H_2S is 2^-. Consequently, the oxidation of H_2S to H_2SO_4 involves additional reaction- steps compared to SO_2, because H_2S is first oxidized to SO_2 and the resulting SO_2 is then oxidized to H_2SO_4. The reactions leading to H_2S oxidation to SO_2 involves: H_2S (hv) → HS^- (O_3, NO_2) → HSO (O,NO) → SO (O_2) → SO2 (Stumm and Morgan, 1996). The SO_2, thus produced, is in turn oxidized to H_2SO_4 by the reactions mentioned above. Note that water activity is an important requirement as the OH^- radical initiates the conversion of H_2S to SO_2 in the regolith (as UV does in the atmosphere). The availability of O_2 in the atmosphere and the temperatures in the near surface environment of Mars determines the rates of these reactions. As the abundance of O_2 in Mars atmosphere is low, i.e. 0.13% and the partial pressure of O_2 in Mars atmosphere is10^{-4} is much less compared to Earth, the oxidative reactions on Mars may be very sluggish (Burns, 1993).

Though H_2S is a minor species in volcanic emissions, it may be of importance in producing secondary sulfides (such as FeS) in subsurface aqueous interactions on Mars. When H_2S dissolves in aqueous acidic solutions, the hydrolysis reaction starts producing HS^- radical initially. At low pH values of 3 to 5, the HS^- concentrations in these solutions are usually low (Stumm and Morgan, 1996). In addition to the restricted O_2 availability in the sub-surface environment on Mars, the ambient temperatures are also extremely low (<60°C) which make the oxidation of HS- to SO very slow. Though small amounts of dissolved oxygen is available for initiating chemical reactions under subsurface conditions, the oxidation rates by these reactions is about a million- times slower compared to Earth (Burns,1993). This type of sub-surface environment may, in fact, be conducive for bacterial survival /growth, where reducing conditions are maintained by partially arresting the oxidation of H_2S. Furthermore, it is likely that part of the H_2S emanated from volcanoes on Mars escapes surface / atmospheric oxidation and dissolve into the acid-sulfate droplets attached to the aerosol particles. It is known that significant amounts of H_2S could dissolve into strong sulfuric acid solutions and remain in molecular form (Carroll and Mather, 1989). The dissolved H_2S in acid solutions undergoes chemical reactions mentioned above and the total reactive H_2S corresponds to the sum of the mole fractions of H_2S, HS^- and S^{2-} molecular species (Stumm and Morgan, 1996). Total H_2S concentration may increase under near-neutral state and such conditions may exist in pore waters in the Martian regolith.

When O2 availability increases, elemental sulfur may also form by the oxidation of H_2S in solutions. Elemental sulfur is commonly found in sulfur-rich, near surface hydrothermal solutions and H_2S-rich spring waters in terrestrial settings. Under anoxic conditions such as the early atmosphere on Earth, the H2S emitted by volcanoes is oxidized to elemental sulfur via reactions H_2S (hv, OH) → HS- and HS^- (HS) → S_2 [Kasting, 2001}. It is likely that such reactions producing elemental sulfur could have occurred in the near-surface environment on Mars.

3.2.2. Acid-sulfate mineral dissolution in soils on Earth and Mars :

The major rock-type near the martian surface is extrusive basalts which contain mainly ferro-magnesian silicates (pyroxenes and olivines), plagioclase feldspar and some accessory oxides. Detailed petrographic studies on SNC meteorites (McSween and Trieman, 1999; McSween, 2002) suggest that the constituent mineral assemblages in these rocks might have undergone chemical weathering and aqueous alteration near the martian surface. Among the constituent minerals, the Fe-Mg silicates are highly vulnerable to chemical weathering reactions while feldspars are relatively less susceptible to acid-sulfate degradation (Burns, 1993).

Among different models proposed for explaining the prominent characteristics of Martian soil, 'the acid-fog model' is one of them (Banin et al., 1997; Settle, 1979; and Clark, 1993). It addresses questions related to chemical weathering of mineral constituents by acid-sulfate solutions on Mars. Hence, we focus our attention on this model as our experimental results may have direct bearing on its implications. The Viking and Pathfinder data yield high concentrations of sulfur (~8% SO_3 equivalent) for Martian soil and suggest that most of the sulfur in salt-rich evaporites is probably present as sulfate as a result of high redox potential of the soil (Banin et al., 1997; Clark et al.,1982; Rieder et al., 1998). The sulfate in the soil is considered to originate mainly from SO_2 released by volcanoes on Mars, which later oxidized to H_2SO_4 in martian atmosphere and regolith (Settle,1979; Clark and Baird,1979; Clark and Van Hart,1981) and settle back on the surface.

In the present study, we restrict our discussion to chemical weathering reactions involving dissolution of pyroxenes and feldspars by acid-sulfate solutions and to the study of release, mobilization and precipitation of the soluble and insoluble salt products by the transgressing solutions at the reactor- sites near the Martian surface. During congruent dissolution of ferromagnesian silicates, structural elements such as Fe^{2+} Mg^{2+} Ca^{2+} and silica are released into solution at rates that are proportional to their concentrations in the host minerals. This usually happens when the acid concentrations are relatively high (Burns,1993; Tosca et al., 2003). When the acid concentrations are low, the dissolution proceeds incongruently. During incongruent dissolution in pyroxenes, the cations from the higher Madelung energy M2 sites are preferentially released into the solution compared to those occupying the lower energy M1 sites (the higher the Madelung energy, the weaker the bond, which makes it easier to dislodge the atom from a given site in the mineral matrix). However, during long-term chemical weathering on Mars, the release of Fe^{2+} Mg^{2+} Ca^{2+} etc from the silicate mineral assembly eventually becomes stoichiometric in a closed system (Burns,1993; Burns and Fisher, 1993). However, in an open system, the leaching efficiencies of the mobilizing solutions determine the relative distribution of the reactive elements in the weathered mineral matrix. Among the major cations released into solution during chemical weathering of pyroxenes, ferrous iron goes to a higher oxidation state when the pH of the oxygenated ground waters exceeds ~3.5 (Nordstrom and Alpers, 1999). In acidic solutions below pH ~4.5, the oxidation of $Fe2^{+}$ to Fe^{3+} is independent of pH and is slow because of low temperatures on Mars.

3.2.3. Secondary mineral deposition :

Precipitation of secondary minerals from these solutions depends on several factors such as the saturation state of the altered mineral, pH of the solutions, and the structure of both the precipitating mineral and the depositing surface, among other parameters (Tosca et al., 2003; Brantly and Chen, 1995). As mentioned above, the dissolution of ferromagnesian silicates

liberate appreciable amounts of ferrous iron, magnesium and calcium and silica into aqueous solutions. In the case of iron, most of the ferrous species released into solutions during acid-sulfate weathering on Earth get oxidized to the ferric state and precipitate as hydroxides. However, it is not known how much of the liberated divalent iron remains un-oxidized in the near-surface and sub-surface environment on Mars, which is controlled by the net oxygen availability. When the acid-sulfate solutions become saturated with respect to ferric hydroxide/ ferrihydrite under excess sulfate on Earth, amorphous schwertmannite-type compounds precipitate at pH values above ~4. This mineral material could be poorly-crystalline sulfate-substituted ferric hydroxide on Mars. According to Bigham et al. (1996), schwertmannite forms in acid-sulfate waters on Earth at a pH range of ~3-5 and ferrihydrite in pH range of ~5-7. Ferrihydrite is converted to relatively stable hematite, if the pH is maintained between 5 and 9, but below pH ~5, it dissolves and re-precipitates as fine grained goethite. From this discussion, it appears that it is not one single iron mineral that precipitates from these solutions on Mars but a mixture of different iron mineral phases may be precipitating under low water/rock ratios.

In contrast, plagioclase feldspars present in basaltic rocks undergo limited dissolution in acid-sulfate waters releasing Ca^{+2}, Na^{+} and Al^{+3} and silica into strongly acid solutions. It appears that hydroxysulfate of Al precipitates over the pH range 4-5 (Bigham and Nordstrom, 2000). It may be noted that part of the aluminum sulfate is leached and the remainder is deposited on grains depending on the pH conditions. Aluminum may precipitate as colloids in these solutions, separate from the Fe precipitates and there is little evidence for mutual substitution of Fe in the Al hydroxysulfates and vice versa. These amorphous $Al(OH)_3$-silica assemblages precipitate under less acidic conditions. When evaporation overtakes, $CaSO_4$ precipitates from these solutions. In anoxic environments, such assemblages of amorphous and dissolved species may form clay silicate minerals near the Martian surface.

3.2.4. Buffer controls and solution-acidity near Mars surface:

Though the mineralogical make-up of the Martian soil is poorly defined, it is believed that the martian soil may contain a variety of clay-silicates such as smectites, palogonites and evaporite-salts such as gypsum etc (Gooding, 1992; Gooding and Keil, 1978; Warren, 1998). Soils, in general, have the capacity to neutralize the transgressing acidic solutions. It depends on the amount of exchangeable bases and the content of carbonates available for chemical reactions. A soil containing appreciable amounts of smectite clay (which can accommodate significant base-contents) can deactivate most of the acidity so that the pH does not drop significantly below ~4. Some sediments from arid temperate regions on Earth are associated with $CaCO_3$, which, in turn, can neutralize large amounts of soil acidity. When the H_2SO_4 concentration is sufficiently high during initial stages of soil weathering, aluminum silicates (feldspars and smectites) rapidly weather to Al-bearing minerals and amorphous silica. Note that most of the acidity produced during H_2SO_4 interactions with the medium is inactivated by the reaction converting saponite to nontronite clays. In principle, all alkalis, Ca and Mg in silicates and carbonates present in the medium are capable of counteracting the decrease in pH under these conditions. Acid-sulfate reactions can release cations such as Mg & Al and silica from silicate mineral lattice under pH <4 and various clay minerals tend to buffer the pH of the solutions at ~4. The mineral assemblages of hydroxysulfates of Fe and Al as well as the oxides and hydroxides of Fe, amorphous silica as well as gypsum, all help in buffering the solutions in maintaining pH ~ 4 under favorable water/rock ratios.

Carbonates are of particular interest because of their potential role in neutralizing acidity in the aqueous solutions. Calcium carbonate can be rapidly dissolved by H_2SO_4 and any excess sulfuric acid remaining after $CaCO_3$ dissolution starts reacting with clay minerals and other silicates (Van Breeman, 1982; Carson et al.,1982). Note that Ca and Mg carbonates, some times in association with gypsum, are found in glasses from EET79901 (Gooding and Meunow, 1986 ; Gooding an Wentworth, 1991) and Shergotty (Wentworth et al.,2003). Several Ca, Mg and Fe-bearing carbonate assemblages are also detected in other SNCs such as nakhlites by Bridges et al. (2001). The occurrence of these carbonates in Martian soil could partially help in maintaining the near- surface solution-acidity around pH ~4. As in the case of Earth, this process on Mars may involve several steps, related to saturation of the medium with bases from gypsum and those released during silicate weathering or bases brought in by lateral leaching or capillary rise from evapo-transpiration (Carson et al., 1982).

Chemical processes occurring in these solutions depend on the saturation / under-saturation, pH, as well as oxidizing / reducing conditions prevailing in the ambient environment on Mars. On Earth, under weak reducing conditions, Fe^{+3} is reduced to Fe^{+2} but not sulfate. Under strong reducing conditions, sulfate sulfur could also be reduced to sulfide as well as Fe^{+3} also reduced to Fe^{+2}. Iron sulfide may form under these conditions. The occurrence of the later, however, seems to probably require the presence of sulfur reducing bacteria such as *Desulfovibro desulfuricans* observed on Earth (Carson et al.1982).

3.3. MAJOR- ELEMENT CORREIATIONS IN GLASSES FROM EET79001, 506 (Lithology A)

In this section, we present the data for individual points (instead of line- averages as before) in impact melt glass veins from EET79001,506 (belonging to Lithology A) to examine the major element distribution among the glass constituents. The glass sample ,506 is an aliquot of a bigger glass inclusion (,8) which was mass-spectrometrically analyzed by Garrison and Bogard (1998) in which they found large concentrations of Martian atmospheric noble gases along with a $^{129}Xe/^{132}Xe$ ratio of 2.5.

Minerals weather and degrade by interaction / digestion with sulfuric acid on Mars and new minerals form from dissolution products under favorable conditions. The dissolved species resulting from acid-sulfate weathering are mobilized from the reaction sites by mass flow or diffusion processes involving leaching or capillary flow. This process may be enhanced by evapo-transportation before they are precipitated in response to pH or concentration gradients in transgressing solutions (Carson et al. 1982). To decipher these complex geochemical relationships transpiring between salts and silicates of major elements in the glass precursor source materials from Martian soils, we study the abundances of FeO and MgO (representing pyroxenes) and the Al_2O_3 and CaO (representing feldspars) in glass sample ,506 of EET79001 (Lith A) plotted against SiO_2 (representing silicates) and SO_3 (representing salts) in Figs.6a -6e.

3.3.1. Pyroxene dissolution : In Figs.6a & 6b, we plot the MgO and FeO abundances against SO_3 determined at different locations in impact melt glass veins in sample EET79001,506 respectively. When SO_3 content increases in Fig.6, MgO content decreases resulting in a negative correlation ($R2 = 0.65$). This indicates that as more acid-sulfate becomes available for pyroxene dissolution, more Mg is dislodged from the M2 sites in pyroxenes, which

is subsequently mobilized by the transgressing solutions to other locations on Mars. The leached mineral residues yield correspondingly lower Mg contents compared to the Lith A host. As magnesium sulfate is highly soluble, it is easily dissolved and mobilized by the transgressing solutions from the reaction sites in the ,506 martian soil precursor materials under limited water/rock ratios. Furthermore, the MgO data trend in Fig.5a suggests that the pyroxenes in precursor soil fines on Mars might have undergone limited dissolution, because the tie-line connecting the mineral residues passes through the Lith A- MgO point as one end-member. From this diagram, one can deduce the MgO abundance in the soil-free rock-fragment component at the EET79001, 506 site by extrapolating the correlation line back to the 0.4% sulfur level, which turns out to be ~17% , similar to that in Lith A.

The FeO-SO_3 pair in Fig. 5b shows also a negative correlation (R2 = 0.32) indicating that FeO behaves similar to MgO in this system. It is known that the removal of Fe from the M2 sites in pyroxenes is somewhat less efficient compared to Mg (i.e. Mg^{+2} is more easily dislodged than Fe^{+2}). As in the case of MgO, an increase in the SO_3 content in the soil-reactor system will lead to an increase in the Fe^{+2} removal from the regolith mineral mix, leading to a decrease in the FeO content of the resultant mineral residue in the un-reacted soil sample. The FeO-SO_3 slope is thus less steep compared to MgO-SO_3 because the release rate of FeO is somewhat less pronounced compared to MgO for the ferromagnesian minerals. This observation indicates that ferrous sulfate which is as soluble as magnesium sulfate is similarly dissolved and mobilized from the soil matrix on Mars surface. This, further, suggests that the Fe^{+2} leached from pyroxenes did not get oxidized to Fe^{3+} and did not precipitate as insoluble ferric sulfate salt at this regolith site on Mars. Based on these results, we infer that the transgressing acidic solutions were operating under reducing environment (which effectively arrested Fe^{+2} oxidation) in the precursor soil fines at the ,506 sampling-site near the martian sub-surface.

As in the case of MgO (Fig.6a), the FeO-SO3 correlation line passes through the data point representing Lith A- FeO point as one end member indicating a limited acid-sulfate digestion of soil fines. As mentioned above, one can deduce the FeO abundance of the soil-free rock fragment component at the EET79001,506 site by extrapolating the correlation line back to 0.4% SO_3 level, which turns out to be similar to that in Lith A (~18% FeO). In other words, the MgO and FeO values, thus deduced for the end member compositions, characterize the soil-free rock- component associated with the regolith material at this EET79001,506 site on Mars. From these results, one infers that the grain sizes in the precursor soil fines for ,506 glass is not very fine–grained. Instead, it is relatively coarse-grained because the starting (end-member) material composition does not reflect the concurrent depletions of FeO and MgO abundances characteristic of the fine-grained fractions, generated as a result of repetitive meteoroid comminution of basalts on Mars / Moon (Hoerz and Cintala, 1997: Horz et al., 1999; Papike et al. ,1981; McKay and Basu, 1979; Hartmann et al., 2001).

3.3.2. Feldspar dissolution : To further examine the mineral dissolution trends in martian soils, we plot below Al_2O_3 & CaO versus SO_3 in Figs. 6b and 6a for ,506 glasses. Al_2O3 vs. SO_3 and CaO vs SO_3 yield positive correlations (in contrast to FeO and MgO) with a regression coefficient R2 = 0.45 and 0.42 respectively. The Al_2O_3 vs SO_3 and CaO vs SO_3 correlation lines pass through the LithA- Al_2O_3 and Lith A- CaO data points indicating them as possible end member compositions. These profiles further indicate a limited acid-sulfate digestion, followed by a closed system deposition of the insoluble precipitate at the reaction sites. The precipitation of the hydroxyl-sulfates of Al and Ca usually takes place at higher pH

values (>5). As pointed above, this deposition likely occurrs under reducing environment on Mars. Because the end-member compositions, thus deduced for Al_2O_3 and CaO in the constituent materials of ,506 glass do not show any plagioclase enhancements with respect to Lith A, we infer that the starting materials in this case are dominated by the coarse-grained soil fractions, which do not display any mineral-specific comminution effects as discussed above. These results deduce for Al_2O_3 and CaO here are consistent with the inferences drawn from FeO and MgO earlier.

The Al_2O_3 vs SiO_2 and CaO vs SiO_2 tie lines (Figs. 6c & 6d) show a flat or horizontal distribution of the data points. This suggests that the acid-sulfate digestion of these regolith fines is relatively moderate and limited, because, though the SiO_2 in the silicate residue varies from 48% to 52 %, the corresponding variations in CaO and Al_2O_3 of the mineral residues are not appreciable. Further, the distribution of the SiO_2 data points indicates that the dissolved silicic acid from the mobilizing solutions had partially precipitated as amorphous silica over the etched grain residues under relatively high pH conditions. This inference is consistent with the observed enhancement of SiO_2 abundance over the Lith A starting materials as shown in Figs. 6d and 6c. Regarding the correlations between SiO_2 and Al_2O_3 & CaO in the case of ,506 glasses (Figs. 6c & 6d), the role of feldspars is limited because Banin et al. (1997) point out that only less than 1% of the total Si content goes into solution during acid-sulfate dissolution of feldspars. Part of the excess SiO_2 observed in Figs. 6c & 6d seems to have resulted from the silicic acid produced by the dissolution of pyroxenes, which subsequently precipitated as amorphous silica as noted above.

As mentioned above, the transgressing aqueous solutions are sufficiently acidic and reducing in nature. Solution pH is the major acid solution variable controlling the dissolution of feldspars. Non-stoichiometric dissolution of feldspars releases alkalies and Ca^{2+} initially while alumino-silicate structures are subsequently hydrolysed and destroyed at a much slower rate because more energy is needed for breaking the Si-O bonds compared to Al-O bonds. Such chemical dissolution of feldspars during weathering results in the formation of leached, cation-depleted layers at grain surfaces (Nesbitt and Muir, 1988). These layers are enriched in residual structural silica and aluminum. In addition, the pH of pore waters in these layers may be substantially higher than that in bulk fluids, which is conducive to the precipitation of secondary salts under weakly acidic conditions (Casey and Bunker, 1990).

Under favorable aqueous (pH ~5) conditions, the released Ca and Al by acidolytic weathering from feldspars may precipitate Ca as $CaSO_4$ (gypsum) and Al as aluminium hydroxysulfate [jurbanite, $Al(OH)SO_4$, $5H_2O$ or basaluminite, $Al_4(OH)10(SO_4)$, $5H_2O$] or amorphous hydroxide (gibbsite)] or sometimes as fine-grained aluminosilicates, on grain surfaces. The partitioning of the dissolved Al and Ca and other cations among the secondary minerals formed, depends on the relative solubility of their sulfate salts. $MgSO_4$ has the highest solubility, followed by ferrous sulfate. Alunogen or basaluminite comes next , whose solubility, in turn, is greater than that of gypsum $CaSO_4$ (Banin et al., 1997; Lindsay, 1979). Based on the simulation experiments of acid-sulfate weathering of plagioclase-rich volcanic tephra from Mauna Kea, Banin et al. (1997) noted that the sulfate among secondary salts preferentially partitioned into gypsum and alunogen (note that their samples did not contain Fe and Mg). Even at high acidities, the Si released from feldspars into solution is only a few percent according to Banin et al. Moreover, there is considerable evidence for the development of Al and cation-depleted Si-rich layers on feldspar surfaces after dissolution in acid region at pH <5 (Bentley,

1995). The correlation trends observed in the case of ,506 study for Al_2O_3 and CaO with SO_3 are consistent with the results obtained in the simulation experiments by Banin et al. (1997). In this context, it may be noted that Gooding and Muenow (1986) and Gooding et al. (1988) found laths and needles of $CaSO_4$ and sulfur-rich aluminosilicate mineraloids imbedded / trapped in a impact-melt EET79001, Lith C glass samples ,234 and ,180. Gooding and Muenow (1986) further observed that aluminosilicate phases were disseminated throughout the glass veins as <10 um size grains. Some of them yielded high sulfur concentrations which were shown to be consistent with the occurrence of oxidized sulfur as sulfate in Lith C during their pyrolysis experiments. In one Lith C sample ,234, sulfate crystals were identified as gypsum or anhydrite of extra-terrestrial origin (Gooding and Muenow,1986). Further, they showed that the SO_2 trapped in these glasses is consistent with the assimilation of sulfate during Lith C melting. These findings by Gooding and Muenow are consistent with the occurrence of secondary mineral salts yielding $Al_2O_3 - SO_3$ and $CaO - SO_3$ positive correlations shown in Figs. 5b and 5a for EET79001,506 glasses.

3.3.3. Silicate-salt mixing : To examine the salt-silicate mixing relations in the Martian soils, we plot SO_3 against SiO_2 in Figs. 6e and 7e for glass samples EET79001,506 and EET79001,507 (presented in the following section) and study them together. First, we discuss the case of ,507 glass samples. A negative correlation between SO_3 and SiO_2, which clearly shows up in ,507 glass study (Fig.7e), indicates that as the SO_3 increases, SiO_2 decreases and vice versa. This suggests that the more the sulfate (SO_3) is deposited on the grains, the less is the un-dissolved silicate (SiO_2) residue remaining in a given grain assemblage. Further, the SO_3-SiO_2 relationship is controlled by another parameter i.e. the leached silicic acid (SiO_2), during acid-sulfate digestion of mineral silicates. Being relatively soluble (pH dependant), silicic acid is mobilized and removed from the reaction sites by the transgressing solutions. The decomposing SO_4 ions complex with cations such as Fe^{2+} , Mg^{2+} and Al^{3+} released into the aqueous medium and deposit by precipitation or evaporation as sulfate salts depending on the water/rock ratios. Solution conditions, such as pH <4 and saturation state, control the deposition rate. As more soluble silica is removed, more insoluble sulfate is deposited in the system apparently leading to a negative correlation between the two element oxides.

On the other hand, one finds a zero correlation (or random distribution) of data points between SO_3 and SiO_2 in the case of ,506 glass samples suggesting that sulfate deposition and silicate removal / mobilization are locally decoupled in this case. This relation could result if the feldspar dissolution products dominate over those from pyroxene dissolution in the weathered grain assemblage. At elevated pH and low oxygen availability (or reducing conditions), the soluble ferrous and magnesium sulfates produced in congruent pyroxene dissolution could be efficiently removed from the mineral reactor system by the transgressing solutions. Insoluble amorphous silica, aluminum hydroxides / hydroxysulfates and gypsum ($CaSO_4$) are left behind as poorly- crystalline precipitates at low water-rock ratios. Hence, the sulfate salts and amorphous silica, arising from unrelated sources, seem to deposit randomly on grain surfaces, leading to a scatter distribution of data points as shown in the SO_3-SiO_2 plot for EET79001,506 glass samples (Fig. 6e).

3.4. MAJOR-ELEMENT CORRELATION TRENDS IN EET79001, 507 (Lith B)

In this section, we present the individual data points (not line-profile averages) of elemental abundances determined along line-traverses in impact melt glass veins and pods in EET79001, 507 glass sample (belonging to Lith B),. This impact-melt glass sample, 507 is an aliquot of a bigger glass inclusion,104, where Garrison and Bogard (1998) found large concentrations of Martian atmospheric noble gases and also a $^{129}Xe/^{132}Xe$ ratio of 2.4. The strontium isotopic studies on this inclusion by Wooden et al. (1982) yielded a $^{87}Sr/^{86}Sr$ ratio which is very different from the ratio of the bulk Lith B host .

3.4.1. Pyroxene dissolution: In Fig. 7a, we plot the FeO and MgO abundances determined in 507 glass veins against SO_3. The SO_3 abundance in these glasses includes contribution from sulfide in varying proportions. Hence, it is labelled as "SO_3". At some measuring points in these glasses, we found SO_3 contents a high as ~21%, which are much higher than the SO_3 content found in Viking and Pathfinder soils (Clark et al., 1982; Rieder et al., 1997). In the FeO vs SO_3 plot (Fig.7a), the SO_3 abundance varies from 0.6% to ~18% and the FeO abundance varies from ~7% to ~25%, showing excellent positive correlation with one another over a wide range. The regression coefficient for this correlation is $r^2 = 0.8$. By extrapolating the correlation trend-line back to $SO_3 = 0.6\%$ (corresponding to the sulfur content in Lith B bulk), we deduce the FeO content in the soil-free rock-fragment component (prior to shock-melting of the grain- assemblage in the precursor martian soil) to be ~10%. As the average FeO content of the bulk Lith B is ~18%, this finding indicates that the FeO content in the glass-precursor martian soil fines in ,507 is depleted by ~56%, when compared to Lith B host. Incidentally, this result suggests that the soil fines prior to shock-melting at Lith B site contains a mineral mixture different from that found at ,506 site (in Lith A), discussed earlier. In the ,507 regolith mix, there seems to be a preponderance of fine-grained Lith B material generated by meteoroid comminution that resulted in significant depletion of the mafic component. At the Lith B site on Mars, this soil mix, dominated by this material, subsequently underwent extensive acid-sulfate weathering. The material thus processed later was shock-melted and got incorporated as glass into ,507 sample. In contrast, the soil material at EET79001,506 (Lith A) site contains a preponderance of coarse-grained Lith A processed material, that did not register features characteristic of enrichment / depletion of components due to mineral-specific meteoroid-comminution on Mars, though that material also underwent limited acid-sulfate weathering on Mars.

Further, we notice in this plot (Fig.7a) that as the SO_3 content increases from 0.6% to 18 %, the FeO content correspondingly increases from 10% (a value much lower than average Lith B- FeO content) to 22% (a value much higher than the bulk Lith B- FeO content). The positive correlation between the oxides of these two elements is consistent with the supposition that the Lith B soil fines might have undergone extensive closed-system acid-sulfate weathering. Consequently, these solutions became enriched in dissolved iron concentrations which finally lead to iron sulfate precipitation, probably as poorly-crystalline ferric hydroxysulfate such as copiapite- or schwertmannite- type. Some goethite might also have co-precipitated. This deposition seems to have occurred from acid solutions under highly oxidizing conditions. The oxidizing nature is evident from the fact that Fe^{2+}, which is released during pyroxene dissolution into solution is converted, making use of dissolved oxygen, to Fe^{3+}, which then precipitated as ferric hydroxysulfate. Hence, sulfate shows a positive correlation with iron over a wide range of

concentrations. Alternatively, this correlation could also be generated if the Fe^{2+} remained un-oxidized in solution and the dissolved Fe^{2+} and SO_3 deposited as ferrous sulfate salt (instead of ferric sulfate) on evaporation under dry martian conditions. However, this is unlikely because Mg, which is also in dissolved state in these solutions along with iron, will crystallize as $MgSO_4$ along with $FeSO_4$ on evaporation to dryness. Hence, MgO and SO_3 are expected to show a positive correlation similarly in this sample. In fact, they do not show such relation. Instead, they yield a flat (or horizontal) correlation between MgO and SO_3, i.e. as SO_3 varies from 0.6 to 18 %, MgO does not change significantly. This is because $MgSO_4$ being highly soluble is efficiently leached out of the grain assemblage by the transgressing aqueous solutions leaving behind only the un-dissolved Mg in the leached pyroxene residue. Further, if Fe was also present in divalent state as Mg, the $FeSO_4$ being also very soluble could have also been easily leached away from the system, which in turn should have resulted in a flat correlation. In fact, Fe did not get mobilized in divalent state. Instead, Fe was oxidized to trivalent state and precipitated as ferric hydroxysulfate when the pH of the solutions reached higher pH levels (pH > 4). These results clearly show that iron precipitated as ferric sulfate indicating the preponderence of oxidizing near-surface environment at the EET79001, Lith B sampling site on Mars.

Furthermore, in Fig.7a, we plot the MgO data for ,507 against SO_3. These two elements show a flat (or horizontal) correlation between them in contrast to the dominant positive correlation observed between MgO and SO_3 in the martian soils at the Viking and Pathfinder sites (Clark, 1993) as discussed in the next section. This discrepancy in Mg behavior between EET79001,507 glasses and Viking / Pathfinder soils seems to result because of the following reason. In the case of sample ,507, magnesium which is deposited as poorly-crystalline $MgSO_4$ due to acid-sulfate weathering under low water/rock ratios is easily dissolved by the transgressing solutions and transported away from the reaction sites. Further, the material transported by the transgressing solutions might have flowed down the hydraulic gradient on the martian regolith i.e. from volcanic highs (such as Tharisis, Elysium or Olympus Mons) to valley plains (such as Ares, Utopia or Chryse Planum) where the magnesium sulfate bearing solutions yield poorly-crystalline $MgSO_4$ on evaporation (Warren,1998). Though the SO_3 content varies from 0.6% to 21%, the MgO content varies little around ~2% in Fig.7a. Note that this Mg content refers to the MgO content of the leached mineral residue in the grain assemblage. When we extrapolate this trend- line to SO_3 = 0.6% i.e. soil-free rock-fragment component, we obtain a MgO content of ~2% for the glass precursor soil fines at the Lith B sampling site on Mars. As discussed in the following section, a similar value is also found for the MgO content for the soil free rock at the Pathfinder site (Rieder et al., 1997; McSween and Keil, 2000).

In Fig.7c, we plot the FeO and MgO abundances against SiO_2 in the ,507 glass veins. We find a negative correlation between FeO and SiO_2, i.e. as the SiO_2 content decreases from 51% to 40%, the FeO content increases from 10% to 23% linearly. As mentioned above in the FeO – SO_3 discussion, the lower value of ~10% FeO (corresponding to ~ 51% SiO_2) indicates that the regolith material at the Lith B site contains silicates significantly depleted in mafic component. Moreover, during the acid-sulfate dissolution of pyroxenes, iron and silicic acid are both released into transgressing solutions congruently if the pH of the solution is low. Silicic acid dissolves rapidly into solutions with pH < 4 and is mobilized from the reaction sites efficiently. In solutions at pH < 4, amorphous silica does not precipitate on grain surfaces. However, in Fig.7c, we notice an increase in FeO abundance with a corresponding decrease in SiO_2 content in glass veins. This suggests that, as the soluble silica is removed and mobilized by acidic solutions, iron is correspondingly precipitated in trivalent state as ferric hydroxysulfate on grain assemblages,

yielding a negative correlation between the two elements on mass balance considerations. Under similar conditions, Mg is removed as soluble $MgSO_4$ by the transgressing solutions from this system efficiently. The MgO remaining in the leached pyroxene residue and SiO_2 in the leached silicate residue yield a flat correlation as observed in $MgO\text{-}SO_3$ system (Fig.7a).

$_3$.4.2. Feldspar dissolution : The role that acid-sulfate solutions play in feldspar dissolution near the ,507 sampling site is delineated using data trends in Figs.7b and 7d. In these figures, the Al_2O_3 and CaO abundances are plotted against SO_3 and SiO_2. First, we address the Al_2O_3 and CaO versus SO_3 correlations in Fig.7b. Here, both Al_2O_3 and CaO correlate negatively with sulfate, i.e. as the SO_3 content increases both Al_2O_3 and CaO abundances show a modest decrease. The $Al2O_3$ and CaO data points, moreover, fit to correlation lines. However, few points, showing higher abundances, plot above the line in Fig.7b. Note that silica also shows lower abundances than the average Lith B-SiO2 content indicating that the dissolved silica is mobilized by the transgressing solutions (at a pH values < 5) from these sites. Under these pH conditions, dissolved Al and Ca could also be mobilized from the grain assemblages, leaving behind mineral residues with depleted cation abundances as seen in Fig.7b and 7d.

During acid-sulfate weathering of feldspars by solutions at pH < 4, after dissolution of a thin surface layer (releasing Al^{3+} from the grain surface into solution), the residual feldspar grain resists further acid-attack by preferential formation of a protective sheath around the grain. The liberated Al^{3+} reacts with sulfate ions in acidic solution, producing alunogen [$Al_2 (SO_4)_3$, n H_2O] which is more soluble than gypsum but less soluble than $MgSO_4$. The Ca^{2+} similarly dislodged from the feldspar matrix into solution, is precipitated as gypsum or remains in solution depending on pH and solution-state. Depending on acid- and cation- concentrations (including solubility-product controls), both alunogen and gypsum are removed from the reaction sites based on their relative solubilities in the transgressing solutions, leaving behind the feldspar residues depleted in Al and Ca. Banin et al., (1997) carried out lab simulation experiments on Hawaian volcanic tephra using acid-sulfate degradation techniques and noted that sulfate preferentially partitions into gypsum and alunogen salts when the cationic constituents of the primary minerals are released in presence of excess sulfuric acid.

As feldspar dissolution progresses incongruently, lesser amounts of Al and Ca are released into solutions because of the inherent resistance of feldspars to continued acid-attack (Nesbit and Muir,1988). Hence, the mineral residues manifest a modest decrease in Al and Ca abundance when plotted against SiO_2. As the SiO_2 decreases significantly from 51 to 40% (removal from both feldspars and pyroxenes), Al_2O_3 and CaO decrease only modestly from 20 - 15% and 11 – 9% respectively (removal essentially from feldspars). These results suggest that, acid-sulfate weathering of the regolith material at the EET79001,507 sampling site on Mars produced end products containing both soluble sulfates (such as magnesium sulfate, alunogen and gypsum) as well as insoluble compounds (such as iron sulfate / hydroxysulfate such as copiapite/ schwertmannite including hydroxides such as goethite). When the acidic solutions percolated through this regolith silicate-salt mix, the soluble salts are preferentially leached out of the system, leaving behind insoluble mineral compounds under favorable water/rock ratios.

4. COMPARISON BETWEEN IMPACT MELT GLASSES IN EET79001 AND VIKING / PATHFINDER SOILS

While attempting to unscramble different mineral components comprising the Martian soils, Clark (1993) proposed a two component model based on major-element systematics observed among Viking samples. This model is essentially concerned with mixing of silicates and salts in Martian soils. One component contains most of Si, Al, Ca and Fe, representing silicates and the other component contains S and Cl (Mg), representing salts. Recently, McSween and Keil (2000), Morris et al., (2000), Waenke et al., (2001) and McLennan (2000) among others have critically examined some of the elemental correlations observed in the case of Viking soils and Pathfinder soils and rocks. As a continuation of the Clark-model, in the present study, we focus our attention on elemental correlation trends in the impact-melt glasses in EET79001, which contain varying proportions of silicate-salt mixtures originating in soils on Mars (presumably originating near young volcanic Martian uplands such as Tharsis or Elysium or Olympus Mons). Below, we compare and discuss the results obtained in this study with those obtained for Viking / Pathfinder soils and rocks by McSween and Keil (2000); Morris et al. (2000); Clark (1993) and Waenke et al., (2001) and McLennan (2000).

4.1. SIO_2 vs SO_3 : Morris et al. (2000) (hereafter referred to as MOL), and McSween and Keil (2000) (hereafter referred to as MK) studied the correlations among major elements using the combined sample-suite of soil and rock data of Pathfinder (Rieder et al., 1997) and soil data from Viking (Clark et al., 1982) after making appropriate data adjustments / corrections. Here, we use the Pathfinder / Viking data given by MOL and MK for plotting in Figs. 8a-8d and 9a-9d, in which we compare the correlation profiles obtained in the case of EET79001,507 with those determined for Pathfinder/Viking soils and rocks. In Fig.8a in this study (and Fig.1 of MK and Fig.39 of MOL), one finds a negative correlation between SO_3 and SiO_2 similar to the one noted by Clark (1993) (regression coefficient r =0.91), i.e. as the SO_3 content increases, the SiO_2 content decreases in the Martian soils and rocks and vice versa. In other words, this correlation suggests that the greater the salt abundance one finds in a given soil sample, the lesser is the silicate abundance in that sample (and vice versa). Note that a similar negative correlation between SO_3 and SiO_2 is also found when we plot the SiO_2 and SO_3 abundances determined in impact-melt glass veins of EET79001,507 in Fig. 7e and 9e. Also the EET79001,507 glasses (r^2 = ~0.75) here and Pathfinder soils / rocks (r=0.91) yield somewhat similar regression coefficients (McSween and Keil, 2000).

Impact melt glasses from another shergottite glass inclusion, DBS Shergotty, (which shows petrographic features similar to that of EET79001,507 and also contains high concentrations of Martian atmospheric noble gases), yielded a similar negative correlation between SO_3 and SiO_2 (Rao et al., 1999b). Though the Viking and the Pathfinder soils are generally considered to be similar, the Pathfinder soils are somewhat enriched in SiO_2 and depleted in SO_3 relative to Viking (Bell et al., 2000). In particular, some Pathfinder soils such as A-2, A-8, and A-10 are found to be relatively rich in SO_3 and poor in SiO_2, consistent with the expectations from acid-sulfate weathering of soil fines near Mars surface. The similarity in the correlations between SO_3 and SiO_2, observed in Viking and Pathfinder soils (which originate from Chryse / Utopia and Ares Vallis regions) and impact melt glasses in EET79001,507 studied here (which presumably originate from young volcanic terrains such as Elysium / Tharsis or Olympus Mons) suggests that this negative correlation may be associated with planet-wide acid-sulfate weathering on Mars.

4.2. FeO and MgO vs SO_3 In Fig.9a (and in Fig.1 of MK and Fig.39 of MOL), SO3 and Fe_2O_3 (FeO) abundances show a positive correlation (regression coefficient, r^2 =0.63) when

Pathfinder rock and soil iron and sulfur data are plotted. Note that the Fe content in soils is reported as $Fe2O_3$ (oxidized) and the Fe content of rocks is reported as FeO (reduced). Based on the element oxide positive correlation observed by MK, the FeO content of soil-free rock (SO_3 = 0%) near Pathfinder is deduced to be ~12% which is in agreement with the value obtained by Rieder et al. (1997) for the assumed Pathfinder soil-free rock. Fig.9a, here yields a slightly higher value (~14%) because we used only selected data (not all the data points) in the plot. Here, in the case of ,507 sample (Fg.6a), SO3 abundances show an excellent positive correlation with FeO (r^2= 0.8), yielding a FeO content of ~11% for the soil- free rock component on the basis that SO_3 = 0.6% representing Lith B. Here, the sulfur and iron abundance variation takes place over a wide range, i.e. the SO_3 content varies from ~1% up to ~18% and the FeO content from ~10 to 24%. Note that the soil- free rock components belonging to these different sampling sites i.e. Pathfinder and EET79001,507 , on Mars surface yield roughly similar FeO content (~11-12%), which is much lower than the FeO content of ~18% of host Lith B (average).

In the case of EET79001,506 glasses, though the range of data variation is relatively limited, one finds a negative correlation between FeO and SO_3 (r^2=0.32) somewhat similar to the one found by Clark (1993) and Morris et al. (2000) for Fe_2O_3 vs SO_3 in Viking soils. This negative correlation is consistent with iron being present in the divalent state because Fe^{2+} hydroxysulfate produced as result of acid-sulfate dissolution (under reducing conditions) could be easily dissolved and mobilized from the reaction sites by the transgressing solutions near Mars surface. Also, the FeO content of ~20% deduced for the end-member rock-residue (sulfur-free) fraction in the EET79001,506 soils is similar to the Fe_2O_3 content of ~22% found for the soil-free rock in Viking soils by Morris et al. (2000) and McSween and Keil (2000)

Below, we examine the MgO systematics for the soil assemblages at Viking, Pathfinder and EET79001 sampling sites. MOL (Fig.39) and MK (Fig.3) and Clark (1993) plot MgO and SO_3 contents for the Pathfinder and Viking soil and rock data and find an excellent positive correlation between these two oxides. Based on this correlation, they deduce the MgO content of the soil- free rock (SO_3 =0) to be ~2%. Wanke et al. (2001) deduced ~1% MgO for the soil-free rock using raw Pathfinder data. In the present study, we plot the MgO contents of the EET79001,507 glasses against SO_3 in Fig. 6a and find a horizontal (or flat) correlation between the two, i.e. as the SO_3 content varies over a large range, the MgO content does not change significantly. By extrapolating this correlation line in Fig.6a back to SO_3 =0.6%, (characteristic of Lith B host), we deduce a MgO content of ~2% for the soil- free rock-residue fraction in the Martian soil fines (MSF) at the EET79001,507 sampling site. Note that these different sampling sites (Pathfinder and EET79001,507) yield a similar MgO content of ~2% for the soil-free rock (or weathered rock residue) in Martian soils.

It is obvious that the SO_3-MgO correlation profile found for EET79001,507 (Lith B) glass is different from that obtained for Viking and Pathfinder soils and rocks in Fig.1 and Fig.39 of MK and MOL respectively. This is because the Mg in the glass precursor materials of EET79001,507 corresponds to the magnesium remaining in the weathered rock–residue, after undergoing heavy- leaching of rock-fragments by the acid-sulfate transgressing solutions. The dissolved $MgSO_4$ resulting from acid-sulfate dissolution of mafic mineral component at this Martian site is mobilized by the transgressing solutions, following the hydraulic gradient to lower geographic locations, depending on the water/rock ratios. On the other hand, the Mg in the soils at Pathfinder and Viking sampling sites results from the secondary salts produced by evaporation of dissolved sulfate transported by the acid solutions to Martian low lands / plains

(Chryse/Utopia and Ares Vallis). The FeO and MgO data in EET79001,506 glasses discussed above indicate that the Martian soils, from which these glasses are produced, had probably undergone moderate or limited dissolution under reducing environment on Mars.

4.3. FeO and MgO vs SiO_2 : Silica is known to be relatively mobile during near- surface aqueous alteration of basaltic rocks on Earth. Acid-decomposition of minerals such as fayalite, forsterite, diopside and albite produces large amounts of silicic acid on Earth (McLennan, 2003). The silica, thus produced, likely precipitates as surface coatings on rocks and mineral assemblages depending on pH and the saturation state of the dissolved SiO_2 in the transgressing solutions. According to Wyatt and McSween (2002), it is likely that the silicic acid may be present as amorphous silica at ~10% concentration levels or more in some regions on Mars. To study the behavior of SiO_2 in Martian soils, here, we plot FeO and MgO abundances measured in Pathfinder soils and rocks against SiO_2 in Figs. 8b and 8c respectively. In Fig. 8b, FeO correlates negatively with SiO_2. When MgO is plotted against SiO_2 for the Pathfinder in Fig.8c, it also shows a negative correlation between the two. But, when we plot MgO vs. SiO_2 in the case of EET79001,507 (Fig.7c) , it shows a horizontal or flat correlation between the two similar to the case of MgO–SO_3 relationship (Fig.7a). The explanation provided here for the MgO-SO_3 correlation is equally applicable to the MgO-SiO_2 relationship. But, in the case of EET79001 ,506 (and other Lith A glasses such as ,77and ,18), both FeO and MgO (as well as Al_2O_3 and CaO) show a weak negative correlation with SiO_2 because of restricted or limited acid-sulfate dissolution of Martian soil at this site. However, note that the increase in SiO_2 content from 47.5% to 52 % in these Lith A glasses is due to the deposition of solubilized silicic acid as amorphous SiO_2 on grain surfaces at relatively high pH conditions near Mars surface. On the other hand, if weathered basalt is found to be ubiquitous near Mars surface (Wyatt and McSween, 2002), it may suggest that the soils and rocks might have undergone extensive acid-sulfate weathering and aqueous alteration near the surface of Mars as observed in the case of EET79001,507 glass. The formation of silica coatings on mineral surfaces as secondary weathering products is widely recognized in terrestrial soils and sediments (Dove, 1995; Brantley and Chen, 1995). Hence, in some samples, we might find evidence for some chemical processes leading to loss or depletion of SiO_2 and in other samples, for gain or enrichment of SiO_2 depending on conditions related to pH and element concentration in the mobilizing solutions. Because of restricted availability of water and extremely low temperatures near the Martian surface, obviously these deposits may form poorly crystalline precipitates, consistent with various spectroscopic observations on the surface of Mars {Bell et al., 2000).

4.4. Al_2O_3 and CaO vs SO3 : Below, we compare the results of feldspars during chemical weathering of soils and rocks at these three different sampling sites (i.e. EET79001, Viking and Pathfinder) near the Martian surface. The Al_2O_3 and CaO abundance data for Pathfinder and Viking rocks and soils are plotted against SO3 in Figs. 9b and 9c in this study (and by MOL and MK in Fig.39 and Fig.$_2$ respectively), where both Al_2O_3 and CaO correlate negatively with SO_3 (regression coefficients r = 0.7 and 0.84 respectively). Further, the range of measured elemental variation in this case is limited, i.e. from ~9 to 11% for Al_2O_3 and it is ~6 to 8% for CaO. Hence, we infer that during acid-sulfate weathering of basaltic materials on Mars, the feldspathic minerals probably underwent limited passive dissolution compared to extensive decomposition of ferromagnesian minerals. This inference is consistent with the results obtained in the case of EET79001 ,507 sample i.e. both Al_2O_3 and CaO similarly show negative correlation trends with respect to SO_3. The range of elemental variation observed in the case of ,507 is also limited, i.e. Al_2O_3 varies from ~17 to 21% and CaO varies from ~9 to 11%. The

negative correlations observed between Al_2O_3 and SO_3 as well as CaO and SO_3 for Pathfinder and Viking rocks and soils are similar to those that we find in the case of EET79001,507 glass. Further, it may be noted that the CaO vs. SiO_2 and CaO vs SO_3 correlation trends (Fig.9c) in these samples are also similar to those observed in Al_2O_3 vs SiO_2 (Fig.7b) and Al_2O_3 vs SO_3 (Fig.9b) systematics, discussed above. Non-stoichiometric dissolution of feldspars under acidic conditions (pH <5) results in the development of Al- and other cation depleted Si-rich layers on the mineral surfaces (Blum and Stillings, 1995; Sposito,1989). These findings indicate that the degree of dissolution of feldspathic minerals during acid-sulfate weathering of basaltic shergottite type materials on the surface of Mars is much less pronounced compared to the mafic mineral dissolution at these three sampling sites.

However, in the case of EET79001,506 glasses, in spite of limited range of data variation, Al_2O_3 shows positive correlation with SO_3 (r^2=0.45). In the case of Viking soils, Clark (1993) earlier found a positive correlation between Al_2O_3 and SO_3 by fitting the regression line to the non-crust data points (note that in the case of Pathfinder soils and rocks, McSween and Keil (2000) and Waenke et al (2001) and others find a positive correlation between these two oxides). The positive correlation found between Al_2O_3 and SO_3 in Viking soils and EET79001,506 glasses suggests that under reducing conditions and high pH, aluminum precipitates as poorly crystalline hydroxysulfate during moderate acid-sulfate dissolution on Mars.

In some cases, dilution effect might control the correlation-systematics. Because of extensive acid-sulfate dissolution of pyroxenes and subsequent deposition of amorphous ferric hydroxysulfate, the sulfate abundance (together with Fe) may get substantially enhanced. Consequently, it will result in lowering of the abundance of the other constituents in a given sample on mass-balance considerations. On the other hand, because of limited and passive chemical dissolution of feldspars, much smaller amounts of Al_2O_3 are released into the solutions from the same sample and mobilized away from the reaction sites on Mars depending on favorable environment. Under these conditions, the insoluble mineral excess added to the sample matrix will act as a diluent in determining the total weight, resulting in lower abundances of oxides such as Al_2O_3 and CaO. This effect may thus contribute to an increase of the negative slope between Al_2O_3 and SO_3 (for example) in the case of EET79001, 507 samples (Fig.7b) as well as in other soils (Fig.9b).

4.5. INTER-ELEMENT GEOCHEMICAL RELATIONSHIPS : In order to put the selected element correlations in perspective, we revisit the observations made earlier in the case of EET79001 glasses and Viking / Pathfinder soils. Combining the data sets for Pathfinder rocks and soils, McSween and Keil, (2000) and Morris et al., (2000) and McLennan (2000); Waenke et al. (2001) point out that FeO (Fe_2O_3) correlates positively with SO_3 as shown in Fig. 8a. In this figure, we plot also the EET79001,507 data for comparison. Note that FeO and SO_3 (Fig.9a & Fig.7a) in the case of EET79001,507 glasses show a similar positive correlation. Further, the slopes of these correlation lines are also somewhat similar, though there is an off-set of FeO abundances of the end-member compositions between these two data sets. The off-set for the end-member FeO abundances between Pathfinder soils and EET79001,507 glasses (which presumably contain impact-molten Martian soil) seems to be a result of the fact that the ,507 glasses are made up of significant amounts of Martian soil fines (MSF) fraction produced by impact-comminution followed by aeolian sorting. As MSF is known to be depleted in mafic component, these glasses show lower FeO abundances relative to the Lith B host material (as discussed in sub-section 3.5). In contrast, in the case of Viking/Pathfinder soils, the end-

member FeO-content is relatively close to Lith B composition, because they have a preponderance of coarse-grained soil fraction in them, where this depletion effects supposedly are not registered. Further, the range of SO_3 abundance in Viking / Pathfinder soils (~8% max) is much less compared to ,507 sample-suite (~18% max). The observation that, as the sulfate content increases in these samples, the FeO content correspondingly increases, indicates that the deposition of insoluble iron sulfate precipitates such as ferric hydroxysulfate (or some combination of amorphous copiapite- or schwertmannite mixed with goethite) on the grain assemblages. It may be noted that, while studying Viking and Pathfinder soils, McLennan (2000) points out that the positive correlation between sulfur and iron in Martian soils may be indicative of a 'secondary sedimentary mineralogy' such as Fe-sulfate.

Furthermore, the data in Fig. 9b shows that the MgO-SO_3 positive correlation observed in the case of Viking soils and Pathfinder soils /rocks is not reproduced in the case of EET79001, 507 glasses. As noted earlier, this is, because, in the case of ,507 glasses, the measured MgO in the glasses corresponds to the Mg content of the rock-residue left over after acid-sulfate leaching of the grain-assemblages. On the other hand, the measured MgO in Viking / Pathfinder soils corresponds to the Mg in the salt mixtures arising from the evaporation of dissolved sulfate mobilized by the transgressing solutions percolating through Martian regolith (discussed in sub-section 4.2). At the same time, during acid-sulfate decomposition of ferromagnesian minerals, soluble silicic acid is also released into solutions depending on the pH. As a result, we notice that, as the SiO_2 content decreases, the FeO content correspondingly increases, showing a negative correlation between the two oxides (Figs.7c and 8a). This takes place because the released SiO_2 from pyroxene dissolution is mobilized away from the reaction sites by transgressing solutions under favorable pH conditions, leaving behind insoluble ferric hydroxy-sulfate as poorly-crystalline deposit on grains. Hence, as more SiO_2 is removed from the system, more iron is precipitated as Fe^{3+} sulfate resulting in a corresponding iron enhancement in the residual samples (Fig.7c and Fig.8a). Note that a similar correlation profile is also observed between FeO and SiO_2 in the case of ,507 glass precursors. These results, therefore, suggest that the acid-sulfate weathering conditions that existed near the EET79001,507 sampling-site on Mars are similar to those that prevailed near the Pathfinder landing sites.

As mentioned before, the MgO vs SO_3 (Fig. 9b) and MgO vs SiO_2 (Fig.7c) plots in the case of ,507 glasses show that the MgO content in the mineral residues remains fairly constant (at ~2-3% level) even though the SO_3 and SiO_2 abundances in the grain assemblage vary from ~1-18 % and ~40-51% respectively. The low MgO abundance in the grain-residues could be accounted for, if the mineral assemblages are low in pyroxene abundance due to the depletion of mafic component in the samples under discussion. In this context, it may be noted that Morris et al. (2000) deduced an MgO content of ~2% for the soil-free rock component at the Pathfinder site. Similarly, the corresponding FeO abundance in the mineral grain residues is ~11-12% (end-member sulfur-free rock value), which is also much lower compared to the Lith B host. Because of impact- comminution and aeolian sorting on Mars, the mafic component depletion occurs in the fine-grained MSF fractions. These results suggest that the ferro-magnesian minerals in the Martian soil mix at this site are heavily digested due to acid-sulfate weathering from which the soluble $MgSO_4$ is efficiently leached out by the transgressing solutions, leaving behind iron mostly precipitated as ferric hydroxysulfate / hydroxide type compounds.

In the case of EET79001,507 samples, the positive correlation observed between FeO and SO_3 in Fig.7a and the negative correlation between Al_2O_3 and CaO against SO_3 in Fig.7b suggest

that the transgressing aqueous solutions are fairly acidic and oxidizing on Mars. In contrast, in the case of ET79001,506 samples, the poor negative correlation between FeO and MgO vs SO_3 (Fig. 6a and Fig. 6b) and the positive correlation between Al_2O_3 and CaO vs SO_3 (Fig.6a and Fig.6b) indicates that the mobilizing solutions are weakly acidic and reducing near the Martian surface. These results suggest that the acid sulfate dissolution of basaltic materials is moderate and inefficient in the case of EET79001,506 samples whereas it is relatively extensive and efficient in the case of EET79001,507 samples near Mars surface.

Feldspathic minerals undergoing acid-sulfate dissolution near Mars surface seem to show a passive relationship between Al_2O_3 and SO_3. Notice the off-set in the Al_2O_3 end-member abundances between the two correlation lines in Fig.9b. It appears that EET79001,507 glasses contain larger amounts of impact-comminuted fine-grained Martian soil fines (MSF) which are presumably enriched in feldspathic minerals relative to the host basaltic material on Mars. In contrast, in the case of Viking / Pathfinder soils, there is a preponderance of coarse-grained soil fraction where such mineral-specific comminution effects are not registered. On the other hand, one finds a positive correlation between Al_2O_3 and SiO_2 in the case of Pathfinder rocks and soils as well as in the case of EET79001,507 glass sample (Fig.7d and 8d) because the decrease in Al_2O_3 positively correlates with decrease in SiO_2 in this system. Note that the Al_2O_3 and SiO_2 species liberated from feldspar dissolution are mobilized by the transgressing acidic solutions without deposition, when the pH is <4. When the pH of acid-sulfate solution is much less than the first hydrolysis constant pK1 (<5), the Al hydrolysis is insignificant. Hence, aluminum is little affected by geochemical reactions and it moves in surface waters as if it were a conservative constituent (Nordstrom and Alpers,1999; Nordstrom and Ball, 1986; Bache,1986). Once the pH of the waters reaches the pK1 value, hydrolysis causes the Al to become insoluble and precipitate as Al $(OH)_3$ (as gibbsite) or other insoluble Al- sulfate compounds such as basaluminnite or Al (OH) SO_4. Under these conditions, the dissolved silicic acid is also mobilized by the transgressing solutions without precipitation on grain surfaces (Nordstrom and Ball (1986); Nordstrom and Alpers, 1999). As both Al and Ca salts remain dissolved in acidic solution, there is no deposition of gibbsite (taking up Al) or gypsum (taking up Ca) on the grains under these pH conditions. These inferences hold good in the case of Viking / Pathfinder soils. Clearly, the major element correlation trends observed in the EET79001,507 glasses are similar to those observed in Pathfinder soils and rocks, though the magnitude of variation is different from one sample to another. Thus, we conclude that the conditions controlling acid-sulfate dissolution of rocks and soils at the Viking and Pathfinder sites are similar to those at the EET79001 sampling site on Mars.

5. SULFATE / SULFIDE SPECIATION IN EET79001 IMPACT GLASS PRECURSOR MATERIALS :

5.1 The sulfur content of bulk lithology A is 0.16%. Approximately similar amount of sulfur (0.19%) occurs in lithology B of EET79001 (Burghlee et al.,1983). This is the expected average sulfur concentration in basaltic shergottites according to Laul et al. (1986). If the impact melt glasses in ,507 of Lith B are formed only out of this basaltic shergottite material, then the expected S content does not match with the observed S content in these glasses. In fact, the observed SO_3 content in 507 glasses varies from ~1 % to ~18% (S = ~8%). The sulfur abundance in Lith C glasses (impact melt glasses in Lith A and Lith B are sometimes referred to as Lith C) is much more than that observed in Lith A or Lith B. It clearly indicates that Lith A or

Lith B material alone cannot generate the measured large S abundances in these glasses and an additional sulfur-bearing component is required for this purpose.

The sulfur contained in bulk Lith A and Lith B is essentially sulfide. It is pyrrhotite with a composition Fe0.93 Ni 0.03 S in Lith A and Fe0.96 S with very little Ni in Lith B (McSween and Jarosewitch, 1983). The Fe/ Ni ratio in Lith A pyrrohitite is ~31. However, the observed Ni content in these glasses is much less, i.e. only 0.02 to 0.04%.

5.2 The question of sulfur speciation in EET79001 glasses was addressed by Gooding and Muenow (1986) using data obtained from the pyrolysis experiments on Lith C samples. They showed that the net oxidation state of S in these glasses is higher than in Lith A indicating that sulfate may be the principal form of sulfur in Lith C glasses. Further, these authors point out that if one considers the bulk composition of Lith C and Lith A to be similar (i.e. ~18% FeO and ~0.18% S) and the typical shergottite liquidus temperature ~ 1200 °C (at 1 atm pressure), then the components Lith A , Lith B and Lith C become saturated with respect to S (Stolper and McSween, 1979). As a result, a basaltic melt containing 20% FeO cannot dissolve more than 0.2 -0.4 % S without purging an immiscible sulfide liquid from the system (Gooding and Meunow, 1986; Wallace and Carmichael, 1992). In the Lith C glass, no discrete grains of iron sulfide were detected during detailed SEM/EDS studies by Gooding and Muenow (1986).

Furthermore, Burgess et al. (1989) addressed the same issue of sulfur speciation in shergottites and other SNCs. Among the SNCs studied by them, Shergotty is of interest to our study because Shergotty and EET79001, Lith B, with which ,507 sample is associated, belong to the same class of SNCs i.e. basaltic shergottites. During step-wise pyrolysis experiments on bulk Shergotty, Burgess et al. found that H_2S equivalent of 1665 ppm S (or 4580 ppm FeS equivalent) was released from their samples in the low temperature (400 to 600 °C) fraction. In the high temperature (700 to 900 °C), SO_2 equivalent of 190 ppm S (or 1020 ppm $CaSO_4$) was released. Based on these results, they determined a S(ox)/S(red) ratio of 0.1 for Shergotty. It may be noted that the ratio of dark-brown impact-melt-glass to igneous bulk in a given sample determines this ratio. During the pyrolysis-combustion of a bulk sample, if the glass to bulk ratio is high, the oxidized sulfur component (sulfate) dominates by preferentially releasing large quantities of SO2 in the high temperature fraction. On the other hand, if the glass to bulk ratio is low, it is the reduced sulfur (sulfide) that dominates by preferentially releasing H_2S in the low temperature fractions. A detailed petrographic sample-examination may be useful in explaining the gas-release data from the pyrolysis experiments. Most of the sulfur in Shergotty was found to be present as sulfide by Burgess et al. This result could be consistent with the above remarks, if their sample contained smaller amounts of dark-brown glass. Here, it may be added that the dark brown impact melt glasses are less common in Shergotty compared to EET79001 (Stoeffler et al., 1986).

In few localized regions in Shergotty, however, dark brown impact- melt glass pockets (0.2 to 1mm in size) were observed by Stoeffler et al. (1986). In these glass inclusions, they report SO_3 contents as high as 4-5%. These high SO_3 contents are similar to the SO_3 contents reported by us in another Shergotty melt glass pocket, DBS 1 / 2 sample (Rao et al., 2000). It may be noted that the DBS 1/2 Shergotty sample, studied by Rao et al. (2000), is an aliquot of a bigger sample which contained high concentrations of Martian atmospheric noble gases (Bogard and Garrison, 1998). While analyzing the impact-melt glasses from other Lithology A of EET79001 (adjacent to Lith B) by SEM/EDS techniques, Gooding and Muenow (1986) and Gooding et al., (1988) showed that Lith C contains an oxidized sulfur (sulfate) component that does not occur in Lith A. They found relict $CaSO_4$ grains imbedded / trapped in these glasses indicating that the

constituent mineral phases probably had undergone incipient melting. The $CaSO_4$ grains are intimately associated with ~10 um grains of $CaCO_3$, which were probably trapped during rapid solidification of quench-textured pyroxene and glass. They concluded that these relict grains formed in an environment that was sufficiently oxidizing to transform sulfide to sulfate and the speciation of sulfur released during Lith C pyrolysis is consistent with sulfate as the principal form of sulfur in these glasses. Recently, the occurrence of more gypsum grains in Shergotty and EET79001 impact glasses was again reported by Wentworth et al. (2003).

6. NEAR-SURFACE WATER DURING RECENT GEOLOGIC HISTORY OF MARS :

Only small amounts of water could be presently accommodated in the Martian near-surface environment. However, MOC images from the MGS spacecraft provide ample evidence for the extensive past-activity of water and ice associated with numerous landforms on Mars (Malin and Edgett, 2000; Baker,2001 and other references therein). In particular, the recently acquired high-resolution MOC images of northern plains on Mars reveal contraction-crack polygonal terrain suggesting a youthful phase of water-related activity on Mars (Baker, 2001). Some of these results are consistent with the flow of liquid water during geologically recent times on Mars (Malin and Edgett, 2001; Carr, 1983). Based on theoretical climate-modeling, Jakosky and Phillips (2001) point out that catastrophic flood channels occur episodically throughout Martian history, requiring large crustal reservoirs of liquid water. Furthermore, the coarse-grained hematite observed at the Mars surface by Christensen et al. (2000) is best explained as resulting from weathering in previously subsurface aqueous systems. In this context, it was shown that the Martian ice can melt under favorable conditions such as dusty snow or when snow is covered by a thick dust layer (Farmer, 1976; Hecht, 2002). The liquid water, thus produced on Mars, as result of ice-melting can flow for several hours without significant freezing because of poor atmospheric convection and low soil conductivity (Haberle et al., 2001). Also, Kuznetz and Gan (2002) note that the large temperature (~20 oC) excursions observed during Pathfinder measurements imply that water ice can easily melt near the Martian surface. Cold trapping of winter condensation could favorably concentrate sufficient amounts of ice in gullies and seasonally melt it when directly exposed to the Sun under normal-incidence insolation during summer time (Hecht, 2002). The recent discovery of high concentrations of hydrogen near sub-surface regions on Mars by GRS from Odessy spacecraft (Boynton et al., 2002) provide direct supporting evidence for the above morphological observations.

The extreme glaciation during the late Proterozoic where the Earth seems to have switched to Mars-like ice-house conditions by freezing the surface of the global ocean is best explained by attributing it to a large change in planetary obliquity (or tilt of the planet's rotational axis with respect to the orbital plane) (Hoffman et al., 1998). The complex variability of Mars obliquity or axial tilt over long time-scales could mobilize water (Jakosky et al.,1995; Lasker and Robutel, 1993) in a way that can explain the relatively recent manifestations of glacial activity such as the melting of near-surface ground ice. The episodic inundation of northern plains on Mars seems to have taken place on a short-term basis (~10^4 years) continuously resulting in melting of permafrost producing water-related landforms throughout Martian history. Furthermore, Jakosky et al. (1995) theoretically examined the behavior of seasonal water cycle over a wide range of obliquities that might have occurred over the last 10 Ma and showed at high obliquities,

ice sublimation could be as high as 1-10 cm / year on Mars, whereas at the present obliquity, the sublimation rate on Mars is as low as 0.1 mm of ice per year. The sublimed ice can be transported as water vapor to equatorial and mid-latitude regions where it condenses eventually on to the surface (Haberle and Jakosky,1990). Once in ~10^5 years, the obliquity of Mars seems to get favorably oriented with respect to the Sun when the temperatures near equator and mid-latitudes are raised above the melting point of ice. Under such favorable conditions, the existing water ice / frozen permafrost may melt and produce transient channels of intense water activity that may last for few years near Mars surface without freezing.

7. ACID-SULFATE WEATHERING CALCULATIONS of EET79001,507 (LITH B)

Here, we calculate the compositions of end-products in the acid-sulfate weathering of basaltic shergottite-type material in the Martian regolith under the assumptions discussed below. For the starting material, we use the shergottite basaltic composition of 56% pyroxene and 29% feldspar plus maskelynite (McSween and Jarosewitch, 1983). The remaining 15% consists of accessory minerals such as oxides and sulfides etc which are not taken into consideration in the following calculations. This material undergoes meteoroid comminution accompanied by aeolian sorting near Mars surface. The fine-grained fractions produced by these physical processes are enriched in felsic component and depleted in mafic component relative to the starting material. Here, we use the adjusted enrichment and depletion factors determined by Horz and Cintala (1997) in the laboratory simulation experiments of meteoroid comminution by bombarding a gabbro target with SS projectiles having impact velocities of 1.4 km/sec. This partially enriched / depleted starting material was subjected to acid-sulfate chemical dissolution. The soluble salts produced, as a result, are dissolved and transported by transgressing solutions on Mars. We assume that all FeO and MgO in the solution results from the dissolution of pyroxenes and all Al_2O_3 in the solution comes from the dissolution of feldspars. CaO is contributed by the dissolution of pyroxenes and feldspars equally into the solution. In the present model, the acid-sulfate solutions are generated from acidic volatiles released by volcanic eruptions into Martian atmosphere . They interact with the enriched / depleted parent basaltic fine materials by dissolving varying proportions of these mineral constituents depending on the acid-sulfate availability under limited water / rock ratios. We consider the following cases in our numerical calculations: Case A = 10% pyroxene and 5% feldspar dissolved into the transgressing solutions, which remove/ mobilize the salt-products $MgSO_4$, H_4SiO_4 and soluble aluminum hydroxysulfate from the system. We consider that when pyroxene is digested, iron released into transgressing solutions as $FeSO_4$ and it will precipitate from the solutions already containing some soluble iron as poorly crystalline iron hydroxysulfate, (the formula assumed here in the calculation is $Fe_2(OH)(SO_4)_2$ i.e $2FeO : 2SO_4$). It is considered that the amount of iron released from pyroxene dissolution precipitates as insoluble $Fe_2(OH)(SO_4)_2$, nH_2O picking up an equivalent amount of Fe from the transgressing solutions which already contain dissolved iron salts from previous mineral weathering regime in Martian regolith. The iron sulfate minerals that precipitate as poorly-crystalline compounds on grain surfaces are not single mineral phases. They seem to be mixtures of copiapite, $[2\ Fe_2(SO_4)_3]\ [Fe(OH)_2].\ 20H_2O$, schwertmannite [Fe8O8 (SO_4) (OH)6], or goethite [FeO (OH), n H_2O] under pH conditions that prevail in these acid solutions. As we do not know the exact composition of the poorly crystalline iron (Fe^{3+}) hydroxysulfate, we consider that two moles of FeO combines with two moles of sulfate to yield the amorphous $Fe_2(OH)(SO_4)_2$ precipitate and use this relation in our

calculation; Case B = 20% pyroxene and 10% feldspar dissolved (and other details same as in Case A) ; Case C = 40% pyroxene and 20% feldspar dissolved (and other details same as in Case A). Using successive model-steps in dissolution and precipitation reactions, we calculate the composition of different major–element oxides in the end products as shown below. We plot the calculated percentage values for Cases A, B and C in Figs. 7a-7e of ,507. The trends generated by the model calculations agree reasonably well with the trends fitted to the measured data points in Figs. 6a-6d, though there is some off-set between the observed and calculated values in some cases. Note that the numbers used for pyroxene and feldspar dissolution calculations are not unique and other combinations are quite likely. By fine-tuning the numerical values chosen in the above calculations i.e appropriately adjusting these parameters, a much better agreement could be achieved between the calculated and observed values. It is important to notice that one set of parameters used in the model calculations is able to reproduce the data trends observed in all the FeO, MgO, CaO and Al_2O_3 versus SO_3 and SiO_2 plots (7a- 7d), including SO_3 versus SiO_2 (Fig. 7e). These results provide credibility to the model and indicate that the glasses likely contain locally-produced , chemically- fractionated soil fines generated as a result of differential comminution and acid-sulfate weathering near Mars surface under limited water / rock ratios prior to impact-melting.

7.1. Mineral abundance and the elemental composition of Lith B given by McSween and Jarosowich (1983) used in these calculations is given below:

Mineral abundance : (McSween and Jarosowich, 1983) also referred to as M&J (1983):

i) Pigeonite=32.2% ; augite=23.9% ; olivine= 0%; Pyroxene(total) = 56.1%
ii)Feldspar + maskelynite = 29.4 %
 # The composition of Lith B (McSween and Jarosewich, 1983) **:**
SiO_2 (49.03%), SO_3 (0.5%), FeO (17.74%), MgO (7.38%), CaO (10.99%) and Al_2O_3 (9.93%)

7.2. Details of the calculations carried out using this model for Cases A, B, and C are shown in Tables 1 to 6.

8. SUMMARY AND CONCLUSSIONS

As a result of constant meteoroid bombardment on Mars surface similar to Moon, impact-induced comminution of bed-rock materials along with collisional destruction of regolith rocks occurs over geological time-scales. This comminution process, together with aeolian sorting on Mars, leads to in-situ generation of a range of grain-sizes among the end products in the regolith. The regolith fine-fraction (MSF) on Mars registers the mineral-specific comminution effects such as enrichment of feldspathic component and depletion of mafic component with respect to the comminuting host phase as found in the case of lunar soil fines on Moon. The degree of enrichment and depletion of these components in Mars soil fines (MSF) differ from those in soil fines on Moon because of the pervasive aeolian activity on Mars. Soil samples originating from different geographic locations on Mars contain varying amounts of the regolith fine fraction (MSF) and the ratio of the coarse to fine fractions in individual samples determine the relative magnitude of enrichment (based on Al_2O_3 and CaO abundances) and depletion (based on FeO and MgO abundances). The wind-blown dust due to the Martian aeolian activity seems to have selectively introduced excess soil fines at the EET79001 sampling site on Mars.

In addition to this mechanical processing, the precursor soil assemblages in the EET79001 glasses have undergone chemical dissolution due to acid-sulfate weathering near Mars surface.

Acid-sulfate mineral decomposition of pyroxenes releases Fe, Mg and SiO_2 into mobilizing solutions, where Fe is precipitated as insoluble ferric hydroxysulfate bearing compounds under oxidizing conditions. The excellent positive correlation observed between FeO and SO_3 in the case of EET79001, 507 glasses provides ample evidence for this type of interaction among regolith grain assemblages on Mars. Further, the mobilization of Mg as soluble $MgSO_4$ by the dissolution of regolith grain assemblages at the reaction sites is consistent with the horizontal correlation found between MgO and SO_3 in ,507 glasses because the measured Mg and S abundances in these glasses correspond to the weathered mineral residues left over from leaching at the Martian site. The removal of SiO_2 as soluble silicic acid from the grain assemblages by the transgressing solutions under relatively low pH conditions is indicated by the negative correlation between FeO and SiO_2 as well as the positive correlation between the Al_2O_3 and CaO decrease and the SiO_2 decrease in abundances found in these glasses. Furthermore, SiO_2 and SO_3 in these glasses negatively correlate with each other showing that as the salt content in the precursor soil fines increases, the silicate content correspondingly decreases and vice-versa. In this context, it may be noted that all these features described above, characterizing the precursor soil assemblages at the EET79001, 507 site on Mars are also shown by Pathfinder soils. The dissolved $MgSO_4$ and soluble silicic acid liberated by mineral decomposition are transported by acidic solutions following the hydraulic gradient into valleys and plains and deposited as poorly-crystalline $MgSO_4$ (evaporites) and amorphous SiO_2. These results indicate that Pathfinder soils had undergone chemical weathering in a relatively oxidizing Martian environment.

On the other hand, if Fe exists as divalent iron sulfate under reducing conditions, it dissolves into the transgressing solutions percolating through the weathered regolith terrain. As a result, it is transported away from the reaction site on Mars. The excellent positive correlation observed for Al_2O_3 and CaO with SO_3, accompanied by a negative correlation of FeO and MgO with SO_3in EET79001,506 glasses clearly show that acid-sulfate weathering under reducing conditions occurred at the EET79001,506 site on Mars. Moreover, the poor correlation of SiO_2 with FeO and MgO as well as Al_2O_3 and CaO observed in the case of EET79001,506 glasses indicates that the intensity of acid-sulfate decomposition of soil grain assemblages at this site is much less pronounced compared to the EET79001,507 site on Mars. Note that the positive correlation between Al_2O_3 and SO_3 and the negative correlation between FeO and SO_3 observed in the case of EET7001,506 precursor soils are consistent with similar correlations shown by Viking soils. These results indicate that Viking soils underwent chemical weathering in a relatively reducing Martian environment.

Few times in a million years, the obliquity of planet Mars becomes favorably oriented with respect to the Sun and the temperatures at near-equatorial regions reach favorable levels, when the existing water-ice and frozen permafrost melt and create transient localized regions of intense water activity (Hecht, 2000; Kuznetz and Gan, 2001; Haberle and Jakosky, 1990). The water thus generated accumulates into subsurface channel network leading to mobile aqueous solutions that provide a transporting medium for soluble salts and minerals near Mars surface.

Here, we present a model where basaltic shergottite-type material is subjected to impact-comminution leading to felsic enrichment and mafic depletion among the end products. The resulting silicate assemblage interacts with acid-sulfate solutions by dissolving varying proportions of the mineral constituents assuming favorable water-rock ratios. The transgressing solutions mobilize the soluble salts from the reaction centers leaving behind insoluble compounds as poorly crystalline precipitates. We calculate the composition of the end products

for each case, considering that soluble $MgSO_4$, silicic acid and Al hydroxysulfate are removed from the system by transgressing solutions under moderate pH conditions, while Fe is deposited as ferric hydroxysulfate type amorphous precipitate. The data generated by the model calculations agree well with the elemental trends fitted to the measured data points. Note that one set of parameters (and assumptions) used in the model calculations is able to reproduce the data trends observed for both positive and negative correlations concerning FeO & MgO as well as Al_2O_3 & CaO versus SO_3 & SiO_2, including SO_3 versus SiO_2 in the case of EET79001,507 impact glasses.

ACKNOWLEDGEMENTS ----- We thank the Meteorite Working Group for providing the EET79001 thin sections used in this study. We sincerely thank Craig Schwandt, Sue Wentworth and Vincent Yang for valuable experimental support during EMPA and FE SEM analytical work reported here. We thank Don Bogard, Fred Horz, John Jones and Dan Garrison for discussions about this work. Robert Rushing is thanked for editorial help. MNR is particularly thankful to H. Waenke and G. Dreibus at Max-Plank Institute fur Chemie, Mainz, where part of this work was done as a Visiting Scientist. The work reported here is supported by NASA Astrobiolgy Institute.

REFERENCES

Bache B.W. (1986) Aluminum mobilization in soils and waters. J. Geol. Soc. (London). 143, 699-706.

Banin A., Han F.X., Kan I., and Cicelsky A. (1997) Acidic volatiles and the Mars soil. J. Geophys. Res. 102, 13,341-13,356.

Baker V.R. (2001) Water and the Martian landscape. Nature 412, 228-235.

Becker R.H., and Pepin R.O. (1984) The case for a Martian origin of the shergottites: nitrogen and noble gases in EETA 79001. Earth Planet. Sci. Lett. 69, 225-242.

Bell III J. F., McSween Jr. H.Y., Crisp J. A., Morris R. V., Murchie S.L., Bridges N.T., Johnson J.R., Britt D.T., Golombek M.P., Moore H.J., Ghosh A., Bishop J. L., Anderson R.C, Brueckner J., Economou T., Greenwood J.P., Gunnlaugsson H.P., Hargraves R. M., Hviid S., Knudsen J.M., Madsen .B., Reid R. (2000) Mineralogic and compositional properties of Martian soil and dust. Results from Mars soil and dust. Results from Mars Pathfinder. J. Geophys. Res. 105, 1721-1755.

Bigham J.M., Schwertmann U., Traina S.J., Winland R.L., and Wolf M. (1996) Schwertmannite and the chemical modeling of iron in acid sulfate waters. *Geochim. Cosmochim. Acta* **60**, 2111-2121.

Bigham J. M. and Nordstrom D. K. (2000) Iron and aluminum hydroxysulfates from acid sulfate waters. In Alpers C.N., Jambor J.L., and Nordstrom D.K. (eds) Sulfate minerals: Crystallography, Geochemistry, and Environmental significance. *Reviews in Mineralogy & Geochemistry*, Vol. **40**, pp.351-403. Mineral. Soc. Am., Washington. D.C.

Blumm A. E. and Stillings L. L. (1995) Feldspar dissolution kinetics. In White A. F. and Brantley S.L. (eds) Chemical weathering rates of silicate minerals. *Reviews in Mineralogy*, Vol.**31**, 292-351.

Boctor N.Z., Alexander C.M. O'D., Wang J., and Hauri E. Y. (2003) The sources of water in Martian meteorites: Clues from hydrogen isotopes. *Geochim. Cosmochim. Acta* **67**, 3971-3989.

Bogard D.D. and Johnson P. (1983) Martian gases in an Antactic meteorite? *Science*, **221**, 651-654.

Boynton W.V., Feldman W.C., Squyres S.W., Prettyman T.H., Brueckner J., Evas L.G., Reedy R.C., Starr R., Arnold J.R., Drake D. M., Englert P.A.J., Metzger A.E., Mitrofanov I., Trombka J.I., d'Uston C., Waenke H., Gasnault O., Hamara D.K., Janes D.M., Marcialis R.L., Maurice S., Mikheeva I., Taylor G.J., Tokar R., and Shinohara C (2002) Distribution of hydrogen in the near-surface of Mars: Evidence for subsurface ice deposits. *Science*, **297**, 81-85.

Brantley S.L., and Chen Y. (1995) Chemical weathering rates of pyroxenes and amphiboles. In White A.F., and Brantley S. (eds) Chemical weathering rates of silicate minerals. *Reviews of Mineralogy* vol. **31,** 119-173.

Bridges J.C., Catling D.C., Saxton J.M., Swindle T.D., Lyon I.C., and Grady M.M. (2001) Alteration assemblages in Martian meteorites: Implications for near-surface processes. *Space Sci. Rev.* **96**, 365-392.

Burgess R., Wright I.P., and Pillinger C.T. (1989) Distribution of sulfides and oxidized sulfur components in SNC meteorites. *Earth Planet. Sci. Lett.* **93**, 314-320.

Burghele A., Dreibus G., Palme H., Rammensee W., Spettel B., WeckwrthG., and Waenke H. (1983) Chemistry of shergottites and the shergottite parent body (SPB): Further evidence for the two component model for planet formation. (abs) *Lunar Planet. Sci.* **XIV**, 80-81.

Burns R.G. (1993) Rates and mechanisms of chemical weathering of ferromagnesian silicate minerals on Mars. *Geochim. Cosmochim. Acta.* **57**, 4555-4574.

Burns R. G., and Fisher D.S. (1993) Rates of oxidative weathering on the surface of Mars. *J. Geophys. Res.* **98**, 3365-3372.

Carr M.H. (1983) Stability of streams and lakes on Mars. *Icarus*, **56**, 476-495.

Carroll J.J., and Mather A.E. (1989) The solubility of hydrogen sulfide in water from 0 to 90 oC and pressures to 1M Pa. *Geochim. Cosmochim. Acta* 53, 1163-1170.

Carson C. D., Fanning D. S., and Dixon J.B. (1982) Alfisols ad altisols with acid sulfate weathering features in Texas *Soil Sci. Soc. of Am. Proc.* **37**, 127-146.

Casey W.H., and Bunker B. (1990) Leaching and mineral and glass surfaces during dissolution. In Hochella M.F. and White A.F. (eds) Mineral-water interface geochemistry. *Rev. Mineral.* **23**, 397-426.

Christensen P.R., Bandfield J.L., Clark R.N., Edgett K.S., Hamilton V.E., Hoefen T., Kieffer H.H., Kuzmin R.O., Lane MD., Malin M.C., Morris R.V., Pearl J.C., Pearson R., Roush T.L., Ruff S.W., and Smith M.D. (2000) Detection of crystalline hematite mineralization on Mars by the Thermal Emission Spectrometer: Evidence for near surface water. *J. Geophys. Res.* **105,** 9623-9642.

Clark B.C. (1993) Geochemical components in Martian soil. *Geochim. Cosmochim. Acta* **57**, 4575-4581.

Clark B.C. and Van Hart D.C. (1981) The salts of Mars. *Icarus* **45**, 370-378.

Clark B.C., Baird A. K., Weldon R. J., Tsusaki D. M., Schnabel L., Candelaria M. P. (1982) Chemical composition of Martian fines. *J. Geophys. Res.* **87**, 10059-10067.

Clark B.C. and Baird A.K. (1979) Is the Martian lithosphere sulfur-rich? *J. Geophys. Res.* **84,** 8395-8403.

Dove P.M. (1995) Kinetic and thermodynamic controls on silica reactivity in weathering environments. In White A.F., and Brantley S. (eds) Chemical weathering rates of silicate minerals. *Reviews of Mineralogy* vol. **31,** 235-290.

Farmer C.B. (1976) Liquid water on Mars. *Icarus*, **28**, 279-289.

Garrison D. H., and Bogard D. D. (1998) Isotopic composition of trapped and cosmogenic noble gases in several Martian meteorites. *Meteorit. Planet. Sci.* **33**, 721-736.

Gooding J.L. (1992) Soil mineralogy and chemistry on Mars: Possible clues from salts and clays in SNC meteorites. *Icarus* **99,** 28-41.

Gooding J.L., and Keil K. (1978) Alteration of glass as a possible source of clay minerals on Mars. *Geophys. Res. Lett.* **5**, 727-730.

Gooding J.L., and Meunow D.W. (1986) Martian volatiles in shergottite EETA 79001: New evidence from oxidized sulfur and sulfur-rich aluminosilicates. *Geochim. Cosmochim. Acta* **50**, 1049- 1060.

Gooding J.L., and Wentworth S.J. (1991) Origin of "white druse" salts in the EETA79001 meteorite. (abs) *Lunar Planet. Sci.* **XXII**, 461-462.

Gooding J.L., Wentworth S.J., and Zolensky M.E. (1988) Calcium carbonate and sulfate of possible extraterrestrial origin in the EETA79001 meteorite. *Geochim. Cosmochim. Acta* **52**, 909-915.

Greely R., Kraft M., Sullivan R., Wilson G., Bridges N., Herkenhoff K., Kuzmin R.O., Malin M., and Ward W. (1999) Aeolian features and processes at the Mars Pathfinder landing site. *J. Geophys. Res.* **104**, 8573-8584.

Haberle R.M., McKay C.P., Schaeffer J., Cabrol N.A., Grin E.A., Zent A.P., and Quinn R. (2001) On the possibility of liquid water on present-day Mars. J.Geophys. Res. 106, 23317-23326.

Haberle R.M., and Jakosky B.M. (1990) Sublimation and transport of water from the north residual polar cap on Mars. J. Geophys. Res. 95, 1423-1437.

Hartmann W. K., Anguita J., A. de la Casa M., Berman D.C., and Ryan E.V. (2001) Martian crateing 7: The role of impact gardening. *Icarus*, **148**, 37-53.

Hecht M.H. (2002) Metasstability of liquid water on Mars. *Icarus*, **156**, 373-386.

Hoffman P.F., Kaufman A.J., Halverson G.P., and Shrag D.P. (1988) A neo-proterozoic snowball Earth. *Science*, 281, 1342-1346.

Hoerz F., and Cintala M.J. (1997) Impact experiments related to the evolution of planetary regoliths. Metoritics & Planet. Sci. 32, 179-209.

Hoerz F., Cintala M. J., Rochelle W.C., and Kirk B. (1999) Collisionally processed rocks on Mars. *Science*, **285**, 2105-2107.

Jakosky B.M., Henderson B.G., Mellon M. T. (1995) Chaotic obliquity and the nature of the Martian climate. J. Geophys. Res. 100, 1579-1584.

Kasting J.F. (2001) The rise of atmospheric oxygen. *Science*, **293**, 819-820.

Kuznetz L.H., and Gan D.C. (2002) On the existence and stability of liquid water on the surface of Mars today. *Astrobiology*, **2**, 183-195.

Lasker J., and Robutel P. (1993) The chaotic obliquity of the planets. *Nature*, **361**, 608-612.

Laul J.C., Smith M.R., Waenke H., Jagoutz E., Dreibus G., Palma H., Spettel B., Burghele A., Lipschutz .E., and Verkouteren R.M. (1986) Chemical systematics of the Shergotty meteorite and the composition of its parent body. *Geochim. Cosmochim. Acta* **50**, 909- 926.

Leshin L.A., Epstein S., and Stolper E.M. (1996) Hydrogen isotope geochemistry of SNC meteorites. *Geochim. Cosmochim. Acta* **60,** 2635-2650

Lindsay W. L. (1979) Chemical Equilibria in Soils. John Wiley and Sons. New York.
Malin M.C., and Edgett K. S. (2000) Evidence for recent ground water seepage and surface runoff on Mars. Science, 288, 2330-2333.
McCoy T.J., Taylor G.J., and Keil K. (1990) Zagami: Product of a two-stage magmatic history. Geochim. Cosmochim. Acta 56, 3571-3582.
McKay D.S. and Basu A. (1979) The Apollo 15 highland regolith. *Lunar Planet. Sci. (abstracts)* **X** , 108-110.
McLennan S.M. (2000) Chemical composition of Martian soil and rocks: Complex mixing and sedimentary transport. *Geophys. Res. Lett.* **27**, 1335-1338.
McLennan S.M. (2003) Sedimentary silica on Mars. *Geology* **31**, 315-318.
McSween H.Y. Jr. (2002) The rocks of Mars, from far and near. *Meteoritics & Planet. Sci.*, **37**, 7-25.
McSween H.Y. Jr., and Keil K. (2000) Mixing relationships in the martian regolith and the composition of globally homogenous dust. . *Geochim. Cosmochim. Acta* 64, 2155-2166.
McSween H.Y. Jr., and Treiman A. H. (1999) Martian meteorites. In Papike J.J. (ed) Planetary materials: Rev. in Mineralogy, **36**, 6.1-6.53.
McSween H.Y. Jr. and Jarosewich E. (1983) Petrogenesis of the Elephant Moraine A79001 meteorite: Multiple magma pulses on the shergottite parent body. *Geochim. Cosmochim. Acta* **47**, 1501-1513.
Morris R.V., Golden D.C., Bell III J.F., Shelfer T.D., Scheinost A.C., Hinman N.W., Furniss G., Mertzman S.A., Bishop J.L., Ming D.W., Allen C. C. (2000) Mineralogy, composition and alteration of Mars Pathfinder rocks and soils: Evidence from multispactral, elemental and magnetic data on terrestrial analogue, SNC meteorite and Pathfinder samples.
Nesbitt H.W., and Muir I.J. (1988) SIMS depth profiles of weathered plagioclase and processes affecting dissolved Al and Si in some acidic solutions. *Nature*, **334**, 336-338.
Nordstrom D. K. and Alpers C. N. (1999) Geochemistry of acid mine waters. In: The Environmental Geochemistry of Mineral Deposits. Part A. Processes, Methods and health issues. PlumleeG. S. and Logsdon M. J. (eds.) Rev. Econ. Geol. 6A: 133-160.
Nordstrom D.K. and Ball J.W. (1986) The geochemical behavior of aluminum in acidified surface waters. *Science*, **232**, 54-56.
Papike J.J., Simon S.B., White C., and Laul J.C. (1981) The relationship of the lunar regolith <10 um fraction and agglutinates. Part I: A model for agglutinate formation and some indirect supportive evidence. *Proc. Lunar Planet. Sci.* 12B, 409-420.
Rao M. N., Borg L. E., McKay D. S., and Wentworth S.J. (1999a) Martian soil component in impact glasses in a Martian meteorite. *Geophys. Res. Lett.* **26**, 3265-3268.
Rao M. N., Wentworth S.J., Schwandt C., Yang S. R., and McKay D. S. (1999b) Molten nartian soil in Shergotty meteorite. *Lunar Planet. Sci.* **XXX**, #1626.
Rao M.N., and McKay D.S. (2003) Characterization of Martian soil fines fraction in SNC Meteorites. Lunar Planet. Sci. XXX #1252.
Rao M. N., and McKay D.S. (2003) Evidence for Mars regolith preserved in shergottite EET79001: Differential comminution and chemical weathering records. 6th. Inter. Mars Conf. JPL, Pasadena. CA. #3130.
Rieder R., Economou T., Waenke H., Turkevich A., Crisp J., Brueckner J., Dreibus G., and McSween H.Y. Jr. (1997) The chemical composition of Martian soil and rocks returned by the mobile alpha proton X-ray spectrometer: Preliminary results from the X-ray mode. Science, 278, 1771-1774.

Settle M. (1979) Formation and deposition of volcanic sulfate aerosols. J. Geophys. Res. **84,** 8343-8354.

Shearer C. K., Rao M. N., Papike J. J., McKay D. S., and Schwandt C. S. (2000) Trace element characteristics of Lithology C in Martian meteorite EET79001 : Implications for the composition of Martian soils. In First Astrobiology Conference at Ames Research Center, April, p. 244.

Sposito G. (1989) The Chemistry of Soils. Oxford University Press. New York. Pp. 1-227.

Stoeffler D., Ostertag R., Jammes C., Pfannschmidt G., SenGupta P.R., Simon S.B., Papike J.J., and Beauchamp R.H. (1986) Shock metamorphism and petrography of Shergotty achondrite. *Geochim. Cosmochim. Acta* **50**, 889-904.

Stolper E. M., and McSween H. Y. (1979) Petrology and the origin of shergottite meteorites. Geochim. Cosmochim. Acta 43, 1475 – 1498.

Stumm W., and Morgan J.J. (1996) Aquatic chemistry: Chemical equilibria and rates in natural waters. J. Wiley & Sons. New york. NY. pp. 1-1022.

Swindle T.D., Caffee M.W., and Hohenberg C.M. (1986) Xenon and other noble gases in shergottites. *Geochim. Cosmochim. Acta* **50**, 1001-1015

Symonds R.B., Rose W.I., Bluth G.J.S., and Gerlach T.M. (1995) Volcanic gas studies: methods, results and applications. In: Carroll M.R., and Holloway J.R. (eds.) Volatiles in Magmas *Rev. Mineral.* **30**, 1-60.

Tosca N.J., McLennan S.M., Lindsley D.H., Schoonen M.A.A. (2003) Low-temperature aqueous alteration on Mars: Insights from the laboratory. *Sixth Inter. Conf. on Mars* (abs.) #3178.

Treiman A. H., Gleason J.D., and Bogard D.D. (2000) The SNC meteorites are from Mars. *Planet. Space Sci.* **48**, 1213-1230.

Van Breemen N. (1982) Genisis, morphology and classification of acid-sulfate soils in coastal plains. *Soil Sci. Soc. of Am. Proc.* **37**, 694-697.

Wooden J., Shih C. –Y., Nyquist L., Bansal B., Weismann H., and McKay G. (1982) Rb-Sr and Sm-Nd isotopic constraints on the origin of EETA 79001: a second Antarctic shergottite. *Lunar Planet. Sci.* **XIII**, 879-880.

Wallace P. and Carmichael I.S.E. (1992) Sulfur in basaltic magmas. *Geochim. Cosmochim. Acta* **56**, 1863-1874.

Waenke H., Brueckner J., Dreibus G., Rieder R., and Ryabchikov I. (2001) Chemical composition of rocks and soils at the Pathfinder site. *Space Sci. Rev.* **96**, 317-330.

Warren P. H. (1998) Petrologic evidence for low temperature possible flood evaporitic origin of carbonates in the ALH84001 meteorite *J. Geophys. Res.* **103**, 16759 -16773.

Wentworth S.J., Thomas-Keprta K.L., and McKay D.S. (2003) Evaporites in the Nakhla and Shergotty Martian meteorites: Traces of Mars history. *Astrobiology* (in press).

Wyatt M. B. and McSween H.Y. Jr. (2002) Weathered basalt as an alternative to andesite. *Nature* **417**, 263-266.

Table. 1. Elemental abundance in pyroxenes and feldspars in EET79001 (MJ,1983) used in the calculations:

Oxide	Pyroxene (%)	Feldspar (%)
SiO_2	52	54.2
FeO		0.66
MgO	17.5	
CaO	8.7	11.6
Al_2O_3	1.3	28.7

(Assumptions: We assume that all FeO and MgO come from the dissolution of pyroxenes and
the Al_2O_3 comes from the dissolution of feldspars. CaO comes from the dissolution of pyroxenes and feldspars equally).

TABLE 2. Depletion and enrichment factors used in the calculations
Composition of the starting shergottite basaltic material enriched / depleted according to the adjusted comminution parameters (Hoerz et al., (1997). The values used in the calculations are in between those determined in impact glasses (max values) and those that are determined by Horz et al.

Enrichment Al_2O_3 =40%
Enrichment CaO = 0%
Depletion FeO = 50%
Depletion MgO = 60%
No enrichment or depletion in SiO_2.

Table. 3. Starting material composition after correcting for enrichment / depletion

	SiO_2 (g)	SO_3 (g)	FeO (g)	MgO (g)	CaO (g)	Al_2O_3 (g)	remarks
Lith B comp. (%) (M & J)	49.03	0.5	17.74	7.38	10.99	9.93	
56.1% pyroxene equivalent	27.5 (0)	---	8.87 (D)	2.95 (D)	6.17 (0)	----	
29.4% feldspar equivalent	14.41(0)	----	-----	-----	3.23 (0)	13.9 (E)	
Total (E + D) [P]	41.9	---	8.87	2.95	11	13.9	pyx +feld together

E = enrichment-corrected; D = depletion-corrected, 0 = no enrichment or depletion, calculated using values given by (Horz and Cintala, 1997).

Table. 4. End product composition after 10% pyroxene and 5% feldspar dissolution followed by iron hydroxysulfate precipitation as explained in the text

Components	**SiO_2 (g)**	**SO_3 (g)**	**FeO (g)**	**MgO (g)**	**CaO (g)**	**Al_2O_3 (g)**	remarks
i.[P]	41.9	--	8.87	2.95	11	13.9	
ii. − 10%pyx (dissolved)	− 2.8	---	− 0.89	− 0.3	− 0.62	----	
iii. − 5% feld(dissolved)	− 0.72	----	-----	-----	− 0.16	− 0.7	
iv. $2SO_3$: 2FeO ppted. as $Fe_2(OH)(SO_4)_2$	----	1.8	1.8	----	-----	------	
Sum of i to iv rows	38.3	1.8	9.61	2.65	8.62	13.2	Sum=77.9 (5% corr.added)*
Percent. (%)	**49.2**	**2.3**	**12.3**	**3.4**	**11.06**	**16.95**	**Case A**

Case A : [P] = composition ,after correcting for feldspar enrichment and pyroxene depletion, in the resulting mineral mix (assume 100 g of the Lith B type as the starting material) ;

- as these shergottite glass samples contain variable amounts of oxide and other accessory minerals, we have applied a 5% correction for the effective grammage of the mineral constituents in the soil mix.

Table. 5. End product composition after 20% pyroxene and 10% feldspar dissolution followed by iron hydroxysufate precipitation as explained in the text

Components	**SiO_2 (g)**	**SO_3 (g)**	**FeO (g)**	**MgO (g)**	**CaO (g)**	**Al_2O_3 (g)**	remarks
i.[P]	41.9	--	8.87	2.95	11	13.9	
−20% pyx (dissolved)	− 5.6	---	− 1.8	− 0.6	− 1.24	----	
− 10% feld (dissolved)	− 1.44	----	-----	-----	− 0.32	− 1.4	
$4SO_3$: 4FeO ppted. as $Fe_2(OH)SO_4)_2$	----	+3.6	+3.6	----	-----	------	
Sum of the above four rows	34.86	3.6	10.67	2.35	7.84	12.5	Sum=75.42 (5% corr.added)
Percentage	**46.2**	**4.8**	**14.15**	**3.1**	**10.4**	**16.6**	**Case B**

Case B : [P] = same as above

Table. 6. End product composition after 40% pyroxene and 20% feldspar dissolution followed by iron hydroxysulfate precipitation as explained in the text

Components	SiO_2 (g)	SO_3 (g)	FeO (g)	MgO (g)	CaO (g)	Al_2O_3 (g)	remarks
[P]	41.9	--	8.87	2.95	11	13.9	
− 40% pyx (dissolved)	− 11.2	---	−3.6	−1.2	− 2.48	----	
− 20% feld (dissolved)	− 2.88	----	-----	-----	− 0.64	− 2.8	
$8SO_3$:8FeO ppted. as $Fe_2(OH)(SO_4)_2$	----	+ 7.2	+ 7.2	----	-----	------	
Sum of the above four rows	27.82	7.2	12.47	1.75	6.28	11.1	Sum=66.62 (5% corr.added)
Percentage	**39.8**	**10.3**	**17.8**	**2.5**	**9**	**15.8**	**Case C**

Case C : [P]= same as above

Figure Captions

Fig. 1a – 1d: Digital WDS (wavelength dispersive spectrometer) elemental maps of glass-bearing areas in Et79001 for studying the spatial distribution of specific elements in veins (~20-100 micron size) and pods of Lith C. A is a typical Al map of a glass vein in ,78 (eet79001-78bSP1) ; B is the Al map of glass vein in ,77 (eet79001- 77bSP1) ; C is the Al map of glass vein in ,506 (eet79001-506a3SP1) and D is the Al map of glass vein in ,507 (eet79001- 507a1SP1). The lighter areas in the figures correspond to higher concentrations and the darker areas correspond to lower conecentrations of Al. [Beam voltage : 15 kV ; Beam Intensity : 20 nA ; Definition : 512 X 512 ; Step size (um) : 100 ; X size : 512 ; Y size : 512 ; Dwell time (ns) : 70]. They contain vesicles and relic grains and show granular structure at submicron level.

Figures 2a – 2d : Correlations of structural elements FeO and MgO (for pyroxenes) as well as Al_2O_3 and CaO (for feldspars) with SiO_2 in impact-melt glass veins and pods in several EET79001, Lithology A thin sections (,78 – filled diamond; ,77 – filled square; ,18 - filled triangle; ,20A – cross; and ,506 – asterisk). Lith A composition (filled circle) used for normalization is also shown for comparison. Fig. 2a refers to FeO – SiO_2 plot. Fig. 2b refers to MgO – SiO_2 plot. Fig. 2c refers to Al_2O_3 – SiO_2 plot and finally Fig. 2d refers to the CaO – SiO_2 plot in these glasses. Each data point here represents the average of 20 to 30 measurements in 10X8 um areas consecutively rastered along a line across the vein at relatively homogeneous locations.

Figures 3a – 3d: Correlations of structural elements FeO and MgO (for pyroxenes) as well as Al_2O_3 and CaO (for feldspars) with SO_3 in impact-melt glass veins and pods in several thin sections of EET79001, Lithology A. The symbols identifying these sections are same as in Fig.

2a. Fig. 3a refers to FeO – SO_3 plot; Fig. 3b refers to MgO – SO_3 plot; Fig. 3c refers to Al_2O_3 – SO_3 plot and Fig. 3d refers to CaO – SO_3 plot. The SO_3, which is representative of secondary salts, is shown as "SO_3" because it is a mixture of sulfate and sulfide in varying proportions. In the case of ,506 (as discussed later), note that when the SO_3 content is high, the SiO_2 conent is low whereas in the case of ,20A glasses, in contrast, when the SO_3 content is low the SiO_2 is high. However, in the case of ,77 and 78 glasses these correlation trends between SiO_2 and SO_3 are poorly- reflected because of random mixing of regolith components.

Figure 4: Enrichment of felsic (Al_2O_3, CaO , Na_2O) and depletion of mafic (FeO, MgO, TiO_2) components relative to Lith A in impact-melt glasses of EET79001. The range of the measured abundance values for each element oxide given in the rectangular boxes and the percentage shown is calculated using the maximum abundance value found in each case. The Lith A composition (McSween and Jarosewich, 1983) , used for normalization, is shown in the square boxes in the middle. Positive and negative signs before the numbers denote enrichment and depletion respectively. Impact melt glasses are sometimes referred to as Lith C in literature.

Figure 5 : Comparison of the measured elemental enrichment and depletion factors in EET79001 impact melt glasses with the elemental enrichment and depletion factors determined in the rock debris fine-fraction (< 10 um) resulting from the fragmental gabbro- comminution by repetitive impact in lab simulation experiments (Horz and Cinala, 1997). Total range (min – max) observed in these samples are plotted here as a histogram. Note that the pattern of enrichment and depletion of mineral components in these glasses (representing Martian soils) is similar to those obtained for lab simulation experiments by Horz and Cintala (1997). However, the magnitude of these enrichment / depletion factors found in these glasses (represnting Martian soils) is different from that determined in the lab simulation experiments because of redistribution of the soil fine fraction due to pervasive aeolian activity on Mars. (In this context, it may be noted that these enrichment and depletion factors determined in the case of lab simulation experiments (Horz and Cintala, 1997) are grossly similar to those found in the case of Moon soil fines by Papike et al. (1982) because there is no redistribution of soil fines due to Aeolian activity on Moon.

Figures 6a – 6e : Correlations of structural elements FeO and MgO (for pyroxenes) and $Al2O_3$ and CaO (for feldspars) with SO_3 (secondary salts) and SiO_2 (silicates) in EET79001, 506 impact-melt glasses. Lith A composition, used for normalization here, is also shown for comparison. The regression lines in Fig. 6a and Fig. 6b show that FeO and MgO correlate negatively with "SO_3" whereas Al_2O_3 and CaO correlate positively with "SO_3". Fig. 6a represents MgO – SO_3 plot and CaO – SO_3 plot. Fig. 6b represents FeO – SO_3 plot and Al_2O_3 – SO_3 plot. Further, Fig. 6c contains MgO – SiO_2 plot and CaO – SiO_2 plot whereas Fig. 6d contains FeO – SiO_2 plot and Al_2O_3 – SiO_2 plot of glass vein data in EET79001,506. Note that the regression lines in Figs. 6c and 6d yield poor correlation coefficients indicating that the SiO_2 removed from the regolith mix by acid-sulfate weathering is very limited. As a result the composition of the parent material deduced from the rock-residue in the glass by extrapolating backwards turns out to be a composition close to Lith A. The data in Figs. 6c and 6d further indicate that the dissolved silica from acid-sulfate weathering of parent regolith material is re-deposited over the rock-residue to varying degrees which is consistent with the finding of an increase of SiO_2 from 48% (Lith A) to ~52% in these glasses. This re-deposition of silica requires a chemical weathering environment on Mars where the pH of the mobilizing solutions is relatively high. Fig. 6e shows that the correlation between SiO_2 and SO_3 for ,506 glasses is very

poor because acid-sulfate dissolution of Martian soils in ,506 glass precursors is very limited leading to inefficient mobilization of dissolved SiO_2.

Figures 7a – 7e : Correlations of structural elements FeO and MgO (pyroxenes) and Al_2O_3 and CaO (feldspars) with SO_3 (salts) and SiO_2 in impact melt glass veins in EET79001,507. Lith B composition used for normalization is also shown. SO_3 is shown as "SO_3" because it includes both sulfate and sulfide in varying proportions. The regression lines in Fig. 7a indicates that FeO correlates positively with SO_3 and MgO shows a zero (or flat) correlation with SO_3. In Fig. 7b, Al_2O_3 and CaO both correlate negatively with SO_3. [It is of interest to note here that the SO_3 content in ,507 glasses varies over a large range i.e. 1-18% compared to the limited range in ,506 glasses i.e. 0.4- 1.6%]. Further, the regression lines in Fig. 7c show that FeO correlates negatively with SiO_2 whereas MgO shows a zero or flat correlation with SiO_2 similar to the MgO – SO_3 correlation (the implications of these relationships are discussed in the text). In Fig. 7d both Al_2O_3 and CaO show positive correlation with SiO_2 i.e. the decrease in Al_2O_3 and CaO correlates positively with the decrease in SiO_2. Note that SiO_2 in the rock-residue in these glasses decreases from ~51% to 40%. Fig. 7e shows that SO_3 negatively correlates with SiO_2 indicating that as the salt content increases in these glasses, the silicate content decreases and vice-versa.

Comparison of elemental correlation trends observed in this study with model -weathering calculations : The filled big circles corresponding to A, B, C represent the case A, case B, and case C where different proportions of pyroxenes and feldspars in the basaltic regolith mix are dissolved during acid-sulfate weathering near Mars surface. The dissolved $MgSO_4$ is mobilized by the transgressing solutions, leaving behind amorphous ferric hydroxysulfate precipitates mixed with ferric hydroxide compounds. Smaller amounts of Al_2O_3 and CaO are also removed by dissolution as sulfates including soluble silicic acid resulting from silicate decomposition. Note that one set of assumptions and parameters in the model used for calculating the end-product compositions in Case A, Case B and Case C (shown as big bullets) is able to reproduce all (both negative and positive) elemental correlation trends seen between FeO & MgO and Al_2O_3 & CaO plotted against SO_3 and SiO_2 (as well as SO_3 vs SiO_2) in Figs. 7a to 7e. However, one could see differences in absolute magnitude between the observed and calculated values in some cases because we used only round numbers for the percentages of pyroxenes and feldspars undergoing acid-sulfate dissolution in the basaltic regolith mix, without trying to adjust these numbers to fit to the experimentally observed values.

Figures 8a – 8d : Correlation of SiO_2 with structural elements FeO and MgO (pyroxenes) and Al_2O_3 and CaO (feldspars) in Pathfinder soils and rocks including Viking soils. Fig. 8a is a FeO – SiO_2 plot. Note that Pathfinder rocks and soils show a negative correlation between FeO and SiO_2 similar to the one shown in Fig. 7c for the Martian soils incorporated into EET79001, 507 glasses during impact. Fig. 8b is the MgO – SiO_2 plot. Note that the MgO, here, represents varying amounts of Mg in the weathered rock-fragments in Pathfinder rocks and soils (including Viking soils) whereas, in Fig. 7b, the MgO represents the relatively uniform abundance of Mg in the weathered rock- residue in EET79001, 507 soils. Further, the data suggests that the Mars soils at this site are heavily weathered. Fig. 8c is the Al_2O_3 – SiO_2 plot. Here, one notices a positive correlation between Al_2O_3 and SiO_2 in Pathfinder rocks and soils (including Viking soils) similar to the one shown between Al_2O_3 and SiO_2 in Fig. 7c for the Martian soils incorporated into EET9001, 507 glasses at the time of impact. Fig. 8d is the CaO – SiO_2 plot. Note that the positive correlation between CaO and SiO_2 in Pathfinder rocks and soils is similar

to the one between CaO and SiO_2 in Fig. 7d , observed for Martian soils incorporated into EET79001, 507 glasses.

Figures 9a – 9e : Comparison of the correlation of SO_3 with structural elements FeO & MgO (pyroxenes) and Al_2O_3 & CaO (feldspars) in soils at the three sites EET79001, Viking and Pathfinder on Mars. Fig. 9a is the FeO (Fe_2O_3) – SO_3 plot. Note the similarity in the positive correlation trend between Pathfinder rocks /soils and EET79001,507 soils on Mars. Though there is a good correlation between the two, there is an off-set for the value of the end-product FeO abundance deduced for these two data sets (a detailed explanation for this is provided in the text). Fig. 9b is the MgO – SO_3 plot. The positive correlation between MgO and SO_3 in Pathfinder rocks / soils is different from the flat (or zero) correlation between the two in the case of EET79001,507 precursor soils for which a detailed explanation is provided in the text. Figs. 9c and 9d show Al_2O_3 – SO_3 and CaO – SO_3 plots respectively. Both Al_2O_3 and CaO negatively correlate with SO_3 in Pathfinder rocks / soils similar to the negative correlation between the two as observed in the case of EET79001,507 soils. The reasons for the off-set among the end-product Al_2O_3 abundances deduced from the correlation lines are discussed in the text. Fig. 9e is the SO_3 - SiO_2 plopt. The EET79001,507 data shows a negative correlation between SO_3 and SiO_2. A similar negative correlation between SO_3 and SiO_2 for Pathfinder and Viking soils was shown in Fig.1a of McSween and Keil (2000), in Fig.39 of Morris et al. (2000), Fig.2a of McLennan (2000) and Fig.1 of Clark (1993).

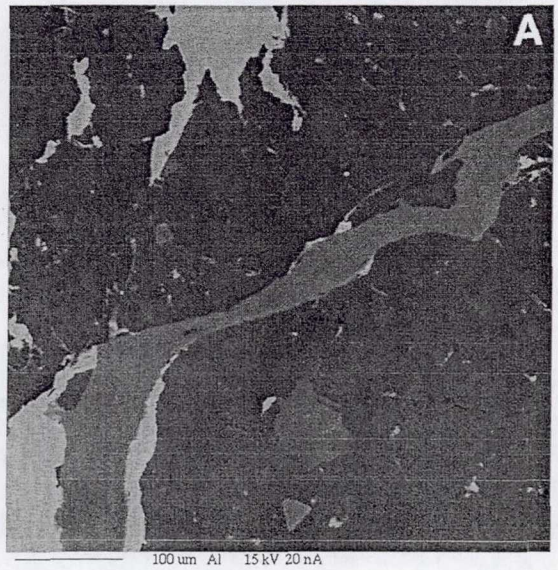
A
100 um Al 15 kV 20 nA

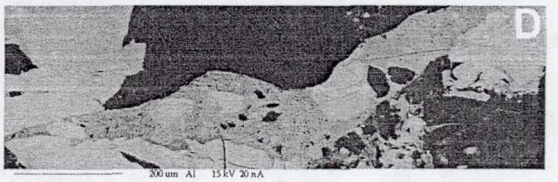
D
200 um Al 15 kV 20 nA

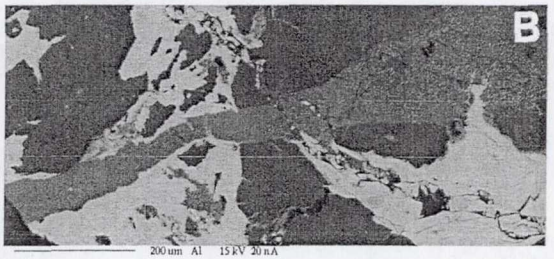
B
200 um Al 15 kV 20 nA


C
50 um Al 15 kV 20 nA

Fig. 1.

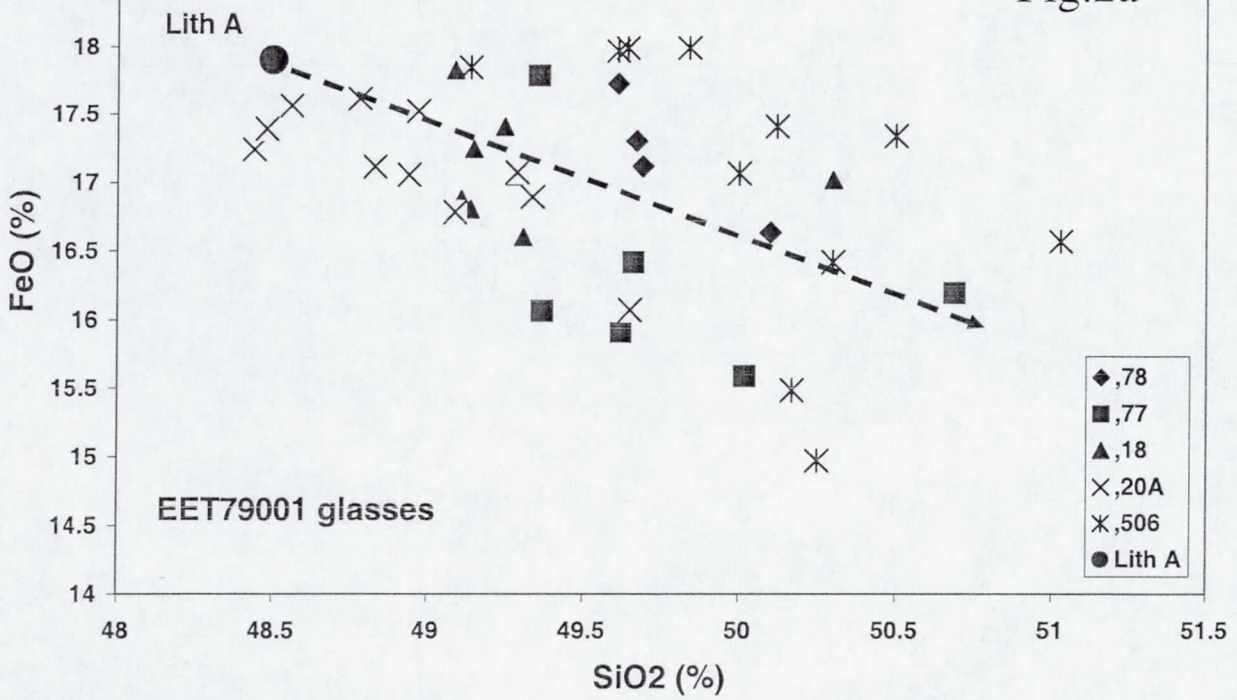
Fig.2a
Lith A
EET79001 glasses
FeO (%)
SiO2 (%)
19
18.5
18
17.5
17
16.5
16
15.5
15
14.5
14
48
48.5
49
49.5
50
50.5
51
51.5
,78
,77
,18
,20A
,506
Lith A

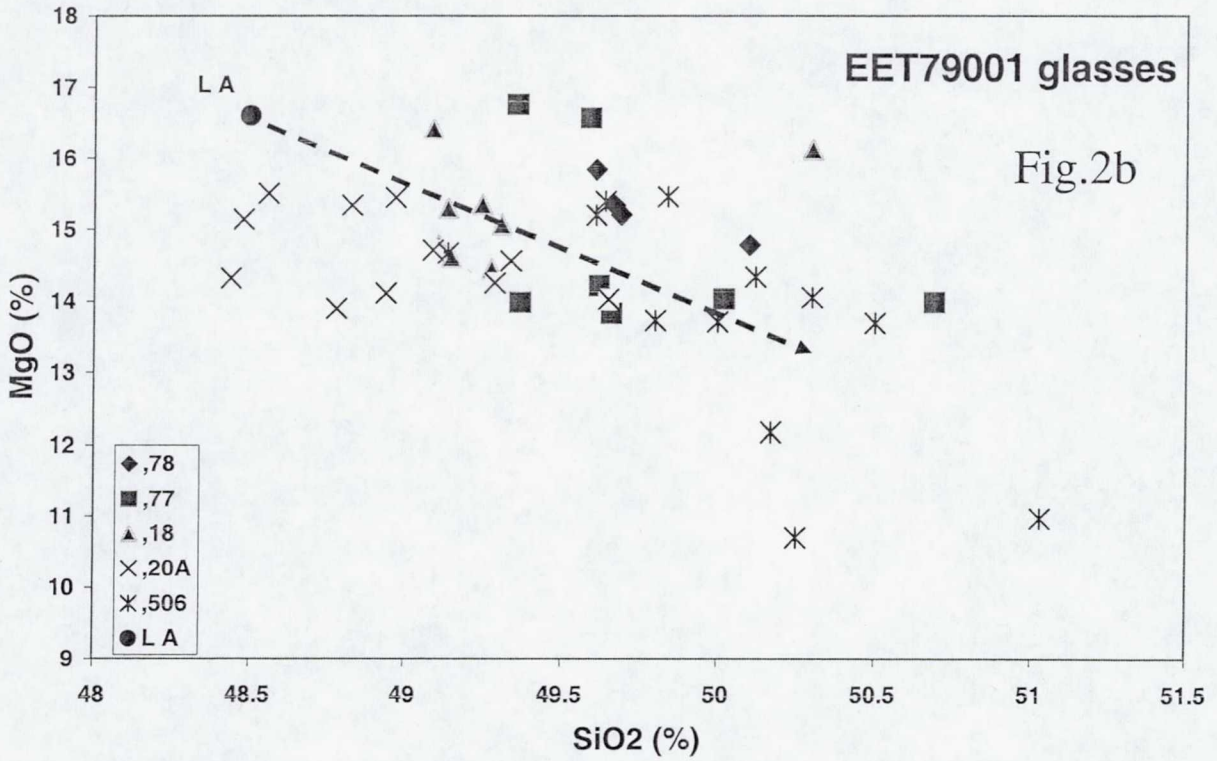
EET79001 glasses
Fig.2b
L A
MgO (%)
SiO2 (%)
18
17
16
15
14
13
12
11
10
9
48
48.5
49
49.5
50
50.5
51
51.5
,78
,77
,18
,20A
,506
L A

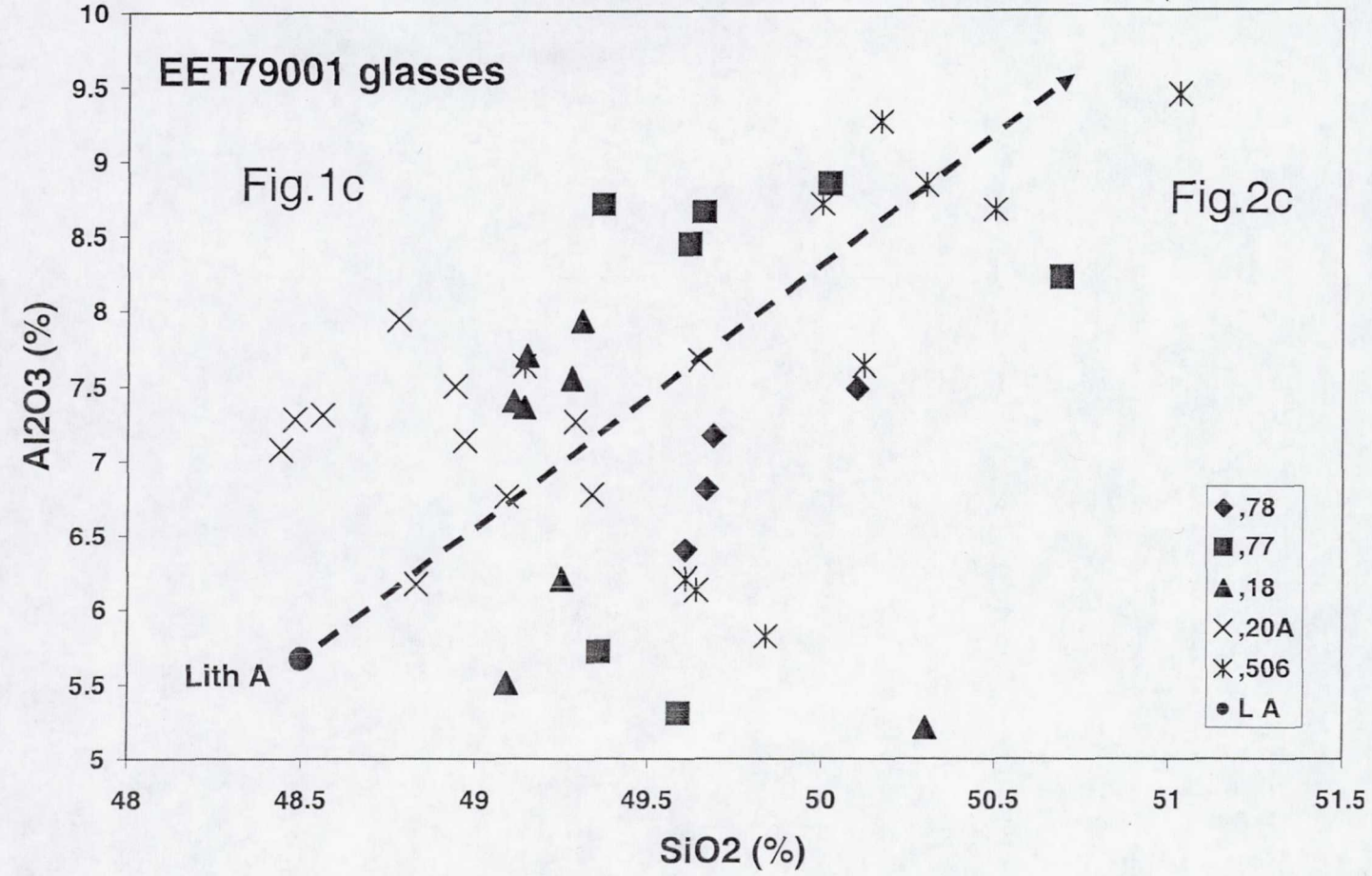
EET79001 glasses
Fig.1c
Fig.2c
Al2O3 (%)
SiO2 (%)
Lith A
,78
,77
,18
,20A
,506
L A
10
9.5
9
8.5
8
7.5
7
6.5
6
5.5
5
48
48.5
49
49.5
50
50.5
51
51.5

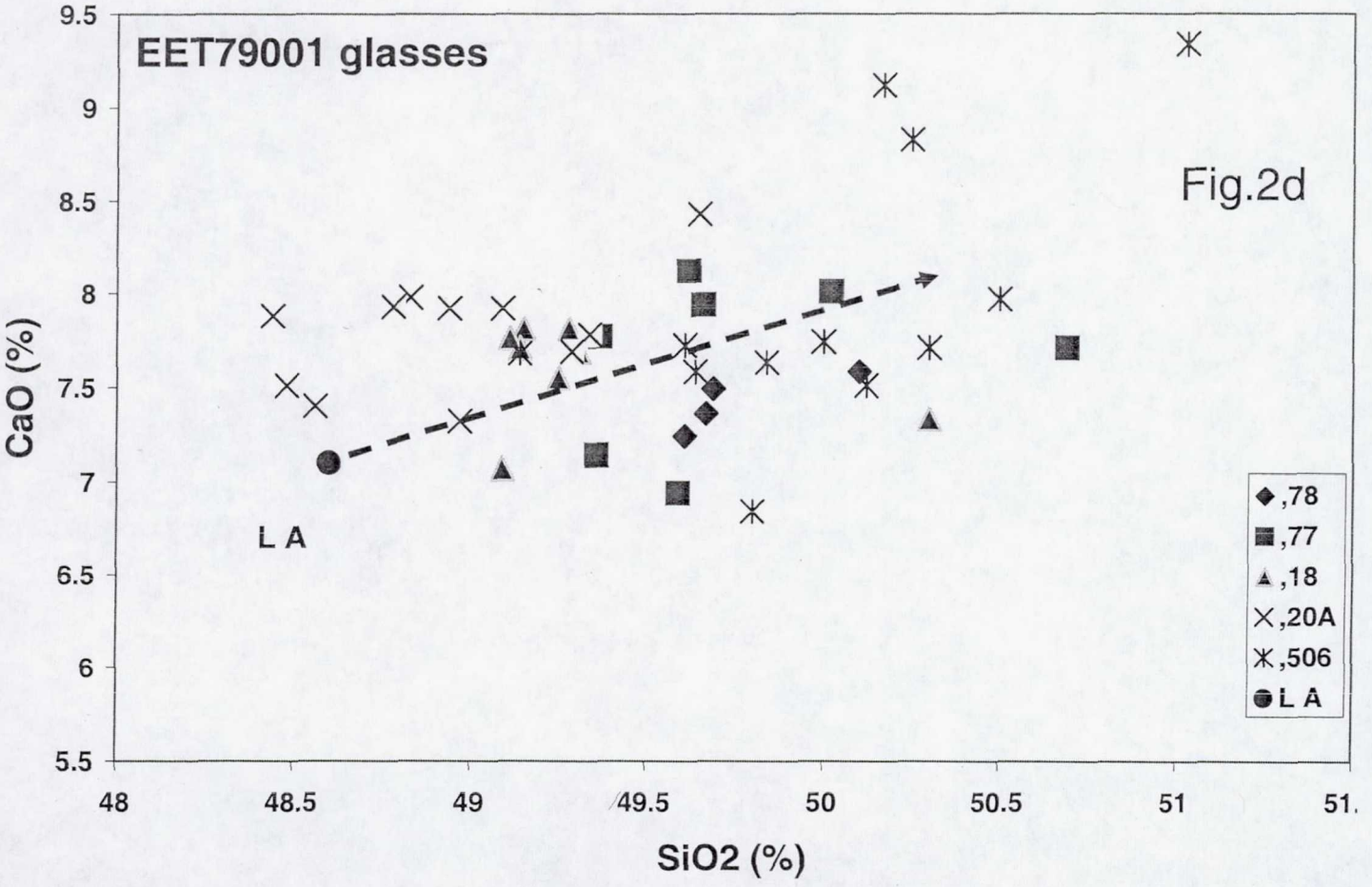
EET79001 glasses
Fig.2d
CaO (%)
SiO2 (%)
L A
,78
,77
,18
,20A
,506
L A
9.5
9
8.5
8
7.5
7
6.5
6
5.5
48
48.5
49
49.5
50
50.5
51

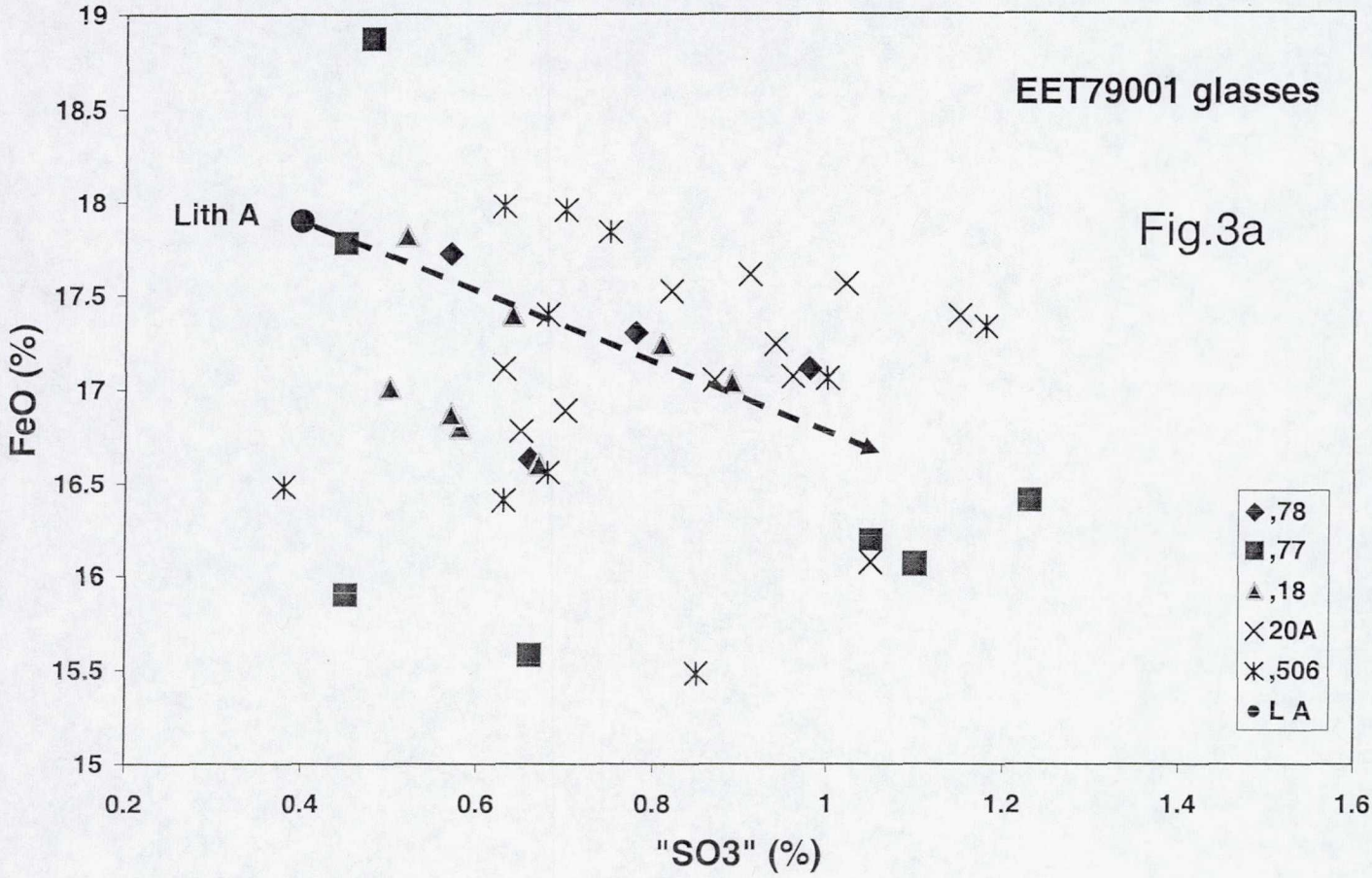
EET79001 glasses
Fig.3a
Lith A
FeO (%)
"SO3" (%)
,78
,77
,18
20A
,506
L A

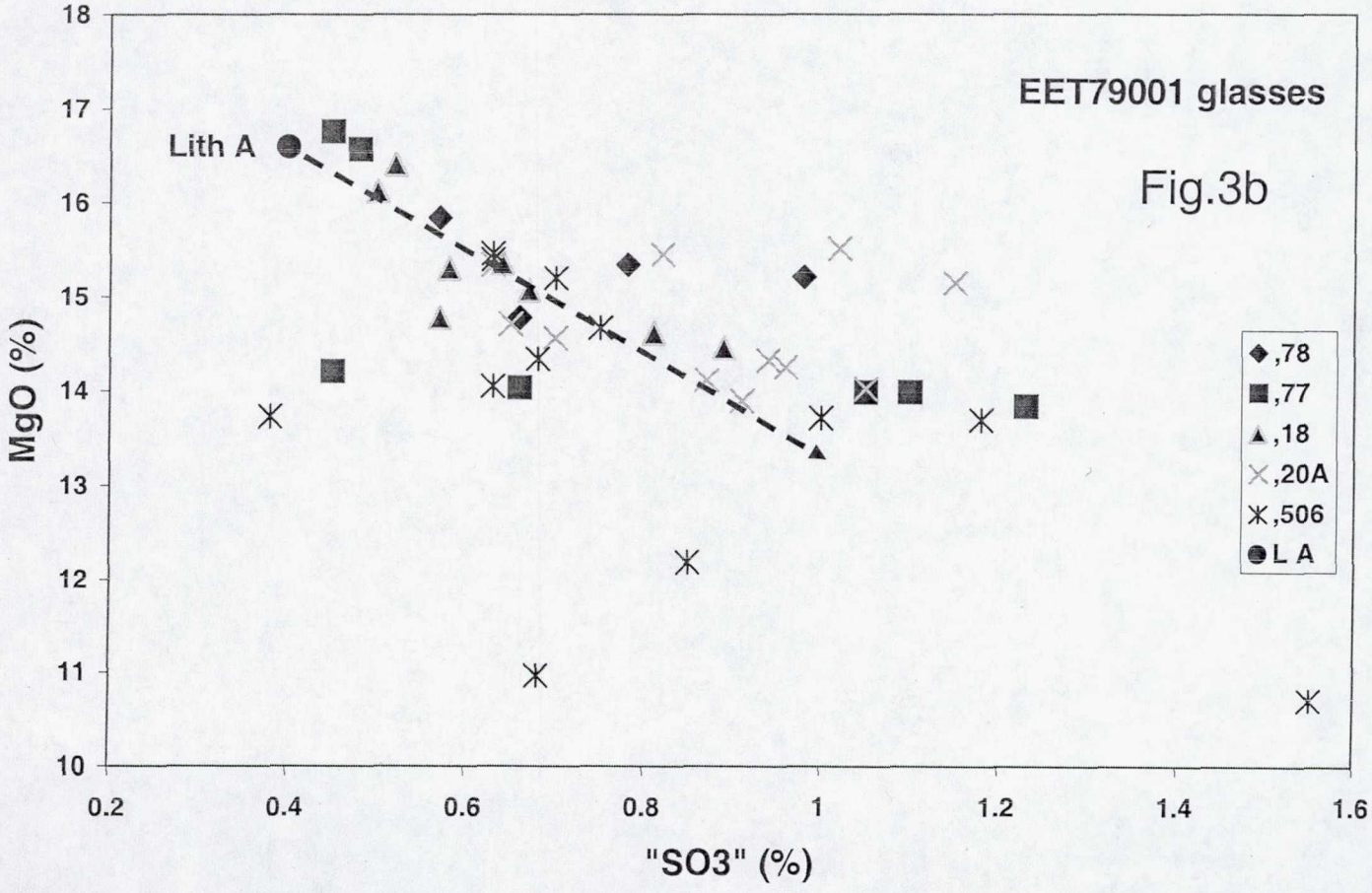
EET79001 glasses
Fig.3b
Lith A
MgO (%)
"SO3" (%)
,78
,77
,18
,20A
,506
L A

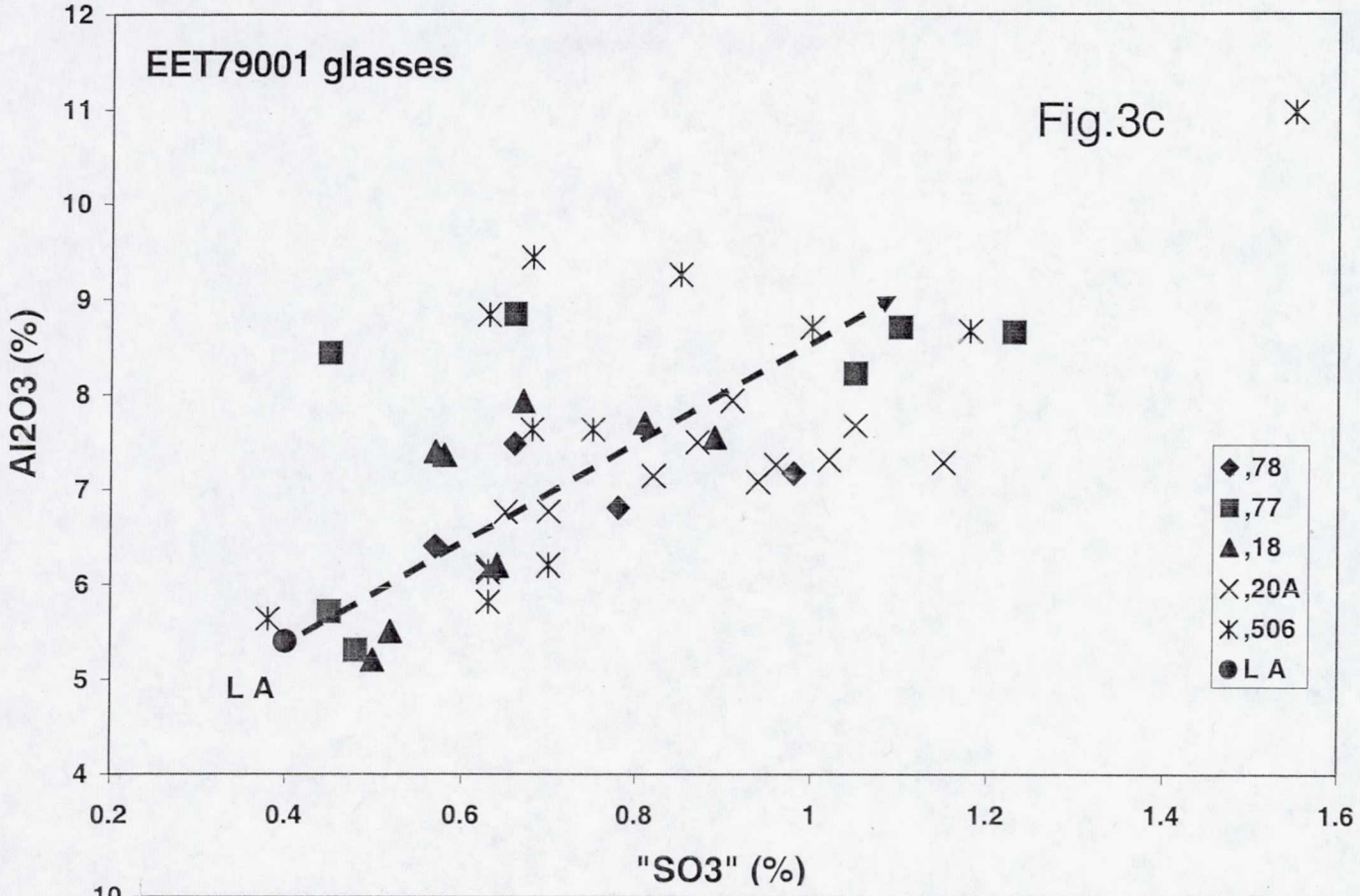
EET79001 glasses
Fig.3c
Al2O3 (%)
"SO3" (%)
L A
,78
,77
,18
,20A
,506
L A

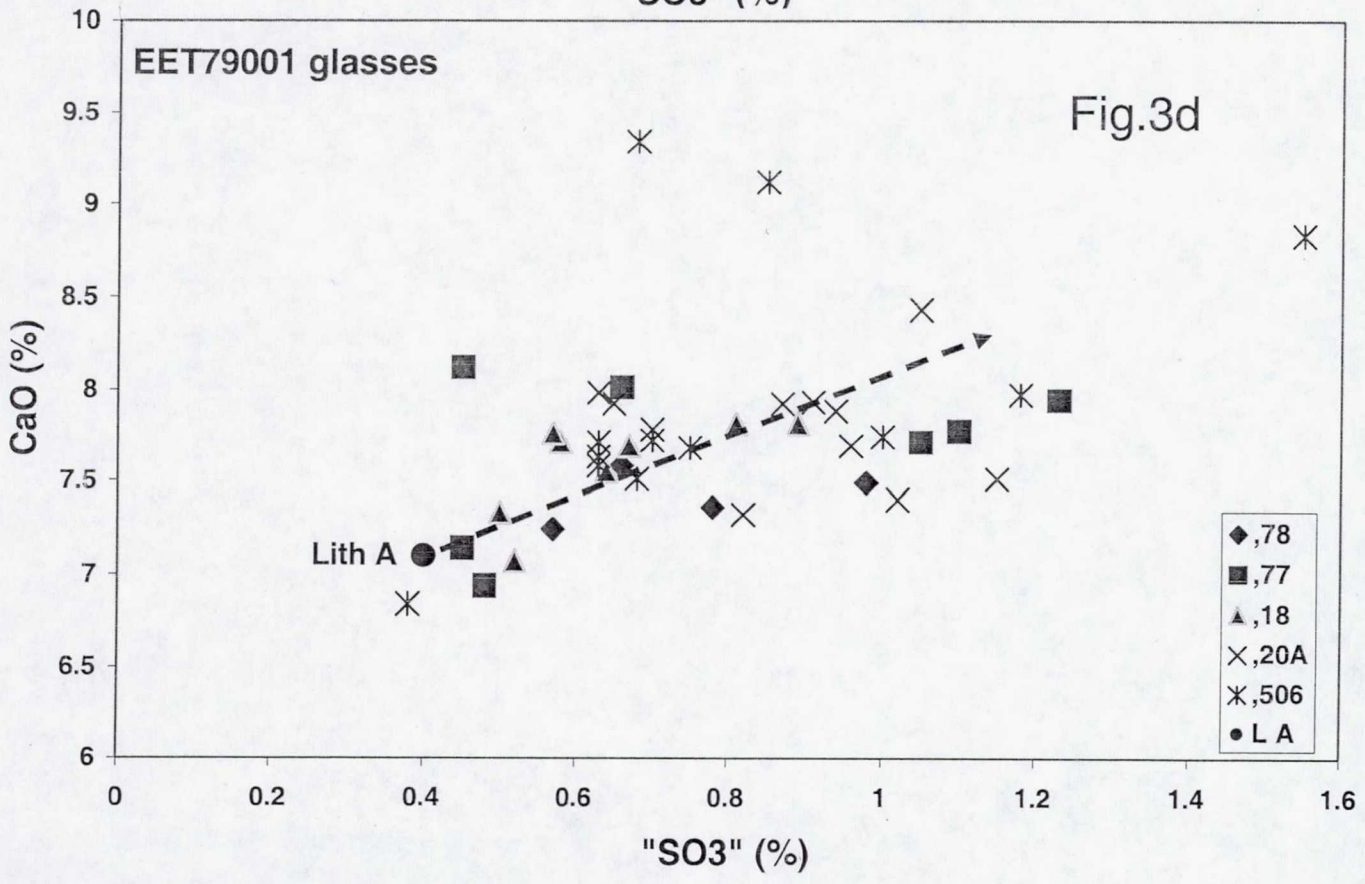
EET79001 glasses
Fig.3d
CaO (%)
"SO3" (%)
Lith A
,78
,77
,18
,20A
,506
L A

Fig. 4

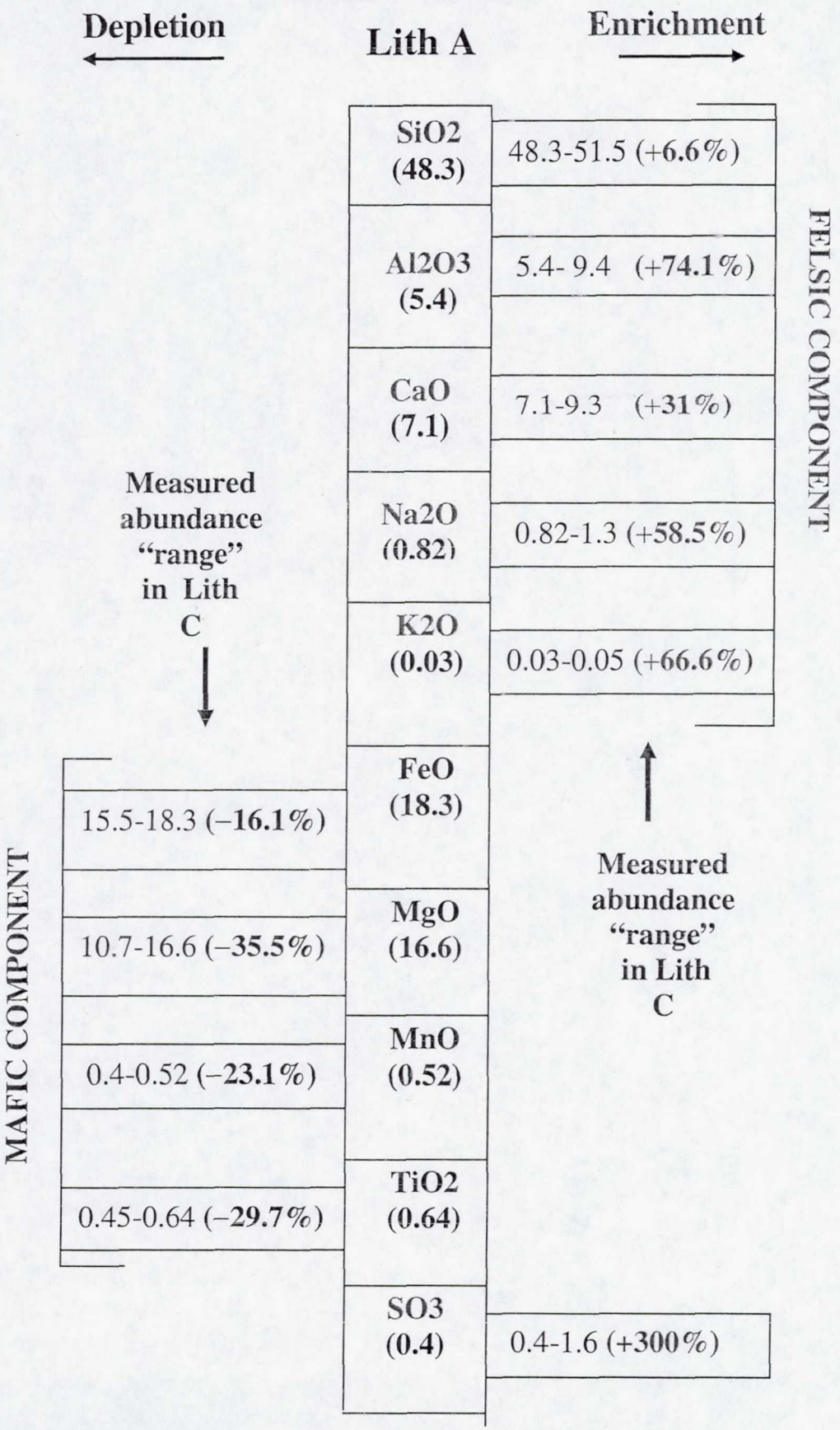
Depletion
Lith A
Enrichment
SiO2 (48.3)
48.3-51.5 (+6.6%)
Al2O3 (5.4)
5.4- 9.4 (+74.1%)
CaO (7.1)
7.1-9.3 (+31%)
Na2O (0.82)
0.82-1.3 (+58.5%)
K2O (0.03)
0.03-0.05 (+66.6%)
FELSIC COMPONENT
Measured abundance "range" in Lith C
FeO (18.3)
MgO (16.6)
MnO (0.52)
TiO2 (0.64)
SO3 (0.4)
0.4-1.6 (+300%)
Measured abundance "range" in Lith C
MAFIC COMPONENT
15.5-18.3 (–16.1%)
10.7-16.6 (–35.5%)
0.4-0.52 (–23.1%)
0.45-0.64 (–29.7%)

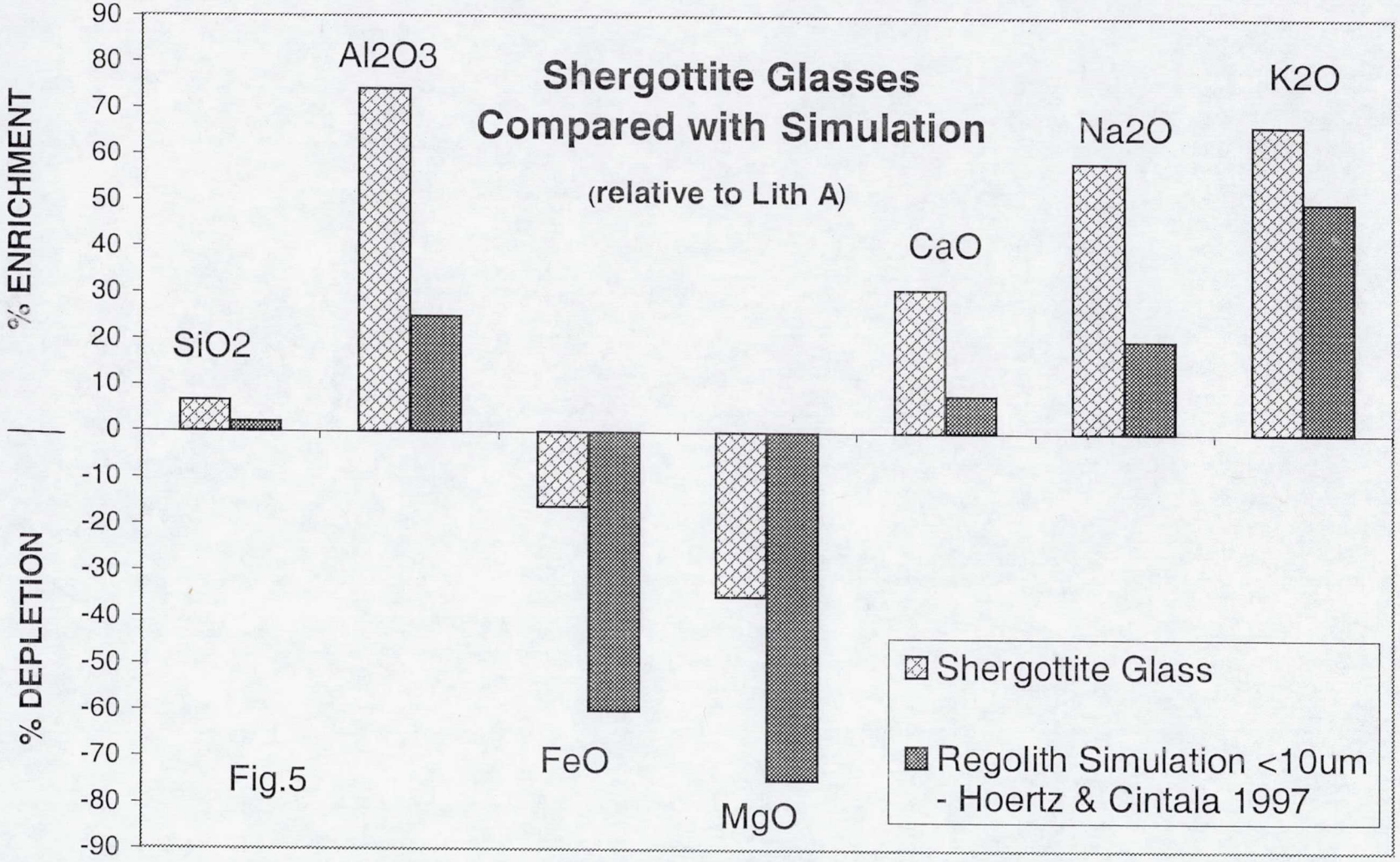
Shergottite Glasses
Compared with Simulation
(relative to Lith A)
% ENRICHMENT
% DEPLETION
90
80
70
60
50
40
30
20
10
0
-10
-20
-30
-40
-50
-60
-70
-80
-90
SiO2
Al2O3
FeO
MgO
CaO
Na2O
K2O
Shergottite Glass
Regolith Simulation <10um
- Hoertz & Cintala 1997

Fig.5

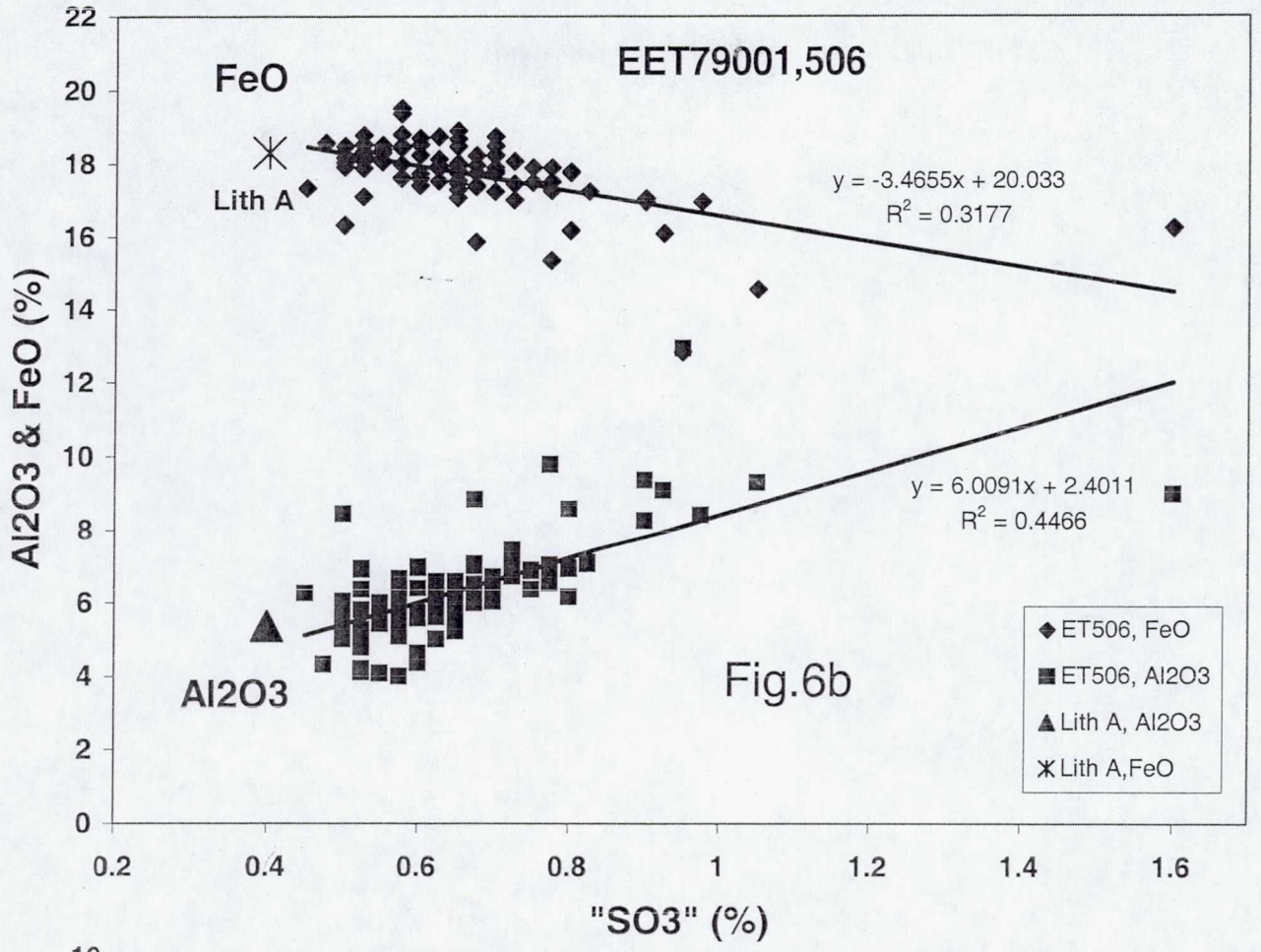
EET79001,506
FeO
Lith A
Al2O3
y = -3.4655x + 20.033
R2 = 0.3177
y = 6.0091x + 2.4411
R2 = 0.4466
ET506, FeO
ET506, Al2O3
Lith A, Al2O3
Lith A,FeO
Al2O3 & FeO (%)
"SO3" (%)

Fig.6b

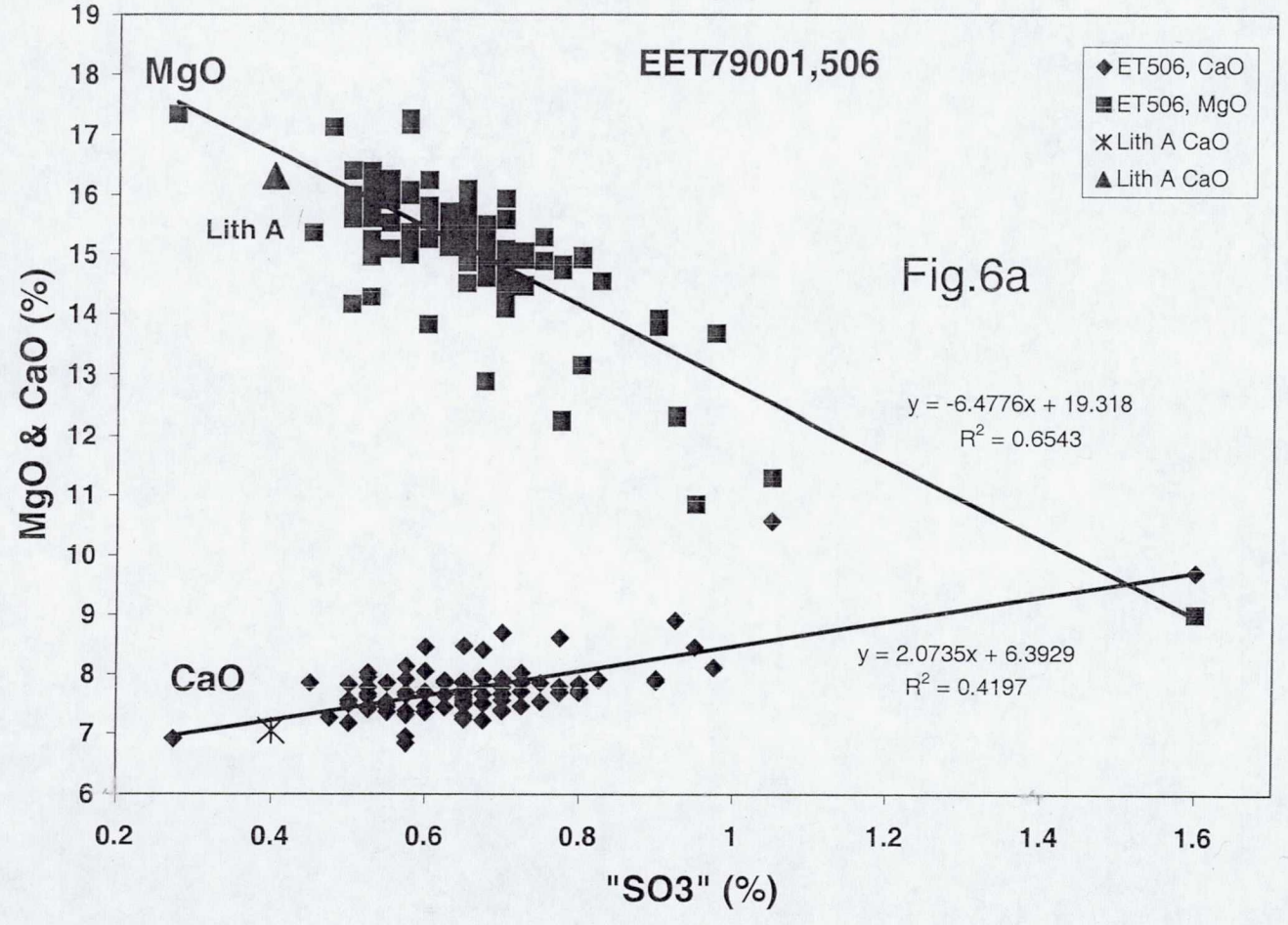
EET79001,506
MgO
Lith A
CaO
y = -6.4776x + 19.318
R2 = 0.6543
y = 2.0735x + 6.3929
R2 = 0.4197
ET506, CaO
ET506, MgO
Lith A CaO
Lith A CaO
MgO & CaO (%)
"SO3" (%)

Fig.6a

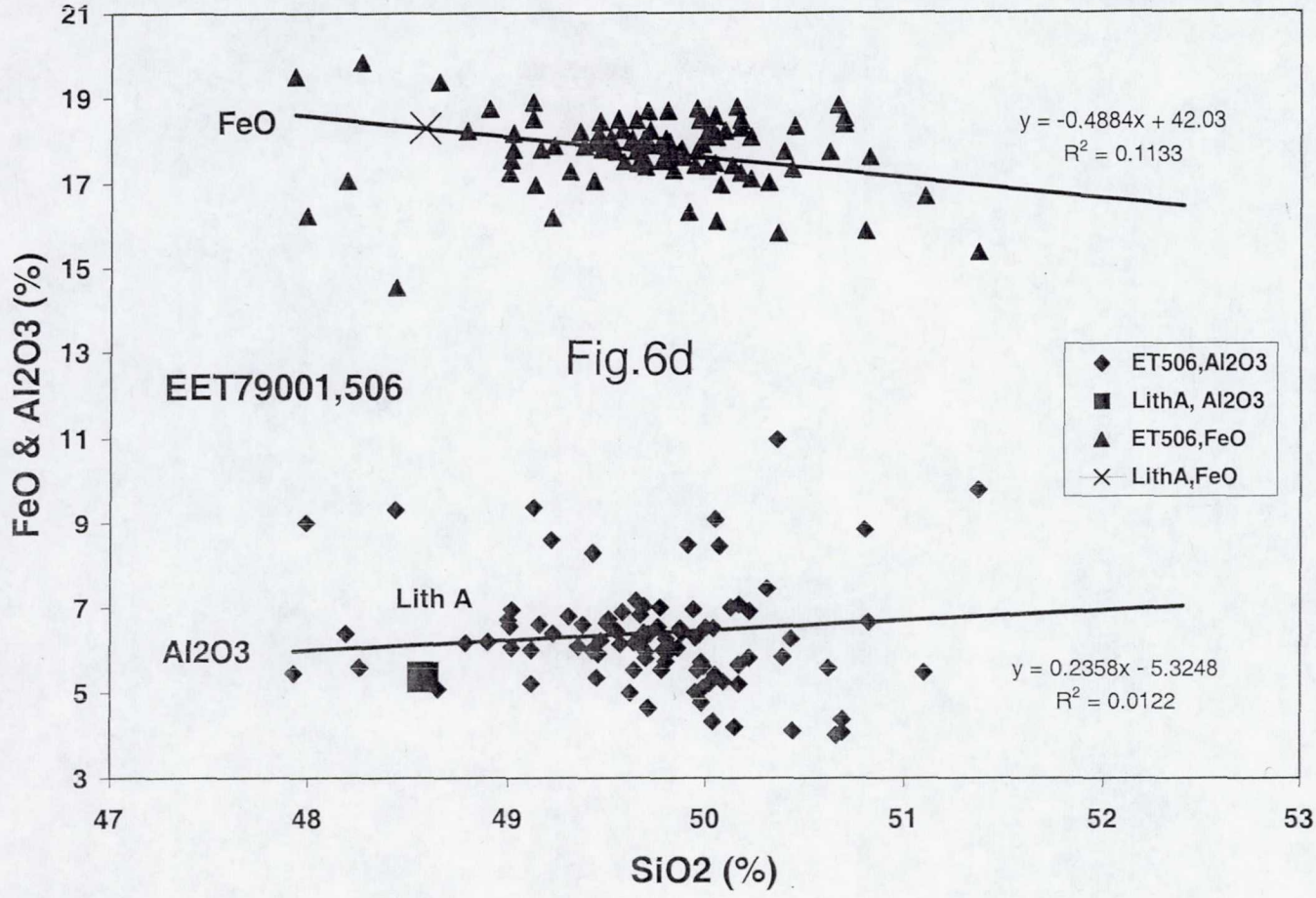
FeO
y = -0.4884x + 42.03
R2 = 0.1133
EET79001,506
Fig.6d
ET506,Al2O3
LithA, Al2O3
ET506,FeO
LithA,FeO
Lith A
Al2O3
y = 0.2358x - 5.3248
R2 = 0.0122
FeO & Al2O3 (%)
SiO2 (%)

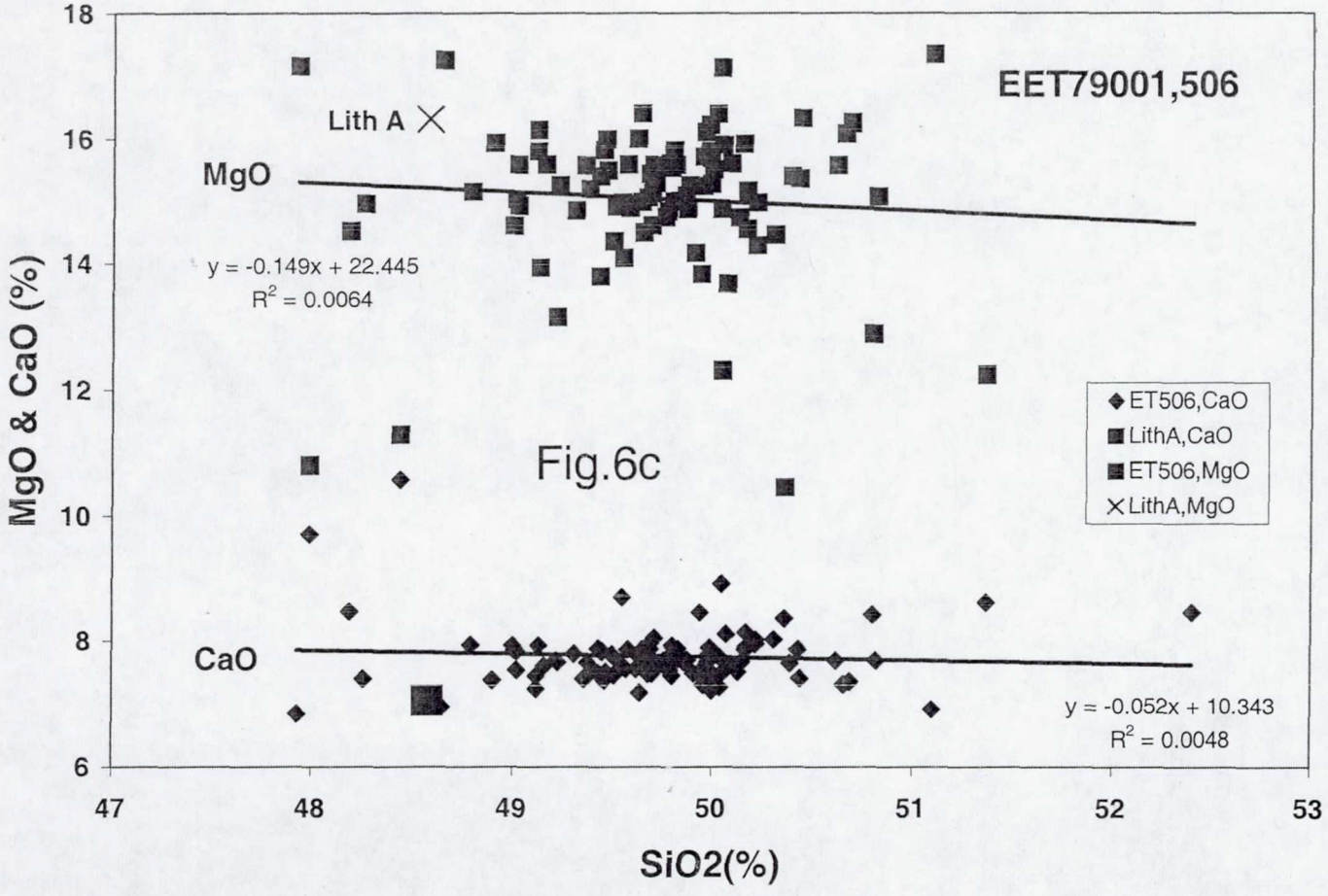
EET79001,506
Lith A
MgO
y = -0.149x + 22.445
R2 = 0.0064
Fig.6c
ET506,CaO
LithA,CaO
ET506,MgO
LithA,MgO
CaO
y = -0.052x + 10.343
R2 = 0.0048
MgO & CaO (%)
SiO2(%)

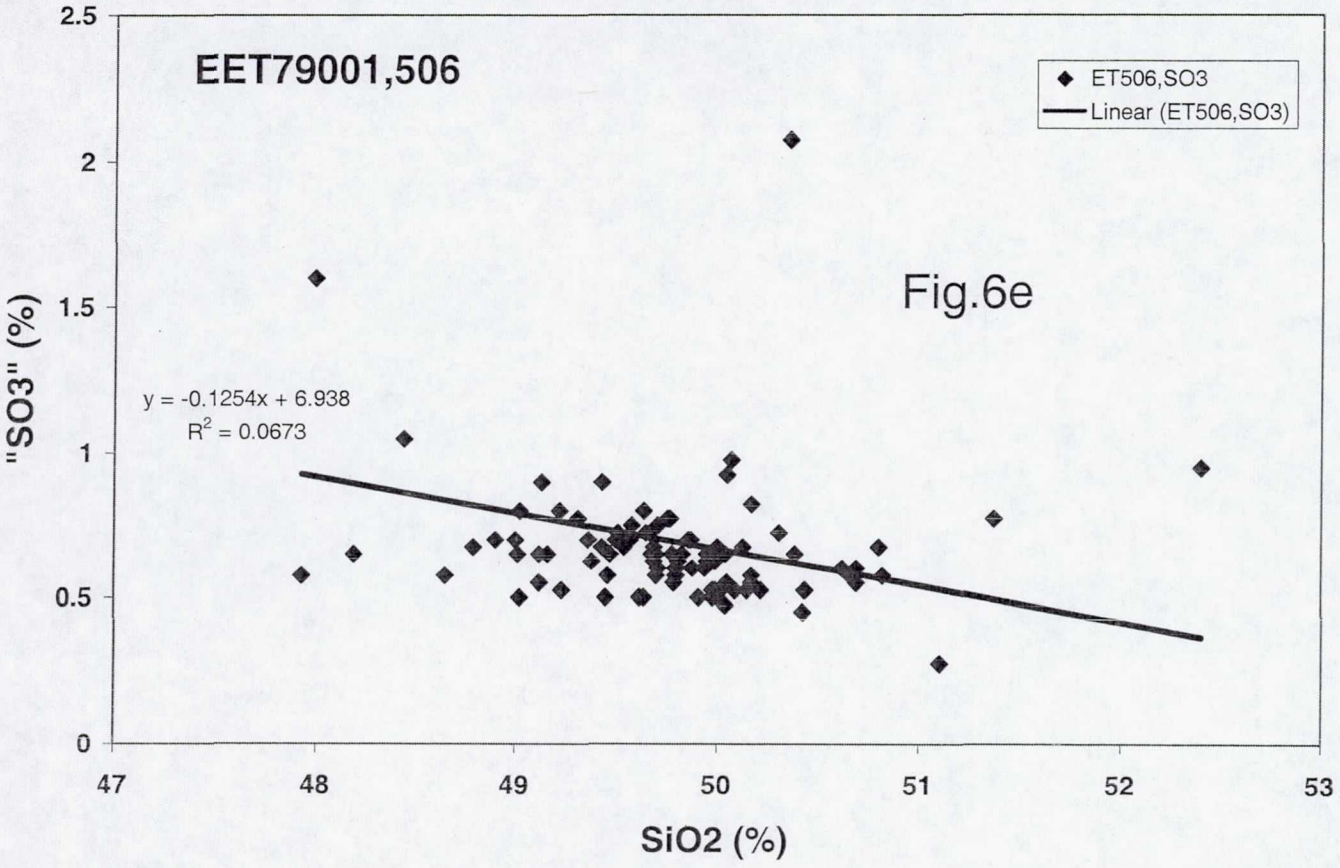
EET79001,506
ET506,SO3
Linear (ET506,SO3)
y = -0.1254x + 6.938
R2 = 0.0673
"SO3" (%)
SiO2 (%)
2.5
2
1.5
1
0.5
0
47
48
49
50
51
52
53

Fig.6e

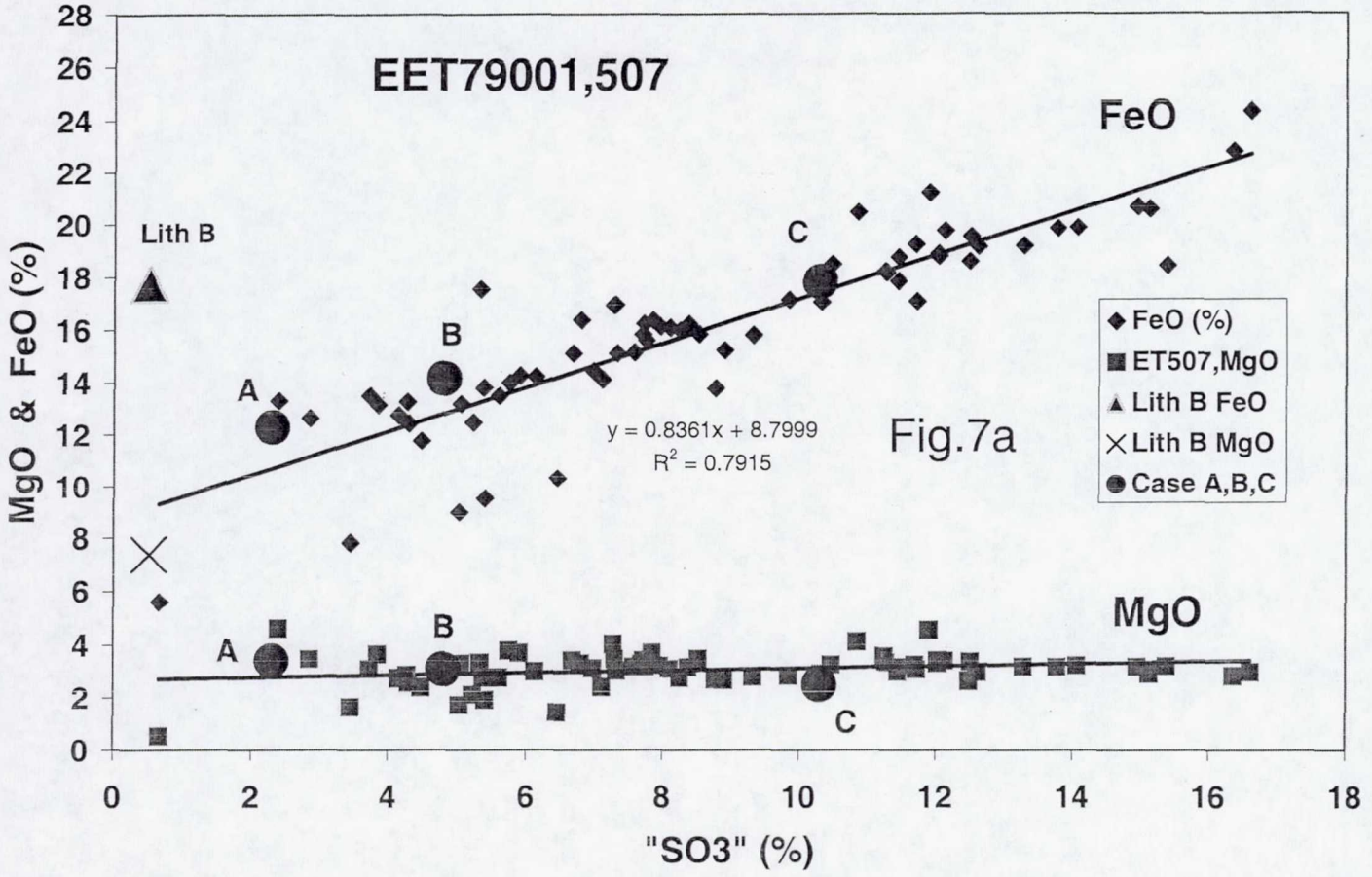
EET79001,507
FeO
MgO
Lith B
A
B
C
y = 0.8361x + 8.7999
R2 = 0.7915
Fig.7a
FeO (%)
ET507,MgO
Lith B FeO
Lith B MgO
Case A,B,C
MgO & FeO (%)
"SO3" (%)

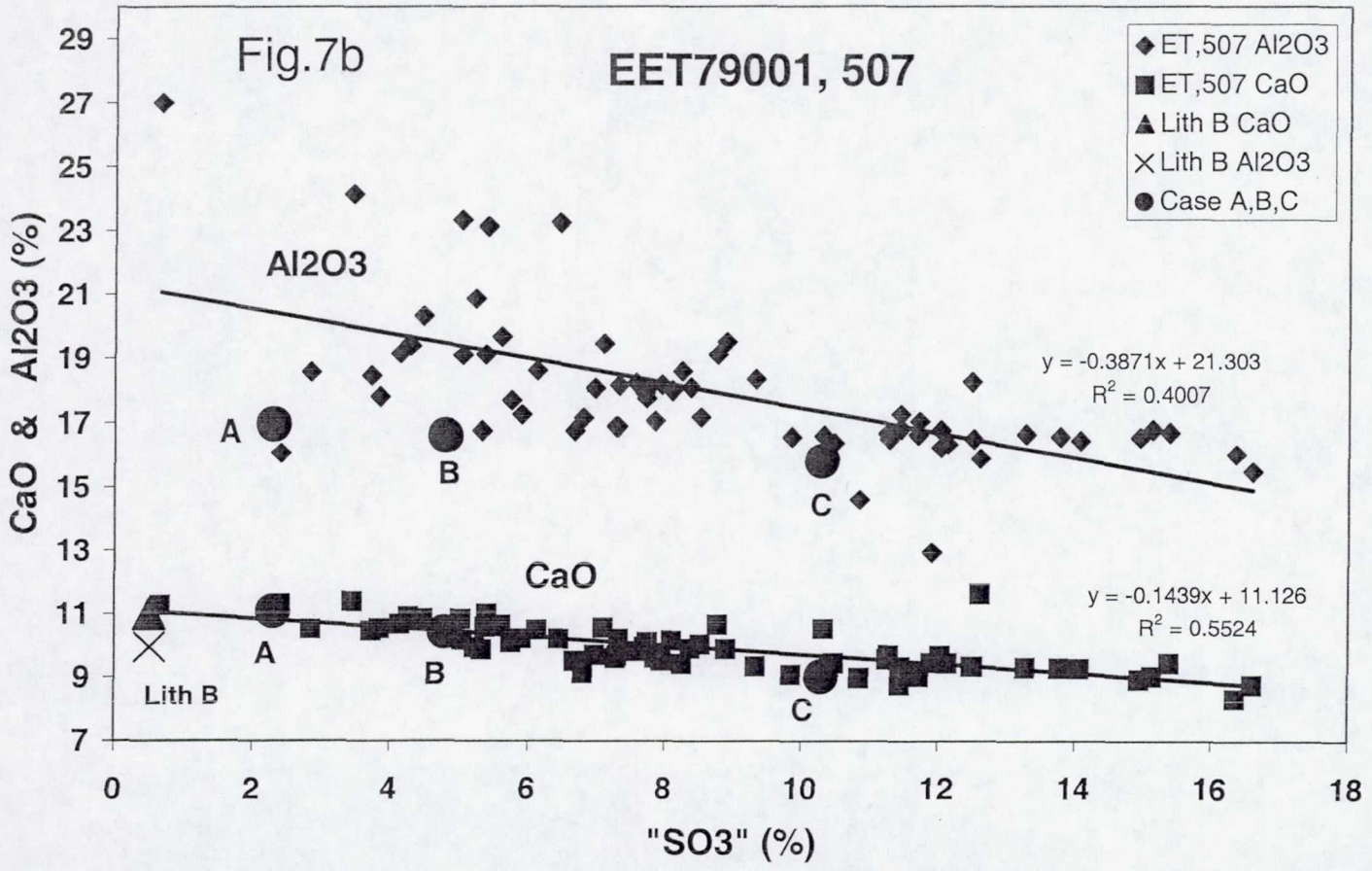
Fig.7b
EET79001, 507
Al2O3
CaO
Lith B
A
B
C
y = -0.3871x + 21.303
R2 = 0.4007
y = -0.1439x + 11.126
R2 = 0.5524
ET,507 Al2O3
ET,507 CaO
Lith B CaO
Lith B Al2O3
Case A,B,C
CaO & Al2O3 (%)
"SO3" (%)

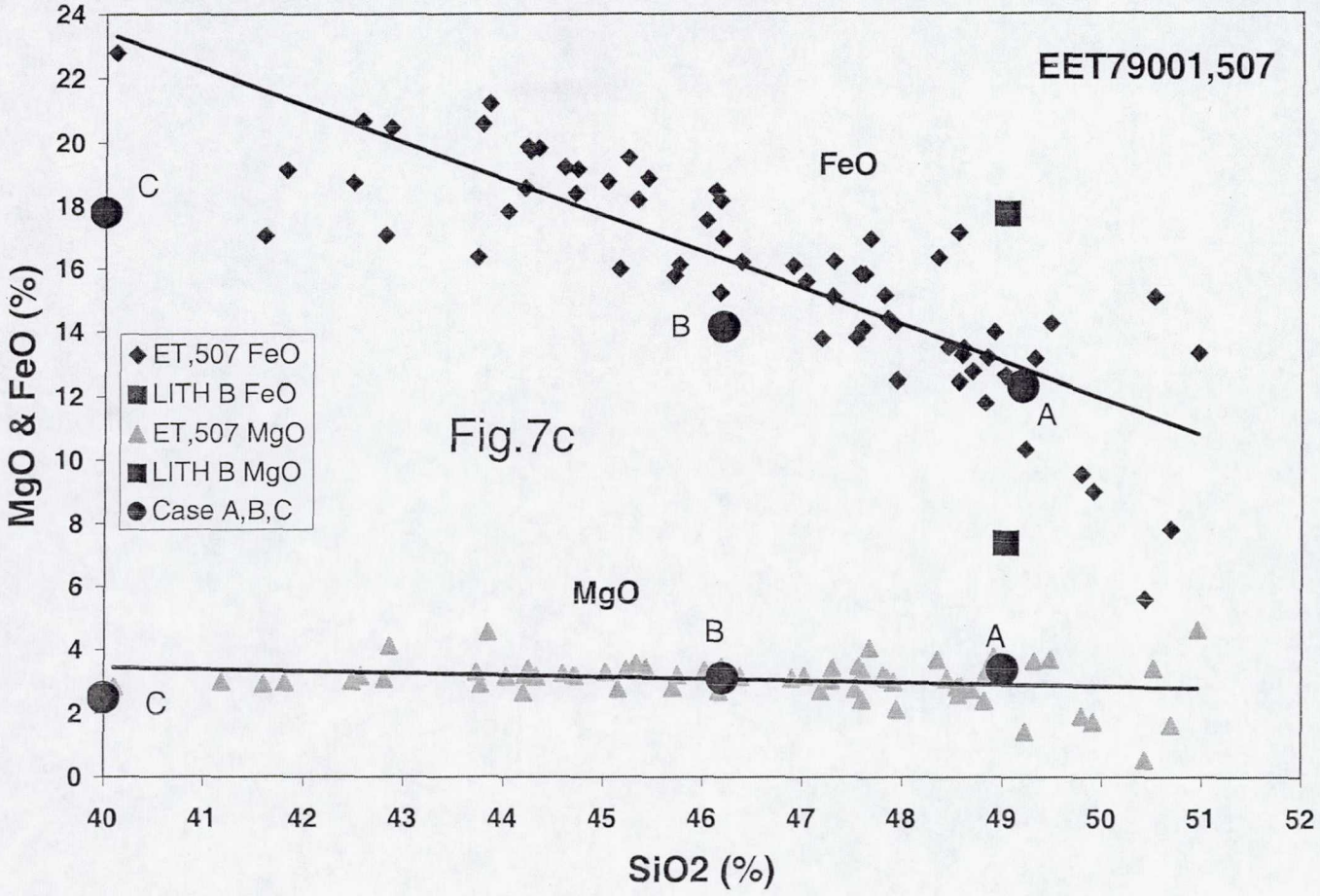
EET79001,507
FeO
MgO
Fig.7c
ET,507 FeO
LITH B FeO
ET,507 MgO
LITH B MgO
Case A,B,C
A
B
C
MgO & FeO (%)
SiO2 (%)

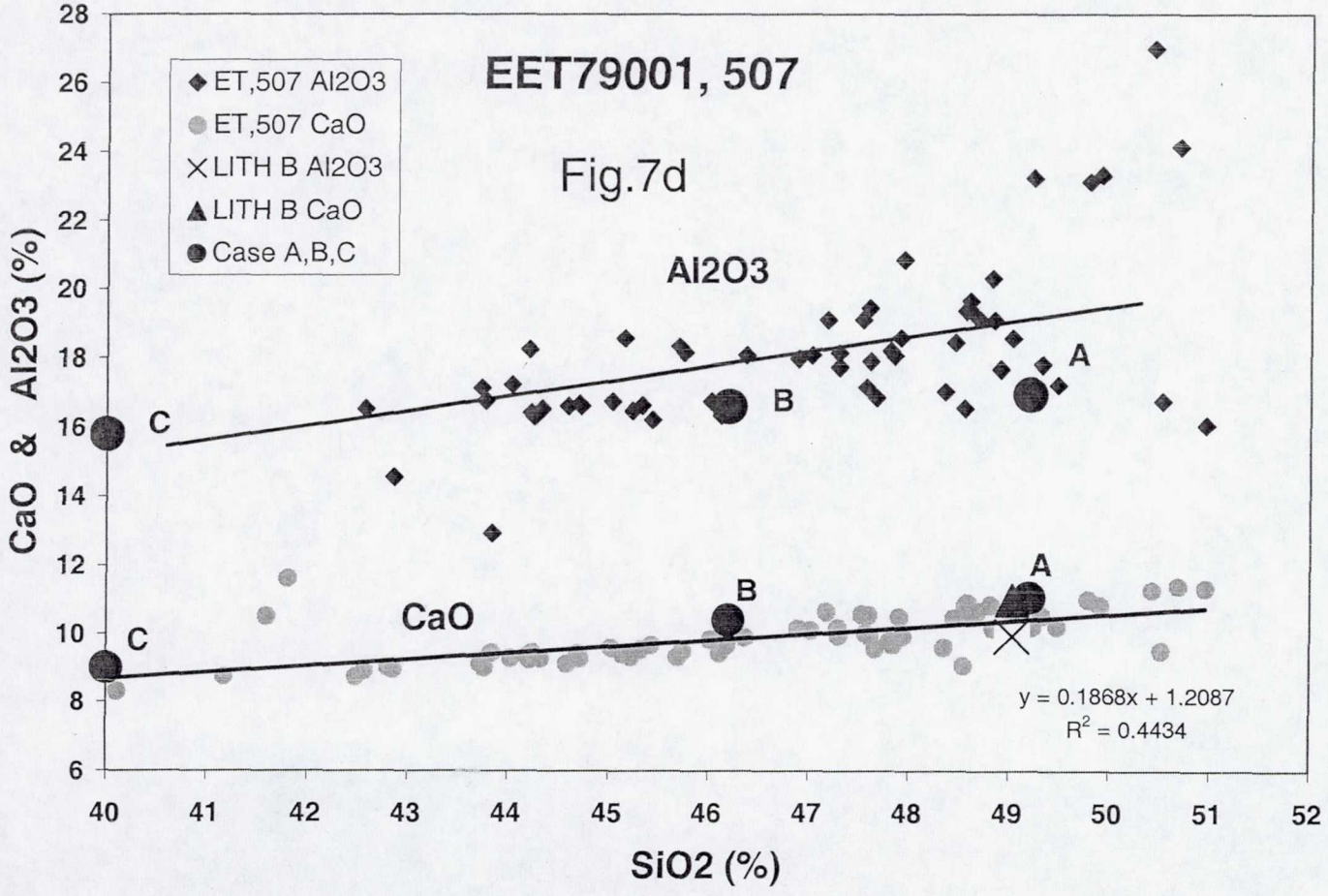
EET79001, 507
Fig.7d
ET,507 Al2O3
ET,507 CaO
LITH B Al2O3
LITH B CaO
Case A,B,C
Al2O3
CaO
A
B
C
y = 0.1868x + 1.2087
R2 = 0.4434
CaO & Al2O3 (%)
SiO2 (%)

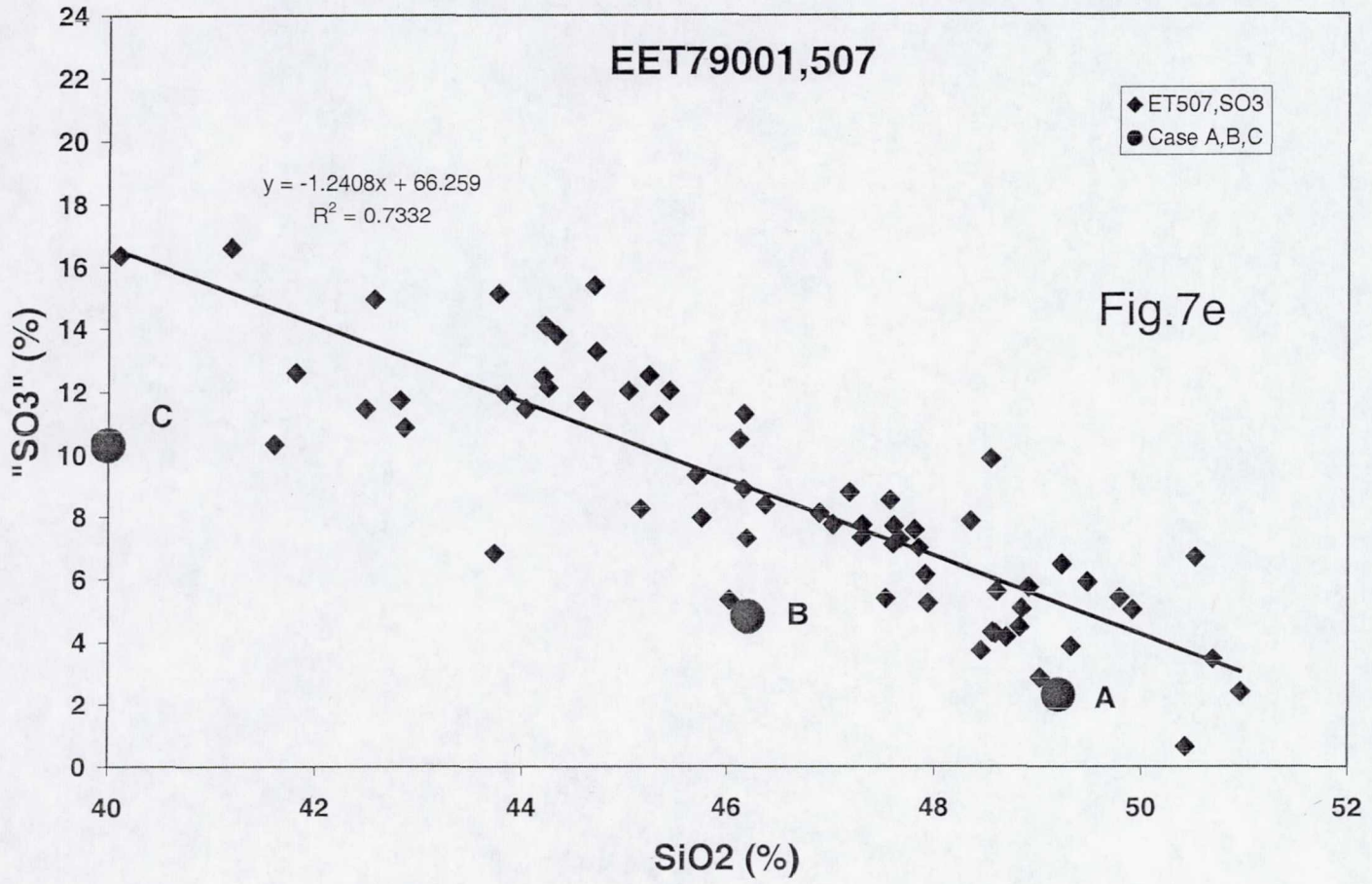
EET79001,507
ET507,SO3
Case A,B,C
y = -1.2408x + 66.259
R2 = 0.7332
"SO3" (%)
SiO2 (%)
A
B
C
0
2
4
6
8
10
12
14
16
18
20
22
24
40
42
44
46
48
50
52

Fig.7e

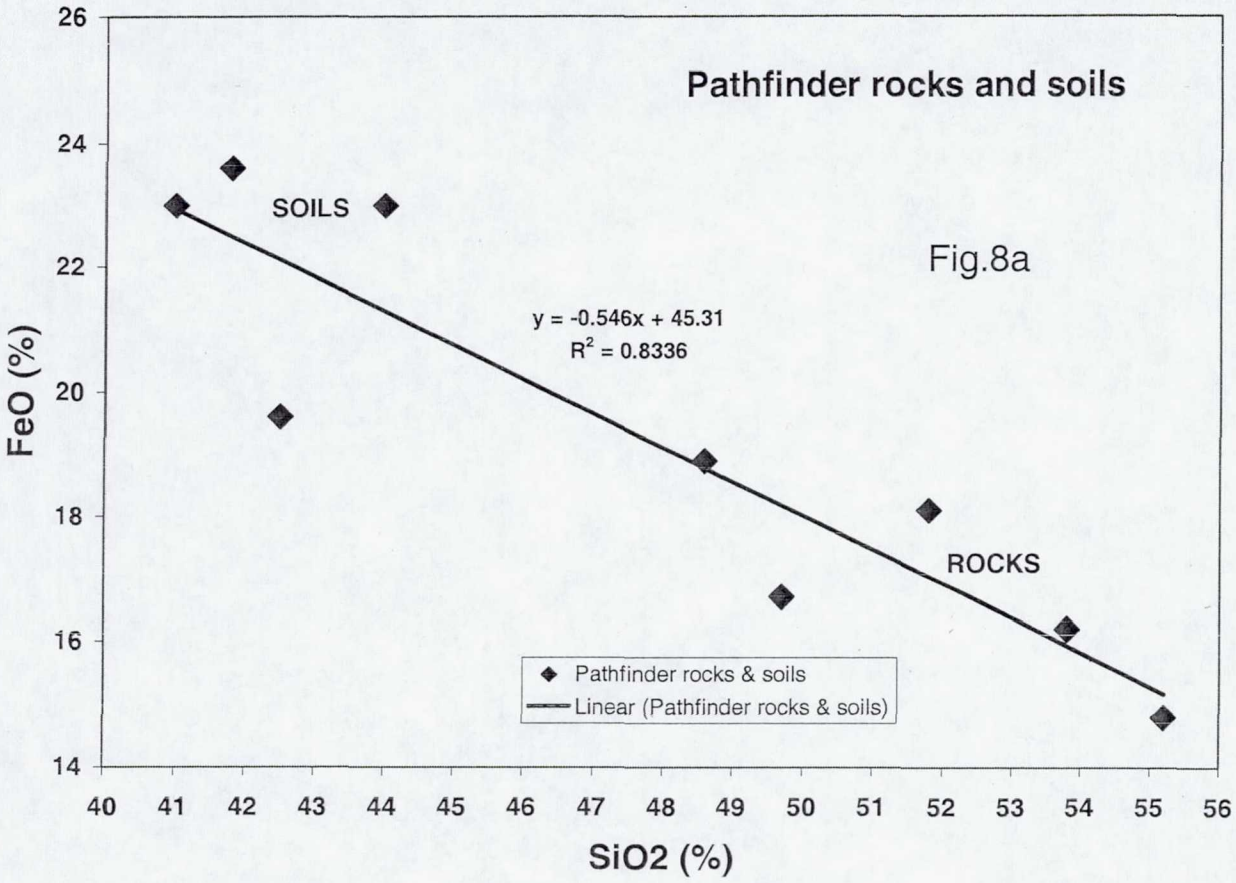
Pathfinder rocks and soils
SOILS
ROCKS
Fig.8a
y = -0.546x + 45.31
R2 = 0.8336
Pathfinder rocks & soils
Linear (Pathfinder rocks & soils)
FeO (%)
SiO2 (%)
26
24
22
20
18
16
14
40
41
42
43
44
45
46
47
48
49
50
51
52
53
54
55
56

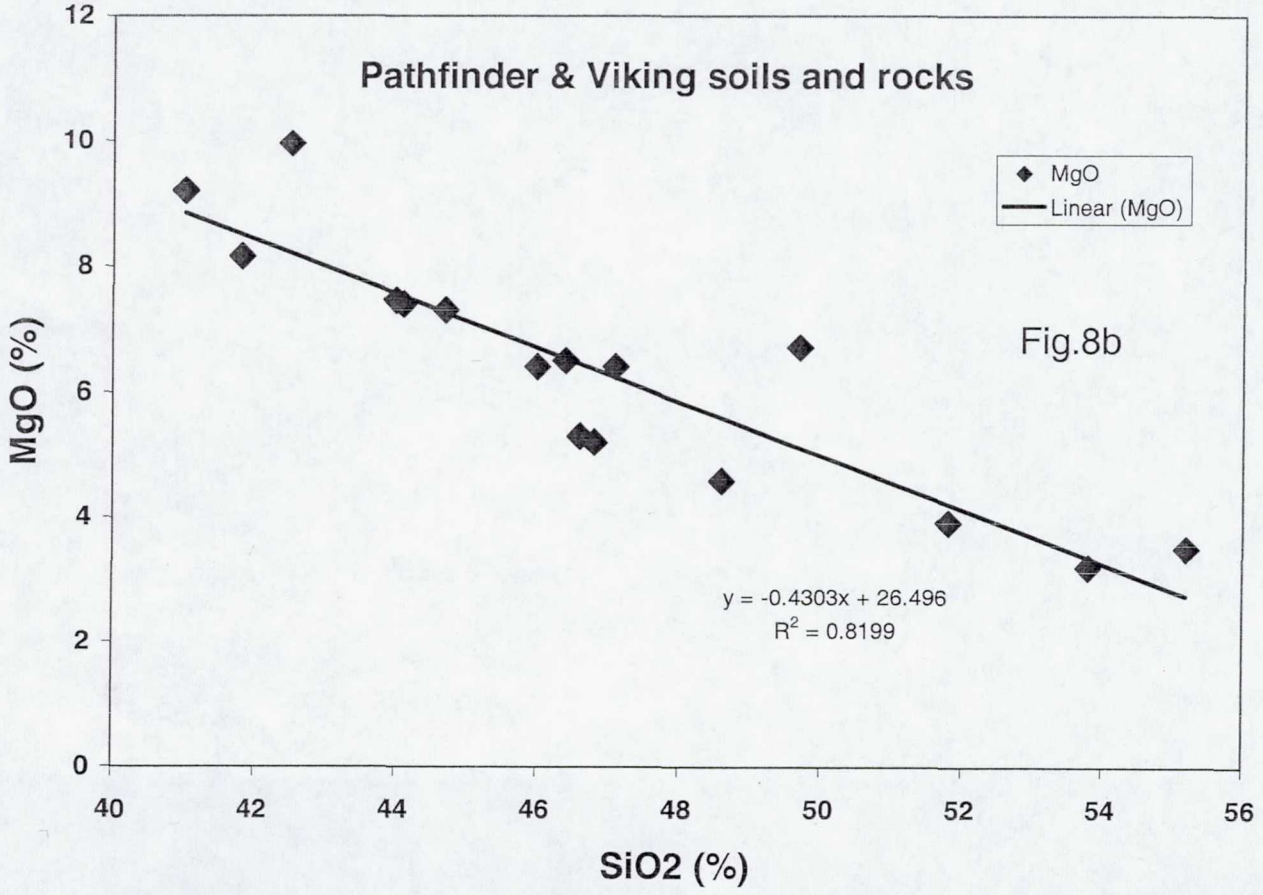
Pathfinder & Viking soils and rocks
MgO
Linear (MgO)
Fig.8b
y = -0.4303x + 26.496
R2 = 0.8199
MgO (%)
SiO2 (%)
12
10
8
6
4
2
0
40
42
44
46
48
50
52
54
56

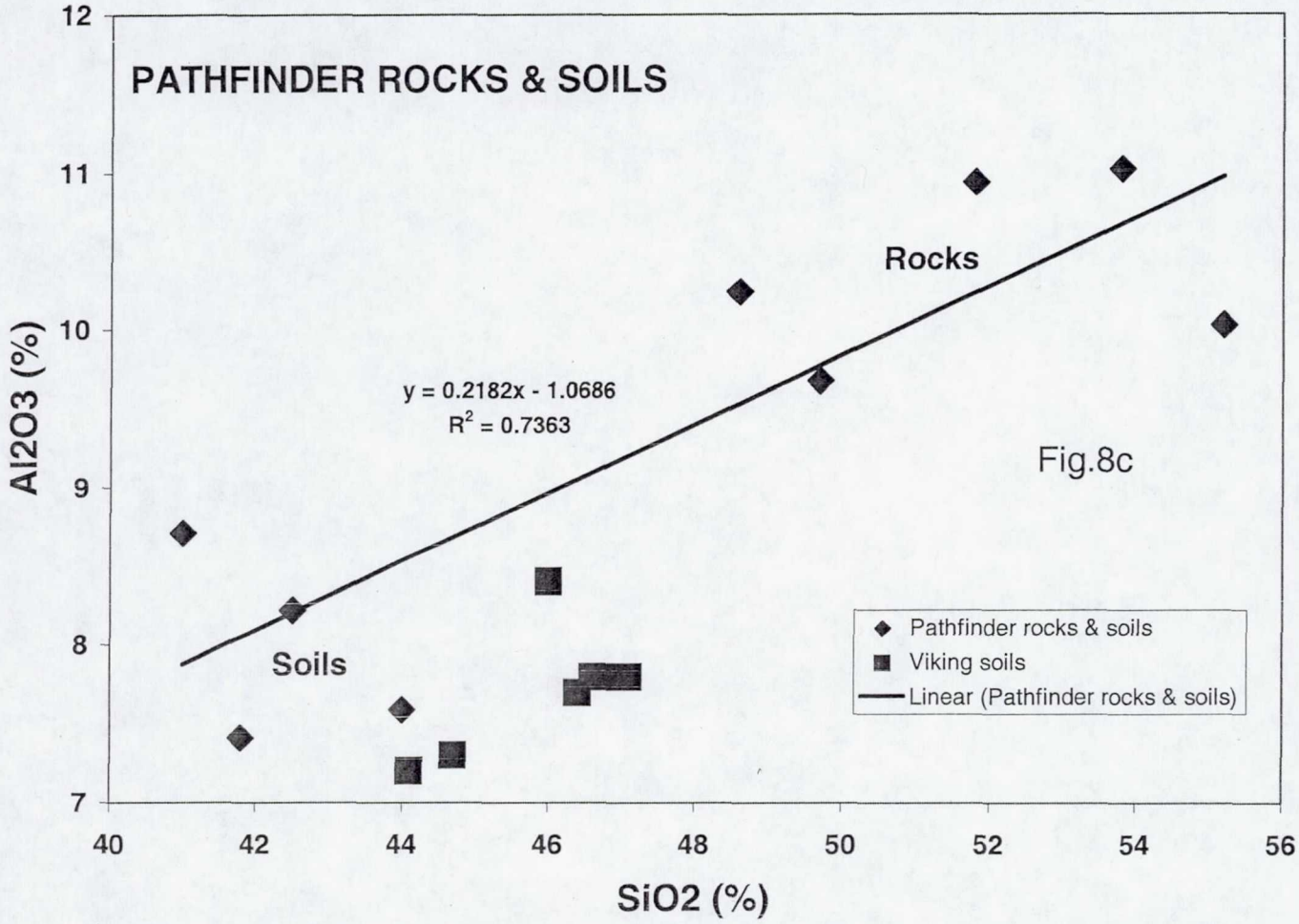
PATHFINDER ROCKS & SOILS
Al2O3 (%)
SiO2 (%)
y = 0.2182x - 1.0686
R2 = 0.7363
Rocks
Soils
Pathfinder rocks & soils
Viking soils
Linear (Pathfinder rocks & soils)
Fig.8c

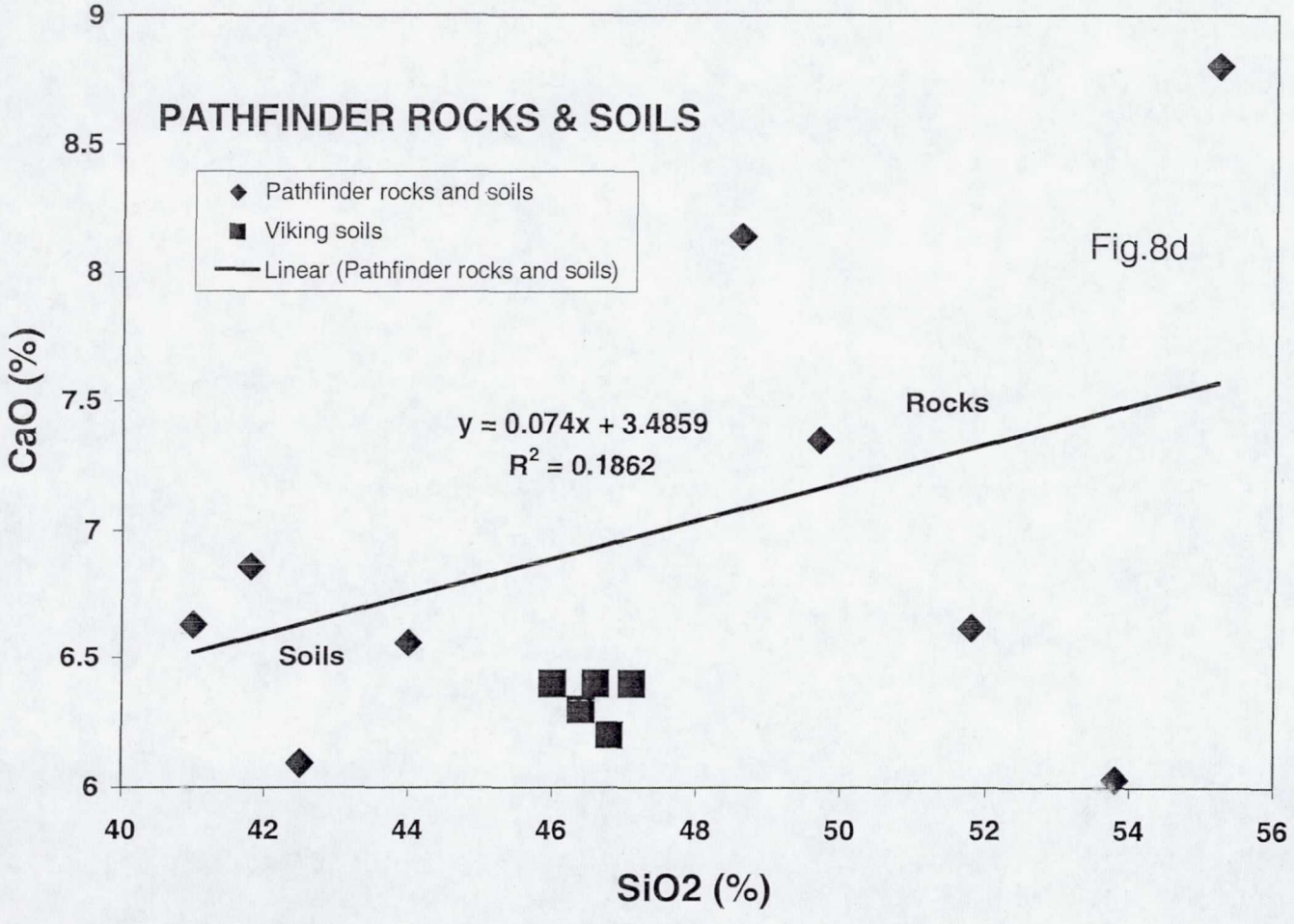
PATHFINDER ROCKS & SOILS
CaO (%)
SiO2 (%)
Pathfinder rocks and soils
Viking soils
Linear (Pathfinder rocks and soils)
y = 0.074x + 3.4859
R2 = 0.1862
Rocks
Soils
Fig.8d

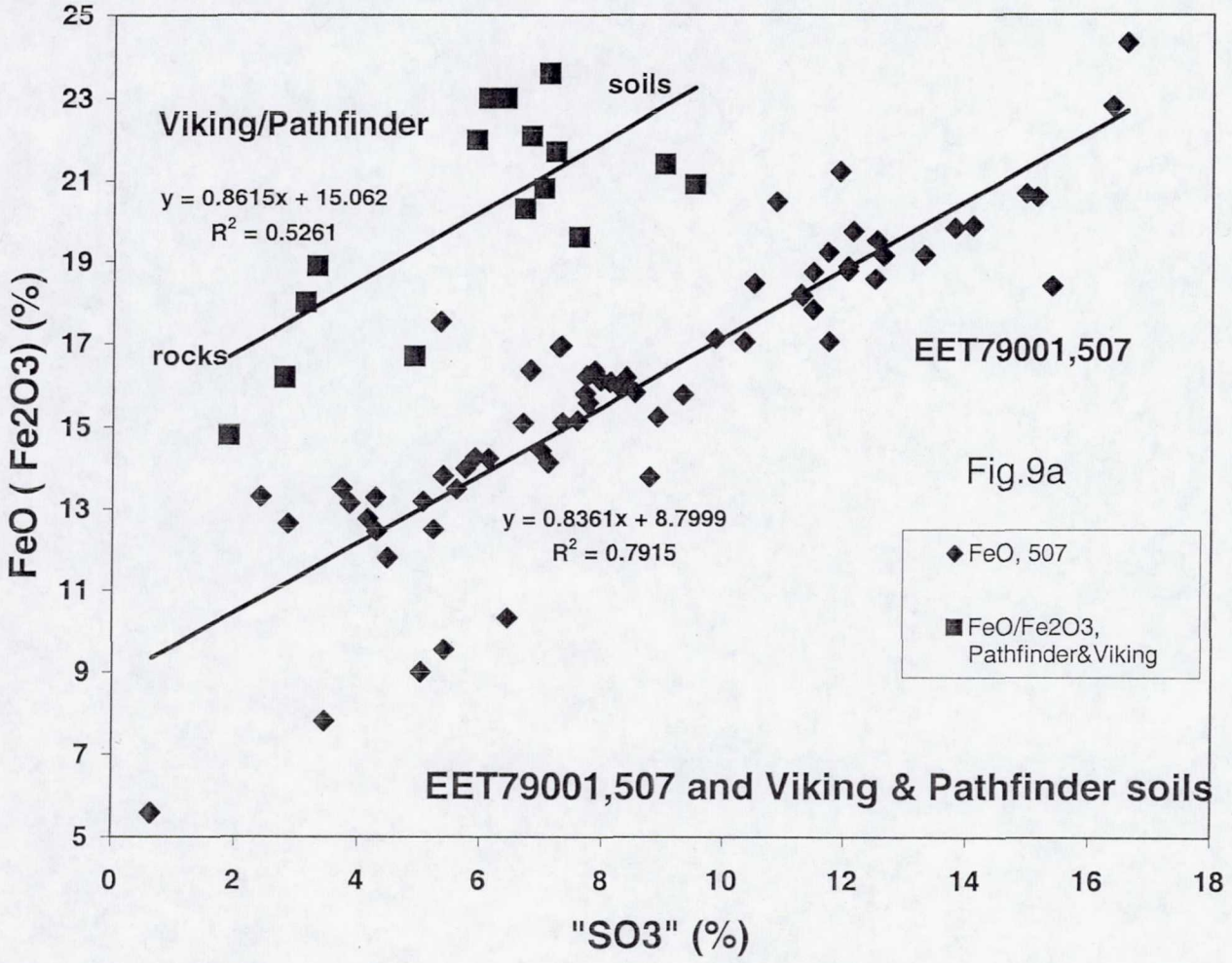
soils
Viking/Pathfinder
y = 0.8615x + 15.062
R2 = 0.5261
rocks
EET79001,507
Fig.9a
y = 0.8361x + 8.7999
R2 = 0.7915
FeO, 507
FeO/Fe2O3, Pathfinder&Viking
EET79001,507 and Viking & Pathfinder soils
FeO (Fe2O3) (%)
"SO3" (%)

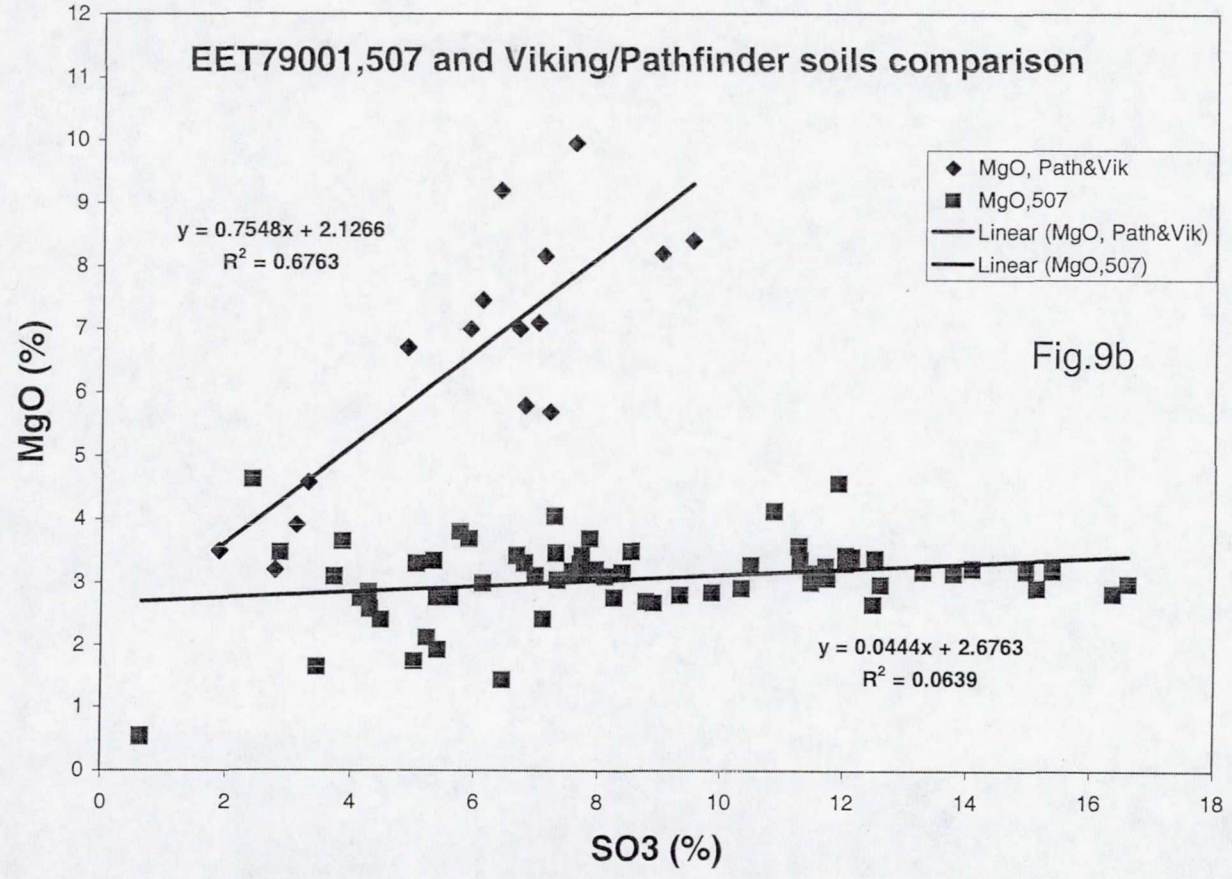
EET79001,507 and Viking/Pathfinder soils comparison
MgO, Path&Vik
MgO,507
Linear (MgO, Path&Vik)
Linear (MgO,507)
y = 0.7548x + 2.1266
R2 = 0.6763
Fig.9b
y = 0.0444x + 2.6763
R2 = 0.0639
MgO (%)
SO3 (%)

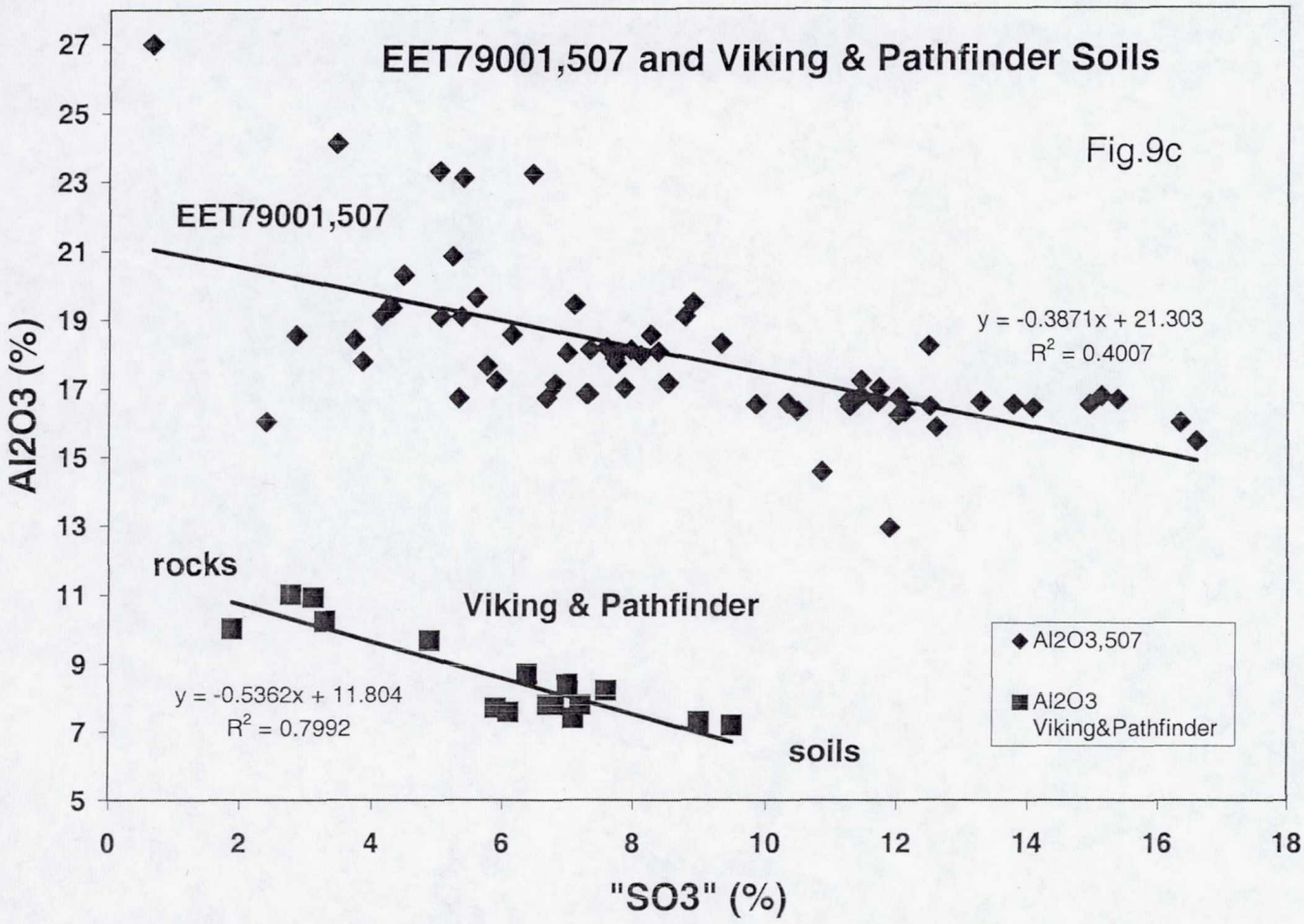
EET79001,507 and Viking & Pathfinder Soils
Fig.9c
EET79001,507
y = -0.3871x + 21.303
R2 = 0.4007
rocks
Viking & Pathfinder
y = -0.5362x + 11.804
R2 = 0.7992
soils
Al2O3,507
Al2O3 Viking&Pathfinder
Al2O3 (%)
"SO3" (%)

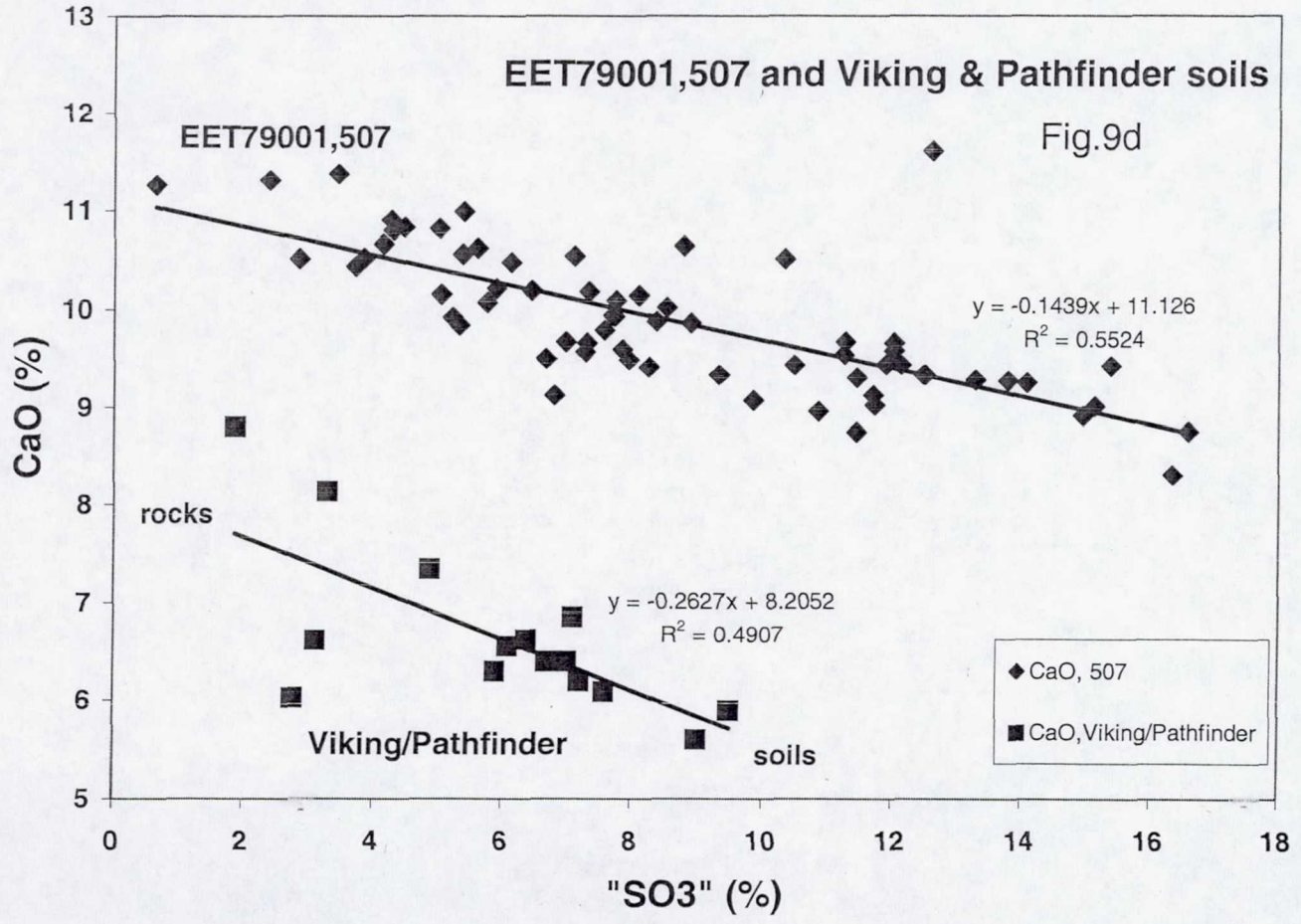
EET79001,507 and Viking & Pathfinder soils
Fig.9d
EET79001,507
y = -0.1439x + 11.126
R2 = 0.5524
rocks
y = -0.2627x + 8.2052
R2 = 0.4907
Viking/Pathfinder
soils
CaO, 507
CaO,Viking/Pathfinder
CaO (%)
"SO3" (%)

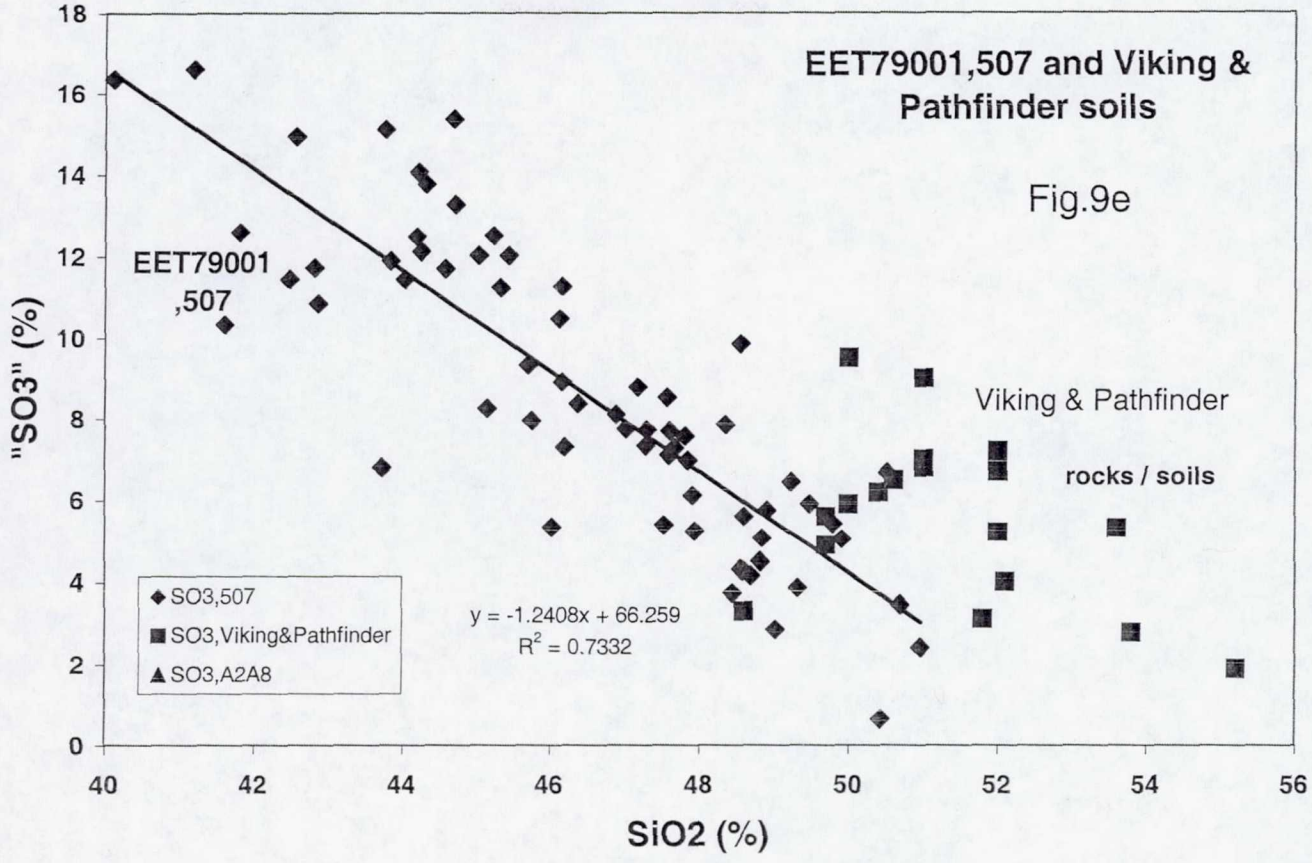
EET79001,507 and Viking & Pathfinder soils
Fig.9e
EET79001 ,507
Viking & Pathfinder
rocks / soils
SO3,507
SO3,Viking&Pathfinder
SO3,A2A8
y = -1.2408x + 66.259
R2 = 0.7332
"SO3" (%)
SiO2 (%)
0
2
4
6
8
10
12
14
16
18
40
42
44
46
48
50
52
54
56